

Charge and Spin Transport in Superconducting Weak Links

Gholamreza Rashedi

Institute for Advanced Studies in Basic Sciences, 45195-159, Zanjan, Iran

Abstract. The coherent mixing of the current states in the superconducting weak link subject to a Josephson phase difference ϕ and subject to an external transport current in the banks is one of the aims of this work. At $\phi = \pi$ the nonlocal mixing of current states produces two vortices close to the point-contact between superconducting bulks. The effect of point-contact reflection in an impenetrable interface and effect of temperature on the vortices have been studied. It is obtained that increasing the reflection of the point-contact destroys the vortices while increasing the temperature restore these vortices. The vortex state is a new version of the interference between the macroscopic states and quantum tunnelling. Also, the weak link between unitary triplet superconductors which have f -wave and $p + h$ -wave pairing symmetry has been studied from the spin and charge current-phase relation point of view. The main result in the second part of this thesis, is the polarization of the spin transport when a junction between triplet superconductors is used. It is observed that the spin current is the result of the misorientation between the gap vectors of two superconductors. In addition, the weak link between two bipolar non-unitary triplet superconductors is studied mathematically. The current-phase relations obtained in third part of this thesis are totally different from the junctions between the unitary spin-triplet superconductors and between the spin-singlet superconductors. The current phase diagrams which have been obtained in this work can be used to distinguish the symmetry of the order parameter in the crystals.

PACS numbers: 74.50.+r, 74.20.Rp, 72.25.-b, 74.70.Pq, 74.70.Tx

1. Introduction

Superconductor is a substance that below a certain temperature (critical temperature T_c) conducts charge current without resistance and also repels the magnetic field. Superconductivity was discovered by Kammerlingh Onnes in a mercury wire at temperatures less than $T = 4.2K$ in 1911 [1]. In 1957, Bardeen, Cooper and Schrieffer (BCS), using the concept of Cooper pairs, proposed a microscopic theory for superconductivity [2]. Cooper had shown earlier that the ground state of a metal, at sufficient low temperatures, will be stable when its electrons are collected as the pairs [3]. BCS theory suggests that Cooper pairs at low temperatures condense into the same quantum state defined by a macroscopic wave function and can travel together without dissipation. Also, the pair amplitude of this wave function as an order parameter in the Ginzburg-Landau (GL) theory of superconductivity, defines the transition between normal and superconducting states [4]. In the limit of $T \rightarrow T_c$, the GL order parameter, is directly proportional to the BCS energy gap, Δ , which is the amount of energy for breaking a Cooper pair. This energy gap carries the information about the pairing symmetry of the electrons.

There are different types of superconductivity. According to the spin states of two electrons in the Cooper pair, superconductor is either spin-singlet or spin-triplet. Since electrons are fermion, the total wave function of a cooper pair should be antisymmetric with respect to electrons: $\Psi_{cooper-pair} = \psi(\mathbf{r}_1, \mathbf{r}_2)\varphi(\mathbf{s}_1, \mathbf{s}_2)$ where \mathbf{r} , \mathbf{s} are spatial coordinates and spins, respectively. For the antisymmetric spin-singlet state, the orbital part of the wave function should be symmetric under the interchange of the electrons and the orbital momentum should be even ($l = 0$, s -wave, $l = 2$, d -wave and $l = 4$, g -wave).

The superconductors with simplest spin-singlet state, $l = 0$, are known as conventional superconductors. All the other type of superconductors including the spin-singlet and spin-triplet with $l \neq 0$, are unconventional superconductors. A s -wave superconductor, has an isotropic order parameter $\Delta(\hat{\mathbf{k}}) = \Delta_0$ in the momentum space, where $\hat{\mathbf{k}}$ is a unit vector pointed on the Fermi surface. Earlier superconductors which had been found in the elements like mercury, are conventional superconductors. Unconventional superconducting compounds which have anisotropic order parameter can be defined using the relation $\sum_{\mathbf{k}} \Delta(\mathbf{k}) = 0$, with summation over the Fermi surface. For the symmetric spin-triplet state, the orbital part of the wave function is antisymmetric and the orbital momentum takes the odd numbers ($l = 1$, p -wave, $l = 3$, f -wave and $l = 5$, h -wave). Here, the terms s -wave, p -wave and *etc* have been used from the terminology of the Hydrogen atom. The pairing state of a spin-triplet superconductor in the spin space is represented by a three dimensional vector $\mathbf{d}(\hat{\mathbf{k}})$, called gap vector. The gap vector determines the order parameter matrix, $\hat{\Delta}(\mathbf{k}) = i(\mathbf{d}(\mathbf{k}) \cdot \hat{\sigma})\hat{\sigma}_y$, in which $\hat{\sigma}_j$ s are Pauli matrices.

Three complex components of gap vector (d_1 , d_2 , d_3) over the Fermi surface are corresponding to three possible spin directions as follow: $|spin\rangle = (d_1 + id_2) \Downarrow$

$\rangle + (-d_1 + id_2)|\uparrow\uparrow\rangle + d_3(|\uparrow\downarrow\rangle + |\downarrow\uparrow\rangle)$. There are many experimental and theoretical works in the case of spin-triplet superconductors from which some important properties of spin-triplet superconductors are listed below:

- 1) The spin-triplet superconductors are generally low T_c superconductors, as compared with the high T_c superconductivity in d -wave superconductors [5, 6, 7].
- 2) The relation between critical temperature and energy gap at zero temperature is different from that of the BCS relation for a s -wave superconductor $\Delta(T = 0) > 1.76T_c$ [8, 9].
- 3) In structures with spin-triplet superconductivity a spin supercurrent can flow generally, while in the case of the spin-singlet superconductivity, the spin current may exist only in the proximity system of the superconductor and a ferromagnet. This means that in the spin-triplet superconductors not only the charge but also the spin of electrons can become superfluid [10, 11, 12].
- 4) Ferromagnetic superconductivity is another interesting phenomenon of spin-triplet state. It had been observed that all conventional superconductors were non-magnetic materials and it was concluded that superconductivity and ferromagnetism are incompatible phases. While, ferromagnetic superconductivity has been observed recently, in some of the triplet superconductors like: $ZrZn_2$, UGe_2 and $URhGe_2$ [13, 14].
- 5) Nonunitary gap vector is another fingerprint of the spin-triplet superconductivity. In the nonunitary spin-triplet state, Cooper pairs may carry a finite averaged intrinsic spin momentum. This nonunitary state is a candidate for the B -phase of superconductivity in the UPt_3 compound (Fig.3). This phase has been observed at the low temperatures and low magnetic fields [15, 16].
- 6) In addition to the temperature and magnetic field, pressure influences the phase transition of triplet superconductors, particularly for the ferromagnetic superconductors [17, 18].
- 7) Another property of some of triplet superconductors is the similarity of their structures with some of the important high T_c superconductors. For example, the Sr_2RuO_4 spin-triplet superconductor is isostructural to the spin-singlet high-temperature superconductor $LaBaCuO$. Here, Sr and Ru atoms are counterpart of $La(Ba)$ and Cu atoms, respectively. Consequently, investigation of this triplet superconductor helps to understand the singlet case [5].

We have to introduce some of unconventional superconducting compounds, particularly those which will be investigated in the following chapters of this work. The uranium compound UPt_3 will be studied in chapter (4) and (6). Then, Sr_2RuO_4 and $PrOs_4Sb_{12}$ compounds will be investigated in chapters (4) and (5), respectively.

The first discovered triplet order parameter, p -wave pairing symmetry, has been observed in the Helium superfluid. Also, p -wave order parameter has been considered as a candidate for the superconducting state in Sr_2RuO_4 by some authors [19, 20]. A famous form of p -wave pairing symmetry in momentum space is $\mathbf{d}(T, \mathbf{k}) = \Delta(T)(k_x + ik_y)\hat{\mathbf{z}}$ in which, $\hat{\mathbf{z}}$ is a unit vector [6]. Another important category of triplet

superconductors is f -wave superconductivity, proposed for the pairing symmetry in heavy-fermion compound UPt_3 in [21, 22] and the compound Sr_2RuO_4 in [5, 23]. The different phases of f -wave superconductivity have different order parameter symmetries in momentum space. For instance, the f -wave axial state symmetry is $\mathbf{d}(T, \hat{\mathbf{k}}) = \Delta_0(T)\hat{\mathbf{z}}k_z(k_x + ik_y)^2$ [24] and the planar state has the form $\mathbf{d}(T, \hat{\mathbf{k}}) = \Delta_0(T)k_z(\hat{\mathbf{x}}(k_x^2 - k_y^2) + \hat{\mathbf{y}}2k_xk_y)$, where, $\hat{\mathbf{x}}$, $\hat{\mathbf{y}}$ and $\hat{\mathbf{z}}$ are the unit vectors [15]. In this work, a nonunitary f -wave gap vector in the B -phase of superconductivity (low temperature and low magnetic field) in UPt_3 compound has been considered. For this nonunitary bipolar state, a gap vector of the form $\mathbf{d}(T, \mathbf{v}_F) = \Delta_0(T)k_z(\hat{\mathbf{x}}(k_x^2 - k_y^2) + \hat{\mathbf{y}}2ik_xk_y)$ has been proposed in the momentum space in [15]. A recently proposed spin-triplet state is the “ $(p + h)$ -wave” pairing symmetry which, has been considered for the superconductivity in $PrOs_4Sb_{12}$ compound in [8]. Of course, two different phases of “ $(p + h)$ -wave” have been observed for superconductivity in the $PrOs_4Sb_{12}$ [25, 26]. Here, A -phase is high magnetic field, high temperature phase but B -phase is low field, low temperature phase [27]. The first model to explain the properties of the A -phase of $PrOs_4Sb_{12}$ is: $\mathbf{d}(T, \hat{\mathbf{k}}) = \Delta_0(T)(k_x + ik_y)\frac{3}{2}(1 - \hat{k}_x^4 - \hat{k}_y^4 - \hat{k}_z^4)\hat{\mathbf{z}}$, where, $\hat{\mathbf{z}}$ is a unit vector. The function $\Delta_0 = \Delta_0(T)$ describes the dependence of the gap vector \mathbf{d} on the temperature T [8]. The second model to describe the gap vector of the B -phase of $PrOs_4Sb_{12}$ is: $\mathbf{d}(T, \hat{\mathbf{k}}) = \Delta_0(T)(k_x + ik_y)(1 - \hat{k}_z^4)\hat{\mathbf{z}}$ [8]. One of the most important types of unconventional superconductivity has been observed in the high T_c superconductor in the ceramic of copper oxide by Bednorz and Müller [28]. This spin-singlet superconductor has a d -wave pairing symmetry, $l = 2$, as $\Delta(\hat{\mathbf{k}}) = \Delta(T)(k_x^2 - k_y^2)$ or $\Delta(\hat{\mathbf{k}}) = \Delta(T)2k_xk_y$, in momentum space. This discovery was a real revolution in the field of superconductivity.

Conventional and unconventional superconductors are usually differentiated by several properties such as anisotropy of the order parameter in the momentum space, heat capacity and heat conductance, density of states, junction behavior and particularly nodes in the momentum space. Node is a direction in the momentum space where no order parameter and superconductivity is effective on the scattering electrons.

One of the most interesting concepts in the field of superconductivity is, superconducting weak link. The weak link experiments are classified in the categories of $S - I - S$, $S - N - S$ and $S - c - S$, in which two superconducting bulks have been separated by a nonsuperconducting interface or point-contact. Here, S , I , N and c denote superconductor, insulator, normal metal and point-contact respectively. The weakness of the link means that the superconducting order parameters are the same as the disconnected massive superconducting bulks. The first configuration had been investigated by Josephson, in which a thin insulator is located between the two superconducting bulks. In the second case, a normal layer has been sandwiched by two superconducting bulks. The third experiment is devoted to the geometry consisting two superconducting bulks which are separated by an impenetrable interface (strong insulator) in which a contact has been prepared for the mixing of two superconducting states. Josephson effect, $S - I - S$, has been investigated in 1962 by Josephson

[29]. He predicted an electrical current flowing between two superconductors while they are separated by an insulator. This insulator layer is very thin and electrons can pass through it, even with the energies less than height of potential barrier of insulator. The flow of current between the superconductors in the absence of an applied voltage is called a Josephson current (there is a phase difference instead of the applied voltage) and the motion of electrons across the barrier is called Josephson tunneling. This tunneling phenomenon, Josephson effect, can be used in the electronic devices such as superconducting quantum interference device (**SQUID**), for detecting the very small magnetic flux (even a flux quantum). The Josephson effect can be influenced by the external magnetic fields through the external phase difference. Consequently, the Josephson junction can be applied to measure the extremely weak magnetic fields, in **SQUID**. The current which flows, (quantum mechanically tunnels through the potential barrier of the interface, has a form $j(\phi) = j_c \sin \phi$ in which, ϕ is the macroscopic phase difference between two superconductors and the critical current j_c depends on the geometry of system (junction). The Josephson effect is a weak link of two massive banks of superconductor, S_1 and S_2 with different phases ϕ_1 and ϕ_2 which are separated by an insulator. The system allows electron to exchange between the two sides of the interface and then establishes the phase coherence in the system as a hole. The Josephson junction can be considered as the mixer between the superconducting quantum macroscopic states. The result of mixing is the supercurrent which flows from one of the banks to the other and it depends on the phase difference $\phi = \phi_2 - \phi_1$ across the weak link. The function $j(\phi)$ depends on the geometry of the system. In the simplest case which had been studied by Josephson, the current has a sinusoidal dependence on the phase but there are many different kinds of the weak links in which the current phase diagrams are not sinusoidal. One of the most famous problems in this category is problem of Kulik-Omelyanchouk ($S - c - S$ junction) which has been investigated in [30]. They have used the Eilenberger equation [31] and using the Green function they have obtained the current-phase diagrams analytically. The current phase relation depends not only on the manner of coupling but also on the properties of the superconducting bulks. Two coupled unconventional superconducting massive bulks have totally different current-phase relation from the conventional superconductivity which was studied by Josephson and later by Kulik and Omelyanchouk. For instance $D - c - D$ weak link which is a special type of $S - c - S$ system, in which D denotes the d -wave and high T_c superconducting bulks and c is the contact, has some new results. The spontaneous current parallel to the junction interface, mid-gap states resulting from the sign change of the order parameter, and the changing period of current $j(\phi)$ to $j(2\phi)$ are different and new results of weak link between unconventional superconducting bulks. In addition, it is observed that the Josephson junction depends not only on the external Josephson phase difference resulting from the external magnetic flux but also on the misorientation angle between two superconducting crystals. In this work, because of similarity between our problem and problem of Kulik-Omelyanchouk, we use the generalized form of their formalism.

This thesis consists of three parts. At first, we are to investigate coherent current

states in the superconducting weak link which has been subjected to the Josephson phase difference ϕ and subjected to the external transport supercurrent state (parallel to the junction interface) in the banks. Earlier it had been observed that at ϕ close to π the mixing of current states produces two vortices in the vicinity of the point-contact between superconducting bulks [32]. In this part we study the effect of transparency coefficient (potential barrier) of the point-contact in an impenetrable interface and effect of temperature on the vortices obtained in the paper [32].

The second part of this dissertation is devoted to the weak link between unitary triplet superconductors. These superconductors have f -wave and $p + h$ -wave pairing symmetry. The former has been proposed for UPt_3 and Sr_2RuO_4 compounds and the later case is considered in $PrOs_4Sb_{12}$ complex. The spin-current in the junction between these unitary triplet superconductors is an important part of this work. The interesting case which is observed in the second part of the thesis, is the polarization of the spin transport using the junction between unitary triplet superconducting bulks. The third and last part of the thesis discusses the case of weak link between non-unitary triplet superconductors. The idea behind the first part of the thesis is suitability of this structure (vortex-like currents) for the investigation of the quantum macroscopic phenomena. For the real system the finite transparency coefficient (finite reflection) which we have investigated is more suitable than ideal transparent point-contact which had been considered in [32]. The second part of the thesis discusses the case of the junction between unitary triplet f -wave and $p + h$ -wave superconductors. First of all we know that the triplet superconductors also the high T_c superconductors are created by a different mechanism of pairing than the phonon-electron interaction. Secondly, the molecular structure of the Ruthenate compound Sr_2RuO_4 is the same as that of the high T_c Cupperate superconductors which are important superconductors and we are interested to understand their properties. Also, the spin polarized transport has a valuable motivation for physicist in the field of spintornics because, the sensitivity and accuracy of the polarized spin-current systems can be used in the measurement technology. The second part of this work can be used to develop the theory of spin-polarized transport systems. The spin transport in the absence of the charge transport is an interesting case to investigate. The third part of the work has been devoted to non-unitary weak links which has intrinsic spin and angular momentum of systems.

The method for investigation of these weak link experiments is the quasiclassical method of Green function. This method had been used by Kulik and Omelyanchouk in paper [30]. They have studied junction through the point-contact between two static conventional superconducting bulks, but, here we have applied this formalism for the case of conventional superconducting bulks with the external transport current in the banks. Also, we have generalized the Kulik-Omelyanchouk formalism for the case of triplet superconducting bulks. We have calculated the analytical Green's function and then we have used that to obtain the current density. The current-phase diagrams are plotted and in some cases the two dimensional profile of the current has been plotted in the space.

Arrangement of the rest of this thesis is as follows. In Chapter (2), we review of the concepts which we use in the rest of the thesis. The quasiclassical approach which is widely used in the field of solid state physics and specially for the case of superconducting systems, will be reviewed. The Kulik-Omelyanchouk problem, that is the ballistic point contact between two superconducting massive bulks will be studied and their results will be reproduced. The effect of transparency coefficient for a point contact with finite reflection in the impenetrable interface between two bulks (related to our problem in the chapter (3)) will be investigated and some analytical relations for this system will be obtained. The Josephson junction between two unitary superconductors will also be studied in chapter (2). We will generalize this approach in the Chapters (4), (5) and (6).

A Josephson effect in the ballistic point contact with transport current on the banks, taking into account the reflection of electrons from the contact, will be investigated in Chapter (3). The contact is subject to the phase difference ϕ and the transport current tangential to the boundary of the contact. As it was shown in [32], in the contact with direct conductivity at $\phi = \pi$ and near the orifice the tangential current flows in the opposite direction to the transport current, and there are two vortices. It is found that by decreasing the transparency, the vortex-like current will be destroyed. On the other hand, as the temperature is increased the vortices are restored. They continue to exist for transparencies as low as $D = \frac{1}{2}$ in the limit of $T \rightarrow T_c$. This anomalous temperature behavior of the vortices is an interesting result which have been obtained.

In Chapter (4), we have studied the spin and charge current in the ballistic Josephson junction in the model of an ideal transparent interface between two misorientated f -wave superconductors subjected to a phase difference ϕ . Our analysis has shown that the misorientation and different models of the gap vectors influence the spin current. The misorientation changes strongly the critical values of both the spin current and charge current. It has been shown that the spin current is the result of the misorientation between the gap vectors. Furthermore, it is observed that the different models of the gap vectors and geometries can be applied to the polarization of the spin transport. In addition, it is observed that in certain values of the phase difference ϕ , the charge-current vanishes while the spin-current flows, despite the fact that although the carriers of spin and charge are the same (electrons).

A stationary Josephson junction as a weak link between $PrOs_4Sb_{12}$ triplet superconductors will be investigated in Chapter (5). Recently, the “ $(p + h)$ -wave” form of pairing symmetry has been proposed for the superconductivity in $PrOs_4Sb_{12}$ compound [25]. The quasiclassical Eilenberger equations are analytically solved for this system. The spin and charge current-phase diagrams are plotted and the effect of misorientation between crystals on the spin current, and spontaneous and Josephson currents is studied. It is found that such experimental investigations of the current-phase diagrams can be used to test the pairing symmetry in the above-mentioned superconductors. Also, it is shown that this apparatus can be applied as a polarizer for the spin current.

In Chapter (6), a stationary Josephson effect in a weak link between misorientated nonunitary triplet superconductors is studied. The non-self-consistent quasiclassical Eilenberger equation for this system has been solved analytically and the current-phase diagrams are plotted for the junction between two nonunitary bipolar f -wave superconducting banks. A spontaneous current parallel to the interface between superconductors has been observed. Also, the effect of misorientation between crystals on the Josephson and spontaneous currents is studied. Such experimental investigations of the current-phase diagrams can be used to test the pairing symmetry in the above-mentioned superconductors. In Chapter (7), the thesis will be finished with some conclusions.

2. Superconducting weak links

When two superconducting bulks are connected to each other by an insulator from which the electrons can tunnel, we have a weak link. The weakness of the link means that the superconducting order parameters have their value in the bulks and they are the same as the disconnected massive superconducting reservoirs. The Josephson effect arises in a weak link of two separated (by insulator) superconducting bulks with different phases. The electrons can be exchanged between two superconducting bulks and the system (two bulks and contact) tends to be the phase coherent. Mixing the superconducting states through the contact or link causes the supercurrent from one of the banks to the other bank. The current is present because of the phase difference between the bulks and this phenomenon can be observed in the absence of any voltage. The phase difference between the bulks which plays a central role in the weak link phenomena can be the result of the external magnetic field which is surrounded by the junction and bulks. The Josephson phase is a kind of the Aharonov-Bohm phase [33]. This phase is related to the magnetic flux which flows from the system as $\phi = \frac{2\pi}{\Phi_0} \oint \mathbf{A} \cdot d\mathbf{l}$, where, $\Phi_0 = \frac{hc}{2e}$ is the quantum of flux and \mathbf{A} is the vector potential. The current in the junction which is a supercurrent and is called Josephson current can be calculated from $j_J = \frac{2e}{\hbar} \frac{\partial E}{\partial \phi}$, in which, the E is the energy of the junction. In the next sections we review some of these weak link experiments analytically. The quasiclassical Eilenberger equations have been used to investigate these weak link systems in this thesis. This method will be explained in Sec.2.1. In Sec.2.2 as an application of the quasiclassical Eilenberger equation, we solve the problem of a conventional superconducting bulk without any contact. These results are exactly the same of results of the standard BCS formalism which can be exerted directly on the uniform bulk system. Sec.2.2 is devoted to the Kulik-Omelyanchouk problem and at the end of this section we have generalized this method to a system of a contact with finite transparency, which is the Zaitsev problem [34]. This problem is as same as our problem in Chapter(3). In Sec.2.3 we have a review in the case of the junction between unitary f -wave superconductors which had been done in paper [6].

2.1. Quasiclassical approach

The normal metals and superconductors can be investigated using the Green functions [35]. It has been shown by Eilenberger that Gorkov equations for the Green function can be transformed to transport-like equations for a quasiclassical Green function [31]. These are called Eilenberger equations. Two conditions for applicability of the quasiclassical approach are that the characteristic length scales should be much larger than the Fermi wavelength and energies must be much lower than the Fermi energy $\varepsilon_F = T_F$, hereafter $k_B = 1$ and $\hbar = 1$ for simplicity. The Green functions which will be used in our work, are Matsubara Green functions written in Nambu space. They are 4×4 matrices in a direct-product space of particle-hole and spin spaces. The general energy integrated Green function in \mathbf{k} -space is of the form $\check{g}(\hat{\mathbf{k}}, \mathbf{r}, \varepsilon_m)$. Here $\varepsilon_m = \pi T(2m + 1)$ are the discrete Matsubara energies $m = 0, 1, 2, \dots$. The odd integer value of $(2m + 1)$ is the

result of Fermion behavior of electrons [36]. Finally, the Eilenberger equation a ballistic case (there is no scattering) is as follows:

$$\mathbf{v}_F \cdot \nabla \check{g} + [\varepsilon_m \check{\sigma}_3 + i\check{\Delta}, \check{g}] = 0, \quad (1)$$

where, \mathbf{v}_F is the Fermi velocity and $\check{\sigma}_3 = \hat{\sigma}_3 \otimes \hat{I}$ in which $\hat{\sigma}_j$ ($j = 1, 2, 3$) are Pauli matrices. This is a first-order differential equation for the Matsubara propagator $\check{g}(\hat{\mathbf{k}}, \mathbf{r}, \varepsilon_m)$ along classical trajectories of quasiparticles. The Eilenberger equation is not enough to make the solution unique and so, a separate normalization condition has to be introduced [31]. With a suitable choice of condition satisfied by physical solutions of Eilenberger equation, normalization is written as $\check{g}\check{g} = \check{1}$. To give a closed system of Eilenberger equations and normalization conditions it should be supplemented by some self-consistency equations for the self-energy $\check{\Delta}$ which will be introduced later in suitable forms. Finally, the Matsubara propagator \check{g} which satisfies the Eilenberger equation, normalization condition, continuity across the interfaces and self-consistency condition can be written in the form [37]:

$$\check{g} = \begin{pmatrix} g_1 + \mathbf{g}_1 \cdot \hat{\sigma} & (g_2 + \mathbf{g}_2 \cdot \hat{\sigma}) i\hat{\sigma}_2 \\ i\hat{\sigma}_2 (g_3 + \mathbf{g}_3 \cdot \hat{\sigma}) & i\hat{\sigma}_2 (-g_4 + \mathbf{g}_4 \cdot \hat{\sigma}) i\hat{\sigma}_2 \end{pmatrix}, \quad (2)$$

where, the matrix structure of the off-diagonal self energy $\check{\Delta}$ in the Nambu space is

$$\check{\Delta} = \begin{pmatrix} 0 & (\Delta + \mathbf{d} \cdot \hat{\sigma}) i\hat{\sigma}_2 \\ i\hat{\sigma}_2 (\Delta^* + \mathbf{d}^* \cdot \hat{\sigma}) & 0 \end{pmatrix}. \quad (3)$$

The $\Delta(\hat{\mathbf{k}}) = \Delta(-\hat{\mathbf{k}})$ refers to the spin-singlet but the $\mathbf{d}(\hat{\mathbf{k}}) = -\mathbf{d}(-\hat{\mathbf{k}})$ has been considered for the case of spin-triplet superconductivity. Fundamentally, the gap (order parameter) has to be determined numerically from the self-consistency equation, while in some cases, we use a non-self-consistent model for the gap which is much more suitable for an analytical calculation. The solution of Eq. (1) allows us to calculate the current densities. The expression for current is:

$$\mathbf{j}(\mathbf{r}) = 4\pi i e T N(0) \sum_{m>0} \langle \mathbf{v}_F g_1(\hat{\mathbf{v}}_F, \mathbf{r}, \varepsilon_m) \rangle_{\mathbf{v}_F} \quad (4)$$

where, $\langle \dots \rangle_{\mathbf{v}_F}$ stands for averaging over the directions of an electron momentum on the Fermi surface and $N(0)$ is the electron density of states at the Fermi level of energy. For the case of the s -wave superconductors our Green matrix changes to a matrix as follows:

$$\check{g} = \begin{pmatrix} g_1 & g_2 i\hat{\sigma}_2 \\ i\hat{\sigma}_2 g_3 & -g_1 \end{pmatrix}, \quad (5)$$

and for the case of the order parameter we have:

$$\hat{\Delta} = \begin{pmatrix} 0 & \Delta i\hat{\sigma}_2 \\ i\hat{\sigma}_2 \Delta^* & 0 \end{pmatrix}. \quad (6)$$

The selfconsistent equation for the spin-singlet case is

$$\Delta(\mathbf{r}, T) = 2\pi\lambda T \sum_{m>0} \langle g_2(\mathbf{v}_F, \mathbf{r}) \rangle_{\mathbf{v}_F} \quad (7)$$

where λ is the electron-phonon constant of interaction and $\langle \dots \rangle_{\mathbf{v}_F}$ is the averaging over directions of \mathbf{v}_F . The other important physical variable which can be derived from this Green function is the density of states. It is related to the diagonal term of the Green matrix as follows:

$$N(E) = N(0) \text{Re}[g_1(\varepsilon_m \rightarrow -iE + 0)] \quad (8)$$

There are many applications of quasiclassical method and in this chapter some of them will be reviewed.

2.2. Superconducting bulks

The simplest case of superconducting system which can be investigated by Eilenberger equation is a single bulk of superconductors without any contact or interaction with other world. In this system all of superconductivity properties are uniform and spatially constant. Because of the uniform properties the gradient term in Eilenberger equation (1) is zero,

$$\left[\varepsilon_m \check{\sigma}_3 + i\check{\Delta}, \check{g} \right] = 0 \quad (9)$$

and the bulk solutions are:

$$g_1 = \frac{\varepsilon_m}{\sqrt{\varepsilon_m^2 + |\Delta|^2}} \quad (10)$$

and

$$g_2(g_3) = \frac{i\Delta(i\Delta^*)}{\sqrt{\varepsilon_m^2 + |\Delta|^2}}, \quad (11)$$

respectively. In conclusion of Eq. (8), the density of states for $|E| \gg |\Delta|$ is as follows:

$$N(E) = \frac{E}{\sqrt{E^2 - |\Delta|^2}}, \quad (12)$$

while for $|E| \leq |\Delta|$ is $N(E) = 0$. This expression has been obtained before from the BCS theory directly and using the particle-hole analysis of a bulk of superconductor. Also, the self-consistent equation for this system is:

$$\Delta(T) = 2\pi\lambda T \sum_{m>0} \frac{\Delta(T)}{\sqrt{\varepsilon_m^2 + |\Delta(T)|^2}} \quad (13)$$

which is the same to the BCS self consistent equation. This latter had been obtained from the second quantization and quantum field theory method. This simple self-consistent equation only can be solved numerically, but near the $T = 0$ and $T = T_c$ it has been solved analytically. Close to the zero temperature the gap function varies in terms of temperature as:

$$\Delta(T) = \Delta(0) - \sqrt{2\pi T \Delta(0)} \exp(-(\Delta(0)/T))$$

and near the $T = T_c$ the gap dependence on the temperature is as follows:

$$\Delta(T) = \left(\frac{8\pi^2}{3\zeta(3)} \right)^{\frac{1}{2}} \sqrt{T_c(T_c - T)}.$$

Also, for the case of the gap function at the $T = 0$ we have $\Delta(0) \simeq 1.76T_c$. So, the current density for this system can be calculated as follows:

$$\langle \mathbf{v}_F \rangle = 0 \Rightarrow \mathbf{j}(\mathbf{r}) = 4\pi ieTN(0) \sum_{m>0} \langle \mathbf{v}_F \rangle \frac{\varepsilon_m}{\sqrt{\varepsilon_m^2 + |\Delta|^2}} = 0. \quad (14)$$

As it is clear from the above expression, the current density for the homogenous superconducting bulks is zero.

2.3. Kulik-Omelyanchouk problem: superconducting weak link through a point contact

We consider the Josephson $S - c - S$ weak link as a microbridge between thin superconducting films of thickness $2a$ (look at Fig.1). The length L and width d of the microbridge, are assumed to be less than the coherence length ξ_0 . On the other hand, we assume that L and $2a$ are much larger than the Fermi wavelength λ_F and use the quasiclassical approach. The point-contact is an ideal transparent area for the electrons and there is not any reflection for the electron. We choose the \mathbf{z} -axis along the interface and the \mathbf{y} -axis perpendicular to the boundary; $y = 0$ is the boundary plane (Fig.1). If the film thickness $d \ll \xi_0$ then in the main approximation in terms of the parameter d/ξ_0 the superconducting current depends on the coordinates in the plane of $\rho = (z, y)$. The open form of the Eilenberger equation for the case of spin-singlet superconducting systems is as follows:

$$\eta \frac{\partial g_{1(n)}}{\partial t} + i\Delta_n^* g_{2(n)} - i\Delta_n g_{3(n)} = 0; \quad (15)$$

$$\eta \frac{\partial g_{2(n)}}{\partial t} + 2\varepsilon_m g_{2(n)} - 2i\Delta_n g_{1(n)} = 0; \quad (16)$$

$$\eta \frac{\partial g_{3(n)}}{\partial t} - 2\varepsilon_m g_{3(n)} + 2i\Delta_n^* g_{1(n)} = 0; \quad (17)$$

where, $t = y/|v_y|$ on the Fermi surface, $\eta = \mathbf{sgn}(v_y)$ and $n = 1, 2$ label the left and right hand superconducting bulks, respectively. Using the quasiclassical approximation, we select the solution the for this problem as follows:

$$g_{1(n)} = \frac{\varepsilon_m}{\Omega} + a_n \exp(-2s\Omega t); \quad (18)$$

$$g_{2(n)} = \frac{i\Delta_n}{\Omega} + b_n \exp(-2s\Omega t); \quad (19)$$

$$g_{3(n)} = \frac{i\Delta_n^*}{\Omega} + d_n \exp(-2s\Omega t); \quad (20)$$

where, $s = \mathbf{sgn}(y)$ and $\Omega = \sqrt{\varepsilon_m^2 + |\Delta|^2}$. By substituting in the Eilenberger equation (1), we obtain:

$$g_{1(n)} = \frac{\varepsilon_m}{\Omega} + a_n \exp(-2s\Omega t); \quad (21)$$

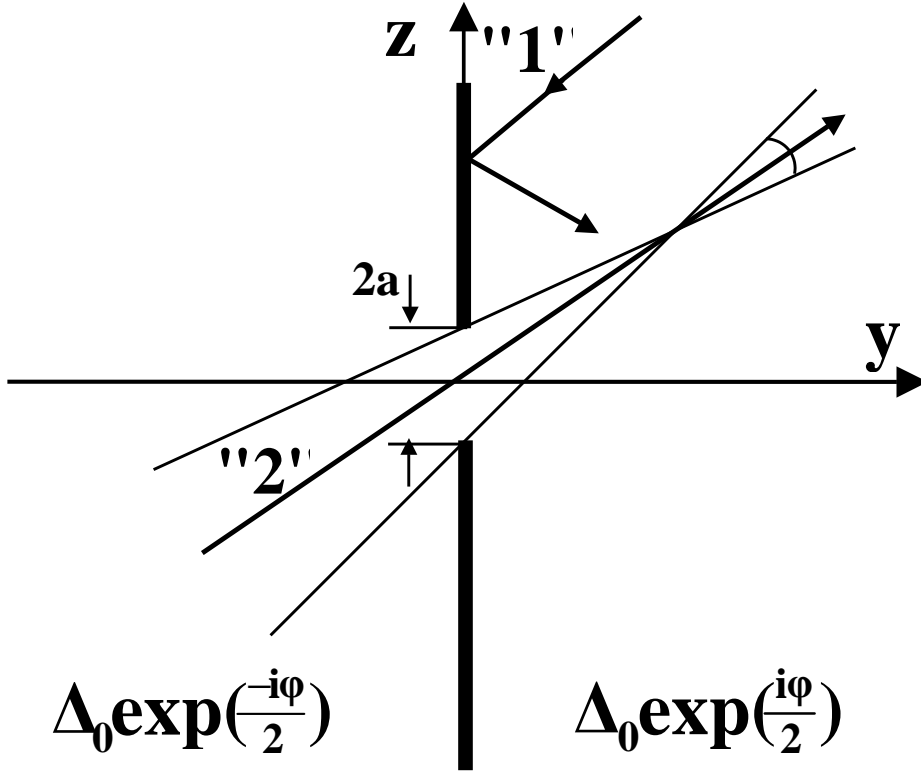


Figure 1. Model of an ideal transparent point-contact as an orifice in the thin impenetrable insulating partition.

$$g_{2(n)} = \frac{i\Delta_n}{\Omega} + a_n \left(\frac{i\Delta_n}{\varepsilon_m - \eta s \Omega} \right) \exp(-2s\Omega t); \quad (22)$$

$$g_{3(n)} = \frac{i\Delta_n^*}{\Omega} + a_n \left(\frac{i\Delta_n^*}{\varepsilon_m + \eta s \Omega} \right) \exp(-2s\Omega t); \quad (23)$$

In the main approximation on the small parameter $a/\xi_0 \ll 1$, the self-consistency can be ignored and the model, in which the order parameter is constant in the two half-spaces

$$\Delta(\mathbf{r}, T) = \Delta(T) \exp\left(\frac{is\phi}{2}\right)$$

in which ϕ is the phase difference between superconductors, can be used. Solutions of Eqs. (1) should satisfy the continuity of solutions across the contact $y = 0, |z| \leq a$ and specular reflection condition for $y = 0, |z| \geq a$. In addition, far from the contact, solutions should coincide with the bulk solutions. Consequently, we find the diagonal term of Green functions which will be used in calculation of the current density, as follows [38]:

$$g_1(y = 0^-) = g_1(y = 0^+) = \frac{\varepsilon_m \cos \frac{\phi}{2} + i\eta\Omega \sin \frac{\phi}{2}}{\Omega \cos \frac{\phi}{2} + i\eta\varepsilon_m \sin \frac{\phi}{2}}. \quad (24)$$

Because of integration over the fermi surface (4) the antisymmetric and imaginary part of Green function remains. It is as follows:

$$\mathbf{Im}(g_1(y=0)) = \frac{\eta|\Delta|^2 \sin \frac{\phi}{2} \cos \frac{\phi}{2}}{\varepsilon_m^2 + |\Delta|^2 \cos \frac{\phi^2}{2}}, \quad (25)$$

and also

$$iT \sum_{m>0} \langle \hat{\mathbf{v}}_F g_1 \rangle = \frac{T}{4} \sum_{m>0} \frac{|\Delta|^2 \sin \phi}{\varepsilon_m^2 + |\Delta|^2 \cos \frac{\phi^2}{2}} = \frac{\Delta(T) \sin \frac{\phi}{2}}{8} \tanh \left(\frac{\Delta(T) \cos \frac{\phi}{2}}{2T} \right) \quad (26)$$

where we have done the angular integration and we have substituted $\langle \mathbf{v}_F \eta \rangle = \frac{1}{2}$ and $\frac{\pi}{4x} \tanh \frac{\pi x}{2} = \sum_{m>0} \frac{1}{x^2 + (2m+1)^2}$ in the above-mentioned relation. Consequently the current density has an expression as follows [30, 38]:

$$I(\phi) = \frac{\pi}{2} S e \Delta(T) N(0) v_F \sin \frac{\phi}{2} \tanh \left(\frac{\Delta(T) \cos \frac{\phi}{2}}{2T} \right) \quad (27)$$

where, in the case of the low temperatures $T \rightarrow 0$ we have $I(\phi) = \frac{\pi \Delta}{e R_0} \sin \frac{\phi}{2}$ [30] while for $T \rightarrow T_c$ we obtain $I(\phi) = \frac{\pi \Delta}{2e R_0} \sin \phi$ [39], in which, $R_0^{-1} = \frac{1}{2} e^2 S N(0) v_F$ is the Sharvin resistance of the junction in the normal state [40] and S is the effective square of the contact. This means that near the critical temperature current-phase relation is sinusoidal like Josephson prediction, while in the low temperatures the current-phase relation is non-sinusoidal and we have some unusual jumps at $\phi = \pi$. Now, we want to investigate the effect of transparency coefficient and reflection of point-contact on the current density which has been studied before by Zaitsev [34]. Using the Zaitsev quasiclassical boundary conditions for the case of Matsubara Green function we have obtained:

$$\mathbf{Im}(g_1(y=0)) = \frac{D \eta |\Delta|^2 \sin \frac{\phi}{2} \cos \frac{\phi}{2}}{\varepsilon_m^2 + |\Delta|^2 (1 - D \sin \frac{\phi^2}{2})}, \quad (28)$$

where D is transparency coefficient which is related to the interface physical properties as the potential barrier against our tunneling phenomenon. The transparency coefficient usually depends on the direction of scattering electron velocity, but here for simplicity we use the constant transparency coefficient formalism. The current density exactly at the contact is as follows:

$$I(\phi) = \frac{\pi}{4} S e \Delta(T) N(0) v_F \frac{\sin \phi D}{\sqrt{1 - D(\sin \frac{\phi}{2})^2}} \tanh \left(\frac{\Delta(T) \sqrt{1 - D(\sin \frac{\phi}{2})^2}}{2T} \right). \quad (29)$$

Obviously, for the low value of transparency coefficient which is called tunneling limit, $D \rightarrow 0$, the current has linear dependence on the transparency and it is a sinusoidal function of phase and we have $I(\phi) = \frac{\pi}{4} S e \Delta(T) N(0) v_F D \sin \phi \tanh \left(\frac{\Delta(T)}{2T} \right)$. So, at the tunneling limit and $T \rightarrow 0$, the current is: $I(\phi) = \frac{\pi}{4} S e \Delta(0) N(0) v_F D \sin \phi$. These two former expressions for current are linear functions of transparency coefficient and sinusoidal functions of phase ϕ . Also in the limit of $T \rightarrow T_c$, the current has the form of: $I(\phi) = \frac{\pi \Delta^2}{8 T_c} S e N(0) v_F \sin \phi D$. This means that at high temperatures the current

is linear function of transparency and has a sinusoidal dependence on the phase. The nonsinusoidal dependence of phase will be happened for both the low temperature and high value of transparency coefficient. Consequently, nonlinearity and nonsinusoidal current-phase relation are coupled with each other. For the density of states using the quasiclassical formalism we obtain:

$$N(E) = N(0) \text{Re}[g_1(\varepsilon_m \rightarrow -iE + 0)] = \frac{E\sqrt{E^2 - \Delta^2}}{E^2 - \Delta^2(1 - D\sin\frac{\phi^2}{2})}. \quad (30)$$

In the limit of $D \rightarrow 1$ we obtain the density of states of the problem of Kulik-Omelyanchouk, $N(E) = N(0)\frac{E\sqrt{E^2 - \Delta^2}}{E^2 - \Delta^2\cos\frac{\phi^2}{2}}$, and in the limit of $D \rightarrow 0$ we have a disconnected system and the density of states for the system tends to the density of states of the bulk, $N(E) = N(0)\frac{E}{\sqrt{E^2 - \Delta^2}}$, as we expect from the BCS theory [35].

2.4. Charge transport in the weak link between unitary and triplet superconductors

In this section we theoretically study the stationary Josephson effect in a small ballistic junction between two spin-triplet superconducting bulks with different orientations of the crystallographic axes. We consider a model of a ballistic point contact as an orifice with a diameter $2a$ in an impenetrable for electrons partition between two superconducting half spaces. We assume that the thickness of interface, d , is much larger than the Fermi wavelength and use the quasiclassical approach. In order to calculate the charge current in point contact we use Eilenberger equations (1) and the normalization condition $\check{g}\check{g} = \check{1}$. For the case of the unitary and pure spin-triplet superconductivity, the Green function matrix (2) is written in the form [6, 37]:

$$\check{g} = \begin{pmatrix} g_1 + \mathbf{g}_1 \cdot \hat{\sigma} & i\mathbf{g}_2 \cdot \hat{\sigma} \hat{\sigma}_2 \\ i\hat{\sigma}_2 \mathbf{g}_3 \cdot \hat{\sigma} & g_4 - \hat{\sigma}_2 \mathbf{g}_4 \cdot \hat{\sigma} \hat{\sigma}_2 \end{pmatrix}. \quad (31)$$

Matrix structure of the off-diagonal self energy $\check{\Delta}$ in Nambu space is

$$\check{\Delta} = \begin{pmatrix} 0 & \hat{\Delta} \\ \hat{\Delta}^\dagger & 0 \end{pmatrix} = \begin{pmatrix} 0 & i\mathbf{d} \cdot \hat{\sigma} \hat{\sigma}_2 \\ i\hat{\sigma}_2 \mathbf{d}^* \cdot \hat{\sigma} & 0 \end{pmatrix}, \quad (32)$$

Also, we have:

$$\hat{\Delta}(\mathbf{k}) = i\mathbf{d}(\mathbf{k}) \cdot \hat{\sigma} \hat{\sigma}_2 = \begin{pmatrix} id_2 - d_1 & d_3 \\ d_3 & id_2 + d_1 \end{pmatrix}. \quad (33)$$

Below we consider a unitary states, for which $\mathbf{d} \times \mathbf{d}^* = 0$. Solutions of Eq. (1) must satisfy the conditions for Green functions and vector \mathbf{d} in the bulks of superconductors far from the orifice:

$$\check{g}(\mp\infty) = \frac{\varepsilon_m \check{\tau}_3 + i\check{\Delta}_{1,2}}{\sqrt{\varepsilon_m^2 + |\mathbf{d}_{1,2}|^2}}; \quad (34)$$

$$\mathbf{d}(\mp\infty) = \mathbf{d}_{1,2}(\hat{\mathbf{k}}) \exp\left(\mp\frac{i\phi}{2}\right), \quad (35)$$

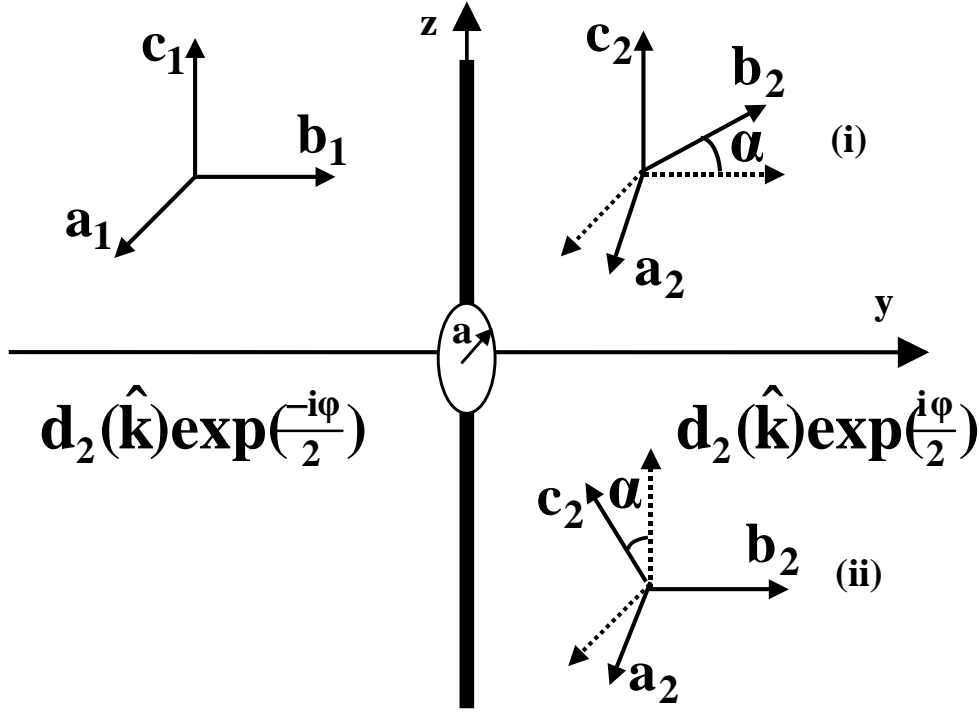


Figure 2. Scheme of an ideal transparent point-contact in an impenetrable flat interface between two superconducting bulks, which are misorientated as much as α .

where ϕ is the external phase difference. Eq. (1) has to be supplemented by the continuity of solutions at the contact plane ($|y| \leq a$) and conditions of reflection at the interface between superconductors, remainder part of the interface ($|y| > a$). Below we assume that this interface is smooth and electron scattering is negligible. The solution of Eq. (1) should be used to calculate the current density. We consider a simple model of the constant order parameter up to the surface. We assume that the order parameter does not depend on the coordinates and in each half-space equals to its value far from the point contact which is called superconducting massive bulk. For this non-self-consistent model the current-phase dependence of a Josephson junction can be calculated analytically. In a ballistic case, the system of 13 equations for functions g_i and \mathbf{g}_i can be decomposed on independent blocks of equations. The set of equations which enables us to find the Green functions are:

$$\eta \frac{\partial g_1}{\partial t} + i(\mathbf{g}_2 \mathbf{d}^* - \mathbf{g}_3 \mathbf{d}) = 0; \quad (36)$$

$$\eta \frac{\partial \mathbf{g}_-}{\partial t} + (\mathbf{d} \times \mathbf{g}_3 + \mathbf{d}^* \times \mathbf{g}_2) = 0; \quad (37)$$

$$\eta \frac{\partial \mathbf{g}_2}{\partial t} + \varepsilon_m \mathbf{g}_2 - i g_1 \mathbf{d} - \mathbf{d} \times \mathbf{g}_- = 0; \quad (38)$$

$$\eta \frac{\partial \mathbf{g}_3}{\partial t} - \varepsilon_m \mathbf{g}_3 + i g_1 \mathbf{d}^* - \mathbf{d}^* \times \mathbf{g}_- = 0; \quad (39)$$

where $\mathbf{g}_- = \frac{\mathbf{g}_1 - \mathbf{g}_4}{2}$, $t = y/|v_y|$ on the Fermi surface and $\eta = \mathbf{sgn}(v_y)$. The Eqs. (36)-(39) can be solved by integrating over the ballistic trajectories of electron in the right and left half-spaces. The general solution satisfying the boundary conditions at infinity is:

$$g_1^{(n)} = \frac{\varepsilon_m}{\Omega_n} + a_n \exp(-2s\Omega_n t); \quad (40)$$

$$\mathbf{g}_-^{(n)} = \mathbf{C}_n \exp(-2s\Omega_n t); \quad (41)$$

$$\mathbf{g}_2^{(n)} = \frac{i\mathbf{d}_n}{\Omega_n} - \frac{ia_n\mathbf{d}_n + \mathbf{d}_n \times \mathbf{C}_n}{s\eta\Omega_n - \varepsilon_m} \exp(-2s\Omega_n t); \quad (42)$$

$$\mathbf{g}_3^{(n)} = \frac{i\mathbf{d}_n^*}{\Omega_n} + \frac{ia_n\mathbf{d}_n^* - \mathbf{d}_n^* \times \mathbf{C}_n}{s\eta\Omega_n + \varepsilon_m} \exp(-2s\Omega_n t); \quad (43)$$

where t is the time of the flight along the trajectory, $sgn(t) = \mathbf{sgn}(y) = s$, $\eta = \mathbf{sgn}(v_y)$ and $\Omega_n = \sqrt{\varepsilon_m^2 + |\mathbf{d}_n|^2}$. Index n numbers left ($n = 1$) and right ($n = 2$) half-spaces. By matching the solutions (40-43) at the orifice plane ($y = 0$), we find constants a_n and \mathbf{C}_n . Exactly at the orifice plane we obtain:

$$\frac{\varepsilon_m}{\Omega_1} + a_1 = \frac{\varepsilon_m}{\Omega_2} + a_2; \quad (44)$$

$$\mathbf{C}_1 = \mathbf{C}_2; \quad (45)$$

$$\frac{i\mathbf{d}_1}{\Omega_1} + \frac{ia_1\mathbf{d}_1 + \mathbf{d}_1 \times \mathbf{C}_1}{\eta\Omega_1 + \varepsilon_m} = \frac{i\mathbf{d}_2}{\Omega_2} - \frac{ia_2\mathbf{d}_2 + \mathbf{d}_2 \times \mathbf{C}_2}{\eta\Omega_2 - \varepsilon_m}; \quad (46)$$

$$\frac{i\mathbf{d}_1^*}{\Omega_1} - \frac{ia_1\mathbf{d}_1^* - \mathbf{d}_1^* \times \mathbf{C}_1}{\eta\Omega_1 - \varepsilon_m} = \frac{i\mathbf{d}_2^*}{\Omega_2} + \frac{ia_2\mathbf{d}_2^* - \mathbf{d}_2^* \times \mathbf{C}_2}{\eta\Omega_2 + \varepsilon_m}; \quad (47)$$

Consequently, the function $g_1(0)$ which determines the current density at the contact is as follows:

$$g_1(0) = \frac{\eta [\mathbf{d}_1 \cdot \mathbf{d}_1 (\eta\Omega_2 + \varepsilon_m)^2 - \mathbf{d}_2 \cdot \mathbf{d}_2 (\eta\Omega_1 - \varepsilon_m)^2]}{\mathbf{d}_1 \cdot \mathbf{d}_1 (\eta\Omega_2 + \varepsilon_m)^2 + \mathbf{d}_2 \cdot \mathbf{d}_2 (\eta\Omega_1 - \varepsilon_m)^2 + 2\mathbf{d}_1 \cdot \mathbf{d}_2 (\eta\Omega_1 - \varepsilon_m) (\eta\Omega_2 + \varepsilon_m)}. \quad (48)$$

Using the $g_1(0)$ one can calculate the current density at the orifice plane $\mathbf{j}(0)$:

$$\mathbf{j}(0) = 4\pi e N(0) v_F T \sum_{m=0}^{\infty} \int d^3 k \hat{\mathbf{k}} g_1(0). \quad (49)$$

Misorientation of the crystals produces a spontaneous current along the interface [41, 42] generally, as can be calculated by projecting vector \mathbf{j} at the corresponding direction. To illustrate the results obtained by computing the formula (48), we can plot the current-phase diagrams for the different models of the pairing symmetry and for two different geometries. These geometries are corresponding to the different orientations of the crystals in the right and left sides of the interface (Fig.2). In the right hand side of the interface, the \mathbf{ab} -plane has been rotated around the \mathbf{c} -axis and the \mathbf{c} -axis has been rotated around the \mathbf{b} -axis by α in geometries (i) and (ii), respectively. Also for the further calculations we need to a certain model of the gap vector \mathbf{d} which is called order parameter vector. There are three models which have been successful to explain properties of the three phases of triplet superconductivity in UPt_3 compound (Fig.3). For the high-temperature and low field phase, A-phase, of superconductivity in UPt_3

Superconducting phases in UPt_3

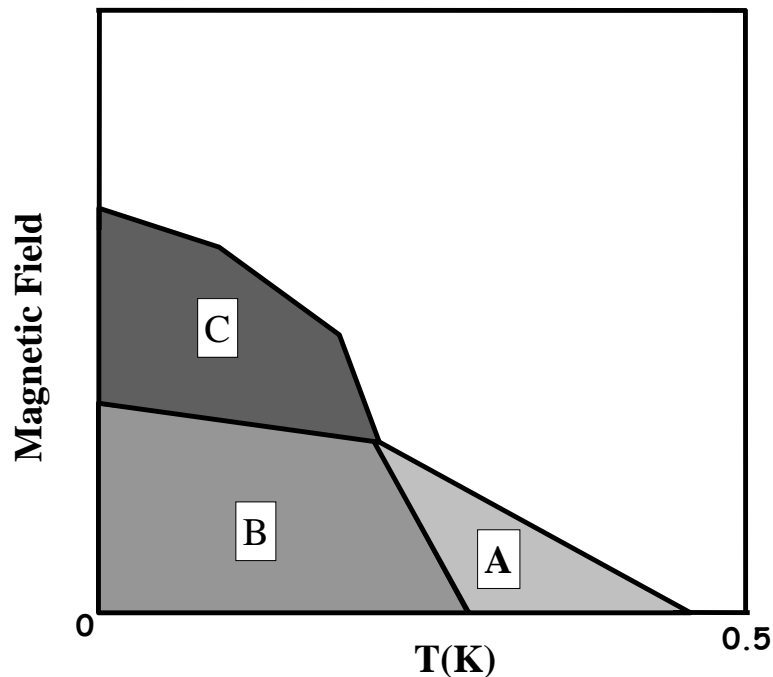


Figure 3. Superconducting phase diagram of heavy fermion UPt_3 compound, in the magnetic field and temperature space.

the order parameter (gap vector) has an equatorial line node and two longitudinal line nodes [6, 15, 16]. This state which is known as the polar state, is as follows:

$$\mathbf{d} = \Delta_0 \hat{z} k_z (k_x^2 - k_y^2). \quad (50)$$

The gap vector dependence in momentum space for the low-temperature and low field phase, B-phase, or the axial state is as follows [6, 15, 16]:

$$\mathbf{d} = \Delta_0 \hat{z} k_z (k_x + ik_y)^2. \quad (51)$$

Here, the longitudinal line nodes are closed and there is a pair of point nodes. The coordinate axes \hat{x} , \hat{y} and \hat{z} are chosen along the crystallographic axes \hat{a} , \hat{b} and \hat{c} as the left of Fig.2. The function $\Delta_0(T)$ describes the dependence of the order parameter \mathbf{d} on the temperature T . Other candidate to describe the orbital states implying the weak effective spin-orbital coupling in the c -phase of superconductivity in UPt_3 compound, is the unitary planar state [6, 15, 16]:

$$\mathbf{d} = \Delta_0 k_z (\hat{x} (k_x^2 - k_y^2) + \hat{y} 2k_x k_y). \quad (52)$$

Using these forms of the triplet order parameters, we can plot the Josephson current-phase relation $j_J(\phi) = j_y(y=0)$ calculated from Eq.49 for a particular value of misorientation angle α under the rotation of \mathbf{ab} -plane, the geometry (i), and rotation around the normal axis \hat{y} or geometry (ii). For simplicity we use the spherical model of

the Fermi surface. The different gap vectors have different current-phase diagrams and such a different behavior can be a criterion for distinguish between the different phases. In some cases, the Josephson current formally does not equal to zero at $\phi = 0$. This state corresponds to a spontaneous phase difference, which depends on the misorientation angle α . The tangential components of current, x and z , as the functions of ϕ are not zero when the Josephson current is zero. This spontaneous tangential current is due to the specific "proximity effect" similar to spontaneous current in contacts between "d-wave" superconductors [42, 43]. The total current is determined by the Green function, which depends on the order parameters in both superconductors. As a result of this, for nonzero misorientation angles the current parallel to the surface can be generated. It can be shown that the current-phase relations are totally different for different models of the gap vector. Because the order parameter phase depends on the momentum direction on the Fermi surface, the misorientation of the superconductors leads to spontaneous phase difference that corresponds to the zero Josephson current and to the minimum of the weak link energy. This phase difference depends on the misorientation angle and can possess any values. It is observed that, in the "f-wave" superconductors the spontaneous current can be generated in a direction parallel to the plane of contact. Generally speaking this current is not equal to zero in the absence of the Josephson current. Finally, study of current-phase diagrams of Josephson junction for different misorientations can be used to distinguish or demonstrate the different phases and different triplet gap vectors of superconductivity UPt_3 .

3. Coherent mixing of Josephson and transport supercurrents

3.1. Introduction

The investigations of Josephson effect manifestations in different systems are continuing due to its importance both for basic science and industry. A point contact between two massive superconductors (S-c-S junction) is one of the possible Josephson weak links. A microscopic theory of the stationary Josephson effect in ballistic point contacts between conventional superconductors was developed in [30]. Later, this theory was generalized for a pinhole model in ^3He [44, 45], for point contacts between "d-wave" [42, 46], and triplet superconductors [6]. The Josephson effect is the phase sensitive instrument for the analysis of an order parameter in novel (unconventional) superconductors, where current-phase dependencies $I_J(\phi)$ may differ essentially from those in conventional superconductors [42, 46]. In some cases the model with total transparency of the point contact does not quite adequately correspond to the experiment, and the electron reflection should be taken into account. The influence of electron reflection on the Josephson current in ballistic point contacts was first considered by Zaitsev [34]. He had shown that reflection from the contact not only changes the critical value of current, but also the current-phase dependence $I_J(\phi) \sim \sin(\phi/2)$ at low temperature which has been predicted in [30]. The current-phase dependence for small values of transparency, $D \ll 1$, is transformed to the $I_J(\phi) \sim \sin \phi$, similar to the planar tunnel junction. The effect of transparency for point contact between unconventional (d-wave) superconductors is studied in the papers [47, 48, 49, 43]. The non-locality of Josephson current in point contacts was investigated in [50]. The authors of [50] concentrated on the influence of magnetic field on the zero voltage supercurrent through the junction. They found an periodic behavior in terms of magnetic flux and demonstrated that this anomalous behavior is a result of a non-locality supercurrent in the junction. This observation was explained theoretically in [51]. In this chapter we want to investigate theoretically the influence of electron reflection on dc Josephson effect in a ballistic point contact with transport current in the right and left banks which are separated by an interface (look at Fig.4). In Ref. [32] for an ideal transparent point-contact in the impenetrable interface, it has been observed that at the phase differences close to the $\phi = \pi$ two antisymmetric vortex-like currents appear (see Fig.8). we want to study the effect of finite transparency (reflection) of the point-contact in the interface, on these vortex-like currents near the contact and at the phase difference $\phi = \pi$. We show that at low temperatures even a small reflection on the contact destroys the mentioned vortex-like current states, which can be restored by increasing of the temperature. In our system which will be investigated in this chapter, a point-contact between two massive superconductors (S-c-S junction) is considered as a possible Josephson weak links. For such systems it is convenient to use Kulik-Omelyanchouk method [30] for the ballistic point-contact. The microscopic theory of the stationary Josephson effect in the ballistic point contacts between conventional superconductors was developed in [30]. Later, this theory was generalized for point-contacts between "d-wave" high- T_c

superconductors in Ref. [42]. The Josephson effect is a phase sensitive instrument for the analysis of an order parameter in novel (unconventional) superconductors, where current-phase dependencies $I_J(\phi)$ may differ essentially from those in conventional superconductors [42, 6]. In some cases the model with ideal transparent point-contact does not correspond to the experiment totally, and the electron reflection should be taken into account. The influence of electron reflection on the Josephson current in ballistic point contacts was first considered by Zaitsev [34]. He had shown that reflection from the contact not only changes the critical value of current, but also the current-phase dependence $I_J(\phi) \sim \sin(\phi/2)$ at low temperature which has been predicted in [30]. The current-phase dependence for small values of transparency, $D \ll 1$, is transformed to the $I_J(\phi) \sim \sin \phi$, similar to the planar tunnel junction. In addition, the non-locality of Josephson current in point contacts was investigated in Ref. [50]. The authors of Ref. [50] concentrated on the influence of magnetic field on the zero voltage supercurrent through the junction. They found an periodic behavior in terms of magnetic flux and demonstrated that this anomalous behavior is a result of a non-locality supercurrent in the junction. This observation was explained theoretically in [51, 52, 53]. Recently an influence of transport supercurrent, which flows in the contacted banks and is parallel to the interface, to the Josephson effect in point contacts has been analyzed theoretically [32]. It was found that a non-local mixing of two superconducting currents results in the appearance of two vortex-like current states in vicinity of the contact, when the external phase difference is $\phi \simeq \pi$. The Josephson current through superconducting weak link is a result of quantum interference between order parameters with phase difference ϕ . Obviously, the finite reflection $R = 1 - D$ of electrons from the Josephson junction suppresses this interference and it must influence the vortex-like current states, which are predicted in [32]. In this chapter, we study the effect of finite transparency on the current-phase dependence and distribution of the superconducting current near the ballistic point contact in the presence of homogeneous current states far from the contact. We show that at low temperatures ($T \rightarrow 0$) the electron reflection destroys the mentioned vortex-like current states even for a very small value of reflection coefficient $R \ll 1$. On the other hand we have found that, as the temperature increases the vortices are restored and they exist for transparency as low as $D = \frac{1}{2}$ in the limit of $T \rightarrow T_c$. The arrangement of the rest of this chapter is as follows. In Sec.(3.2) we describe the model of the point contact, quasiclassical equations for Green functions and boundary conditions. The analytical formulas for the Green functions are derived for a ballistic point contact with arbitrary transparency. In Sec.(3.3) we apply them to analyze a current state in the ballistic point contact. The influence of the transport current on the Josephson current and vice versa at the contact plane is considered. In Sec.(3.4) we present the numerical results for the distribution of the current in the vicinity of the contact.

3.2. Model and equations

We consider the Josephson weak link as a microbridge between thin superconducting films of thickness d . The length L and width $2a$ of the microbridge, are assumed to be less than the coherence length ξ_0 . On the other hand, we assume that L and $2a$ are much larger than the Fermi wavelength λ_F and use the quasiclassical approach. There is a potential barrier in the contact, resulting in a finite probability for the electron that is to be reflected back. In the banks of superconductors a homogeneous current with a superconducting velocity \mathbf{v}_s flows parallel to the partition. We choose the \mathbf{z} -axis along \mathbf{v}_s and the \mathbf{y} -axis perpendicular to the boundary; $y = 0$ is the boundary plane (see Fig.4). If the film thickness $d \ll \xi_0$ then in the main approximation in terms of the parameter d/ξ_0 the superconducting current depends on the coordinates in the plane of the film $\rho = (y, z)$ only. The superconducting current in the quasiclassical approximation

$$\mathbf{j}(\rho, \mathbf{v}_s) = 4\pi ieN(0)T \sum_{m>0} \langle \mathbf{v}_F g_1(\mathbf{v}_F, \rho, \mathbf{v}_s) \rangle_{\mathbf{v}_F} \quad (53)$$

is defined by the energy integrated Green matrix for the case of singlet superconductors which is following:

$$\check{g}(\tilde{\varepsilon}, \mathbf{v}_F, \rho, \mathbf{v}_s) = \begin{pmatrix} g_1 & g_2 i\hat{\sigma}_2 \\ i\hat{\sigma}_2 g_3 & -g_1 \end{pmatrix}, \quad (54)$$

and for the case of the order parameter we have:

$$\hat{\Delta} = \begin{pmatrix} 0 & \Delta i\hat{\sigma}_2 \\ i\hat{\sigma}_2 \Delta^* & 0 \end{pmatrix}. \quad (55)$$

This Green matrix in the ballistic case satisfies the Eilenberger equations as follows [31, 54]:

$$\eta \frac{\partial g_{1(n)}}{\partial t} + i\Delta_n^* g_{2(n)} - i\Delta_n g_{3(n)} = 0; \quad (56)$$

$$\eta \frac{\partial g_{2(n)}}{\partial t} + 2\tilde{\varepsilon} g_{2(n)} - 2i\Delta_n g_{1(n)} = 0; \quad (57)$$

$$\eta \frac{\partial g_{3(n)}}{\partial t} - 2\tilde{\varepsilon} g_{3(n)} + 2i\Delta_n^* g_{1(n)} = 0; \quad (58)$$

where, $t = y/|v_y|$ on the Fermi surface, $\eta = \mathbf{sgn}(v_y)$ and $n = 1, 2$ label the left and right hand superconducting bulks, respectively. Using the quasiclassical approximation, we select the solution the for this problem as follows:

$$g_{1(n)} = \frac{\tilde{\varepsilon}}{\Omega} + a_n \exp(-2s\Omega t); \quad (59)$$

$$g_{2(n)} = \frac{i\Delta_n}{\Omega} + b_n \exp(-2s\Omega t); \quad (60)$$

$$g_{3(n)} = \frac{i\Delta_n^*}{\Omega} + d_n \exp(-2s\Omega t); \quad (61)$$

where, $s = \mathbf{sgn}(y)$ and $\Omega = \sqrt{\tilde{\varepsilon}^2 + |\Delta|^2}$. Here $N(0)$ is the density of states at the Fermi level, $\tilde{\varepsilon} = \varepsilon_m + i\mathbf{p}_F \cdot \mathbf{v}_s$, \mathbf{v}_F and \mathbf{p}_F are the electron velocity and momentum on the Fermi

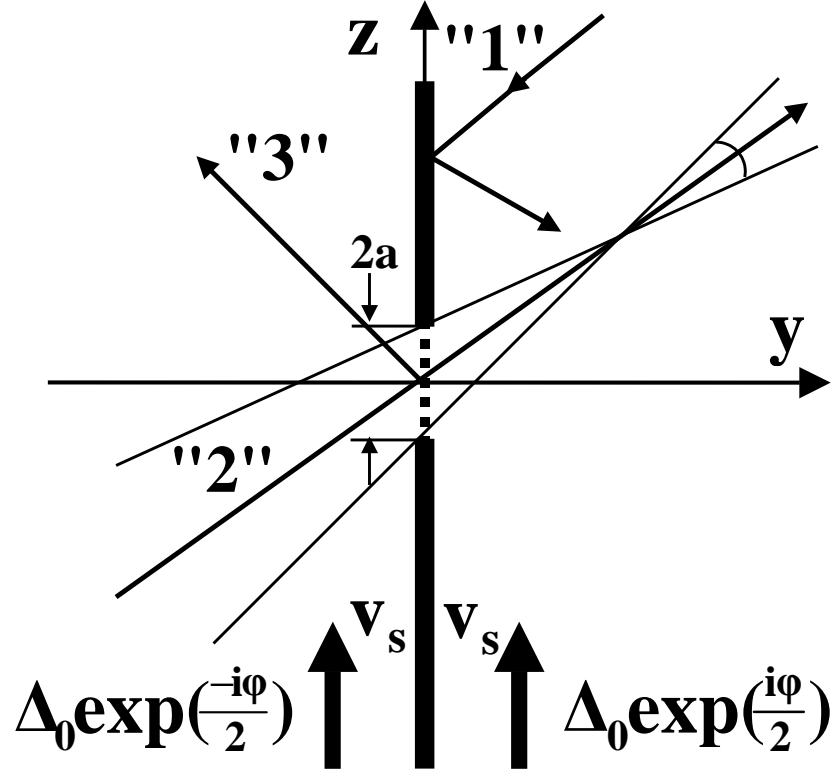


Figure 4. Model of the point-contact with finite reflection coefficient as a slit in the thin impenetrable insulating partition.

surface, $\varepsilon_m = (2m + 1)\pi T$ are the Matsubara frequencies, m is an integer number, \mathbf{v}_s is the superfluid velocity and T is the temperature. Eqs. (3.2) should be supplemented by the equation for the superconducting order parameter Δ

$$\Delta(\rho, \mathbf{v}_s, T) = 2\pi\lambda T \sum_{m>0} \langle g_2(\mathbf{v}_F, \rho, \mathbf{v}_s) \rangle_{\mathbf{v}_F} \quad (62)$$

where λ is the constant of pairing interaction and $\langle \dots \rangle_{\mathbf{v}_F}$ is the averaging over directions of \mathbf{v}_F . After substitute in the Eilenberger equation (1), we obtain:

$$g_{1(n)} = \frac{\tilde{\varepsilon}}{\Omega_n} + a_n \exp(-2s\Omega_n t); \quad (63)$$

$$g_{2(n)} = \frac{\Delta_n}{\Omega_n} + a_n \left(\frac{\Delta_n}{\tilde{\varepsilon} - \eta s \Omega_n} \right) \exp(-2s\Omega_n t); \quad (64)$$

$$g_{3(n)} = \frac{\Delta_n^*}{\Omega_n} + a_n \left(\frac{\Delta_n^*}{\tilde{\varepsilon} + \eta s \Omega_n} \right) \exp(-2s\Omega_n t); \quad (65)$$

As it was shown in [30] in the zero approximation in terms of the small parameter $a/\xi_0 \ll 1$ for a self-consistent solution of the problem it is not necessary to consider Eq. (62). The model, in which the order parameter is constant in the two half-spaces $\Delta(\rho, \mathbf{v}_s, T) = \Delta(\mathbf{v}_s, T) \exp(\text{sgn}(y) \frac{i\phi}{2})$ (ϕ is the phase difference between superconductors), can be used.

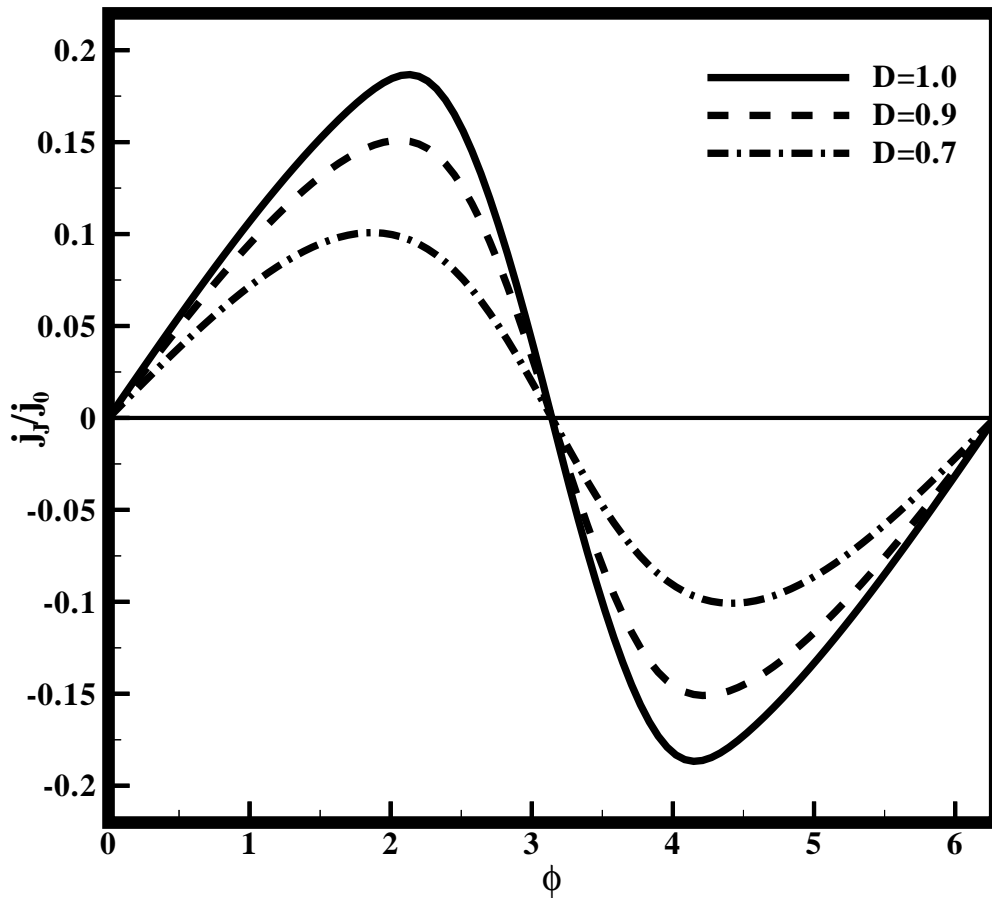


Figure 5. Josephson current j_J versus phase ϕ for $T/T_c = 0.1$, $q = 0.5$ and $j_0 = 4\pi |e| N(0) v_F T_c$.

In the same approximation the velocity \mathbf{v}_s does not depend on the coordinates. The Eq. (62) enables us to calculate a spatial distribution of the order parameter $\Delta(\rho)$ in the next order approximation in terms of the parameter a/ξ_0 . Solutions of Eqs. (1) should satisfy Zaitsev's boundary conditions ([34]) across the contact $y = 0, |z| \leq a$ and specular reflection condition for $y = 0, |z| \geq a$. In addition, far from the contact, solutions should coincide with the bulk solutions. The Zaitsev boundary conditions [34] have been considered in [54], but some improvements are necessary for using these boundary conditions. These improvements have been done in [55]. The Zaitsev boundary conditions at the contact can be written as [34, 54, 55]

$$\hat{d}^l = \hat{d}^r \equiv \hat{d} \quad (66)$$

$$\frac{D}{2-D} \left[\left(1 + \frac{\hat{d}}{2}\right) \hat{s}^r, \hat{s}^l \right] = \hat{d} \hat{s}^l \quad (67)$$

where

$$\widehat{s}^r = \check{g}^r(\mathbf{v}_F, y=0) + \check{g}^r(\mathbf{v}_F', y=0) \quad (68)$$

$$\widehat{d}^r = \check{g}^r(\mathbf{v}_F, y=0) - \check{g}^r(\mathbf{v}_F', y=0) \quad (69)$$

with \mathbf{v}_F' being the reflection of \mathbf{v}_F with respect to the boundary and D is the transparency coefficient of point contact. Indexes l and r denote that the Green function are taken at the left ($y = -0$) or right ($y = +0$) hand from the barrier. Similar relations also hold for \widehat{s}^l and \widehat{d}^l . The first boundary condition implies that the antisymmetric part of Green function is continuous, this is a form of charge conservation, because the antisymmetric part of Green function is related to the current directly. But the second boundary condition means discontinuity in symmetric part of Green function. This discontinuity is the result of potential barrier as the interface. In general, D could be momentum dependent. For simplicity in our calculations we assumed that D is independent of the Fermi velocity direction.

3.3. Current-phase dependencies for Josephson and tangential currents

Making use of the solution of Eilenberger equations (1), we obtain the following expression for the current density (53) at the slit [56]:

$$\mathbf{j}(y=0, |z| < a) = 4\pi e N(0) T v_F \sum_{m>0} \left\langle \widehat{\mathbf{v}}_F \left(\frac{\tilde{\varepsilon}\Omega - i\eta D \Delta^2 \sin \frac{\phi}{2} \cos \frac{\phi}{2}}{\tilde{\varepsilon}^2 + \Delta^2 [1 - D(\sin \frac{\phi}{2})^2]} \right) \right\rangle_{\widehat{\mathbf{v}}} \quad (70)$$

where, $\Omega = \sqrt{\tilde{\varepsilon}^2 + \Delta^2}$, $\widehat{\mathbf{v}} = \mathbf{v}_F/v_F$ is the unit vector and $\eta = \mathbf{sgn}(v_y)$. In the case, $\mathbf{v}_s \neq 0$, the current (70) has both \mathbf{j}_J and \mathbf{j}_z components. The tangential current \mathbf{j}_z depends on the order parameters phase difference ϕ and is not equal to the transport current \mathbf{j}_T on the banks, in other words the total current is not equal to the vector sum of Josephson and transport currents. For the case $\mathbf{v}_s = 0$, at the contact the tangential current is zero and the normal component, i.e. the Josephson current is as found for the finite transparent contact in [34]. Detaching explicitly the Josephson current \mathbf{j}_J and the spatially homogeneous (transport) current \mathbf{j}_T that is produced by the superfluid velocity \mathbf{v}_s , we can write the current as the sum of three terms: \mathbf{j}_J , \mathbf{j}_T , and the "interference" current \mathbf{j}_{int} . Also we have

$$\mathbf{j} = \mathbf{j}_J(\phi, D, \mathbf{v}_s) + \mathbf{j}_T(\mathbf{v}_s) + \mathbf{j}_{int}(\phi, D, \mathbf{v}_s) \quad (71)$$

The "interference" current takes place in the vicinity of the contact, where both coherent currents $\mathbf{j}_J(\phi)$ and $\mathbf{j}_T(\mathbf{v}_s)$ exist (see also the next subsection). At first we consider the current density (70) for temperatures close to the critical temperature ($T_c - T \ll T_c$). From Eqs. (70) at the contact and for the temperatures close to the critical temperature we have:

$$\mathbf{j} = j_0 \sum_{m>0} \left\langle \widehat{\mathbf{v}}_F \mathbf{Im} \left(\frac{\tilde{\varepsilon}\Omega - i\eta D \Delta^2 \sin \frac{\phi}{2} \cos \frac{\phi}{2}}{\tilde{\varepsilon}^2 + \Delta^2 [1 - D(\sin \frac{\phi}{2})^2]} \times \frac{(\tilde{\varepsilon}^*)^2 + \Delta^2 [1 - D(\sin \frac{\phi}{2})^2]}{(\tilde{\varepsilon}^*)^2 + \Delta^2 [1 - D(\sin \frac{\phi}{2})^2]} \right) \right\rangle_{\widehat{\mathbf{v}}} \quad (72)$$

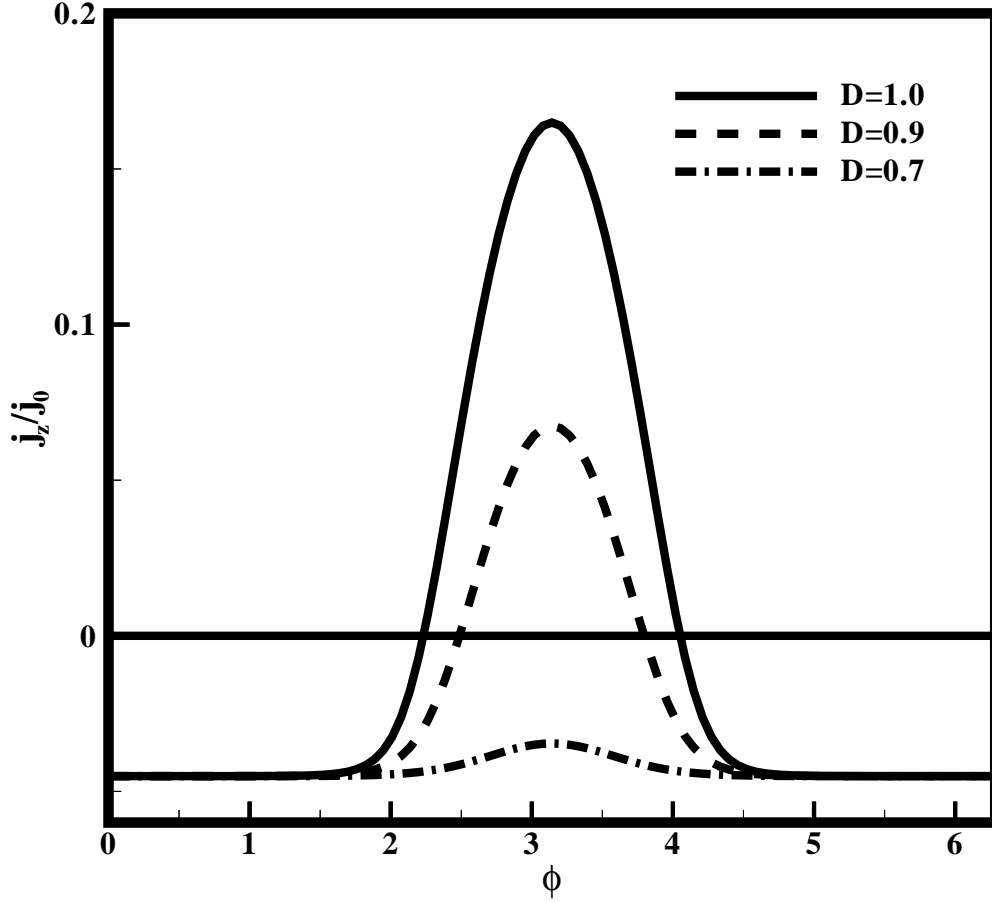


Figure 6. Tangential current j_z versus phase ϕ for $T/T_c = 0.1$ and $q = 0.5$.

where, $j_0 = 4\pi |e| N(0)v_F T_c$ and numerator and denominator of the Green function fraction has been multiplied by the expression $(\tilde{\varepsilon}^*)^2 + \Delta^2 [1 - D(\sin \frac{\phi}{2})^2]$, to escape of the complexity problems. It is well-known that for the temperatures close to the critical temperature, $\Delta(T \rightarrow T_c) \ll T_c$. Consequently, we use the Taylor expansion in terms of the small parameter $\frac{\Delta(T \rightarrow T_c)}{T_c}$. So at the contact we have:

$$\mathbf{j} = j_0 \sum_{m>0} \left\langle \hat{\mathbf{v}}_F \mathbf{Im} \left((\tilde{\varepsilon} \tilde{\varepsilon}^*)^2 + \tilde{\varepsilon}^2 \Delta^2 [1 - D(\sin \frac{\phi}{2})^2] + \frac{1}{2}(1 - i\eta D \sin \phi) \Delta^2 (\tilde{\varepsilon}^*)^2 \right) / \varepsilon_m^4 \right\rangle_{\hat{\mathbf{v}}} \quad (73)$$

we obtain [56]:

$$\mathbf{j}_J(\phi, D, \mathbf{v}_s) = \frac{1}{2} AD \sin \phi \mathbf{e}_y \quad (74)$$

$$\mathbf{j}_T(\mathbf{v}_s) = -\frac{1}{3} Ak \mathbf{e}_z, \quad (75)$$

$$\mathbf{j}_{int}(\phi, D, \mathbf{v}_s) = \frac{1}{3} AkD(1 - \cos \phi) \mathbf{e}_z. \quad (76)$$

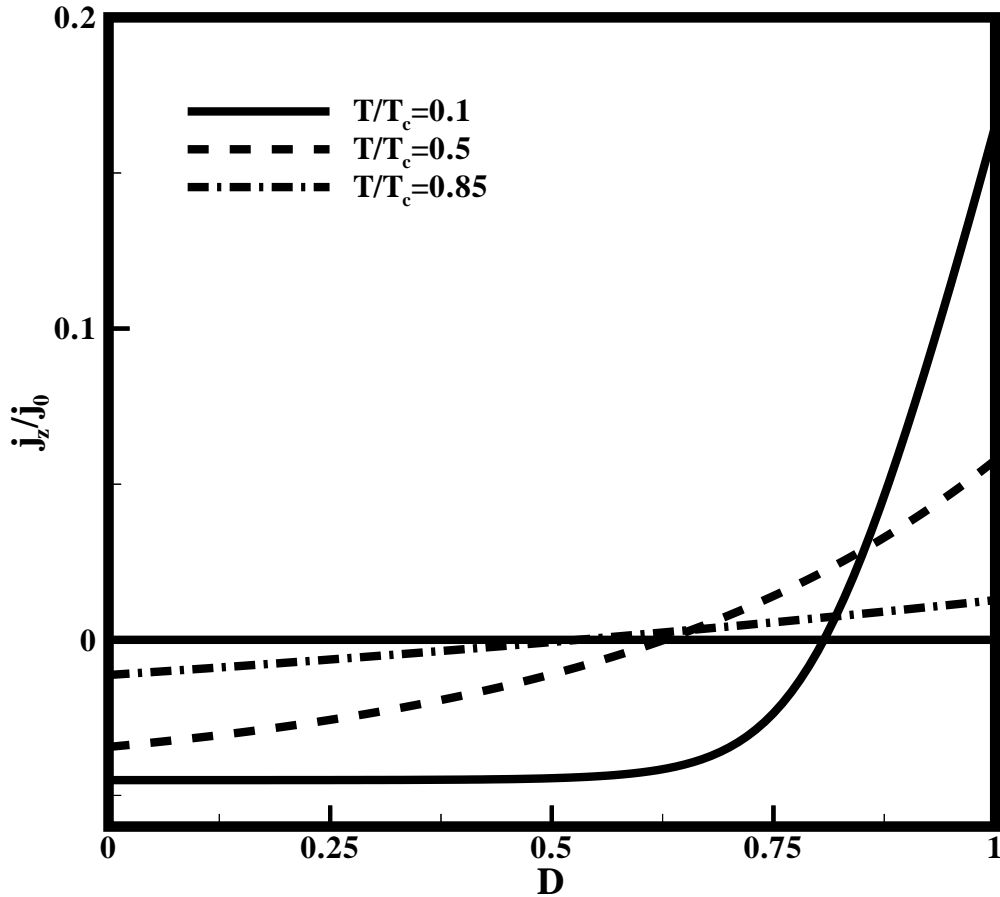


Figure 7. Tangential current j_z versus the transparency D at $\phi = \pi$ and $q = 0.5$.

where $A = \frac{1}{16}j_0 \frac{\Delta^2}{T_c^2}$, $k = \frac{14\zeta(3)}{\pi^3} \frac{v_s p_F}{T_c}$, \mathbf{e}_i is the unit vector in the i -direction. This consideration shows how the current is affected by the interplay of Josephson and transport currents. At the contact the "interference" current \mathbf{j}_{int} is anti-parallel to \mathbf{j}_T and if the phase difference $\phi = \pi$, $\mathbf{j}_{int} = -2D\mathbf{j}_T$. When there is no phase difference (at $\phi = 0$), we obtain $j_{int} = 0$. So at transparency values D up to $\frac{1}{2}$ the total tangential current at the contact flows in the opposite direction to the transport current. Thus, for such D in the vicinity of the contact, two vortices should exist. At arbitrary temperatures $T < T_c$ the current-phase relations can be analyzed numerically. In our calculations we define the parameter, q , in which $q = \frac{p_F v_s}{\Delta_0}$ and $\Delta_0 = \Delta(T = 0, v_s = 0)$. The value of q can be in the range $0 < q < q_c$ and its critical value q_c , corresponds to the critical current in the homogeneous current state [57]. At $T = 0$, $q_c = 1$ and the gap Δ does not depend on q . In Fig.5 and Fig.6, we plot the Josephson and tangential currents at the contact as functions of ϕ at temperatures far from the critical (namely, $T = 0.1T_c$) and for $q = 0.5$ and for different values of transparency D . Far from $\phi = \pi$,

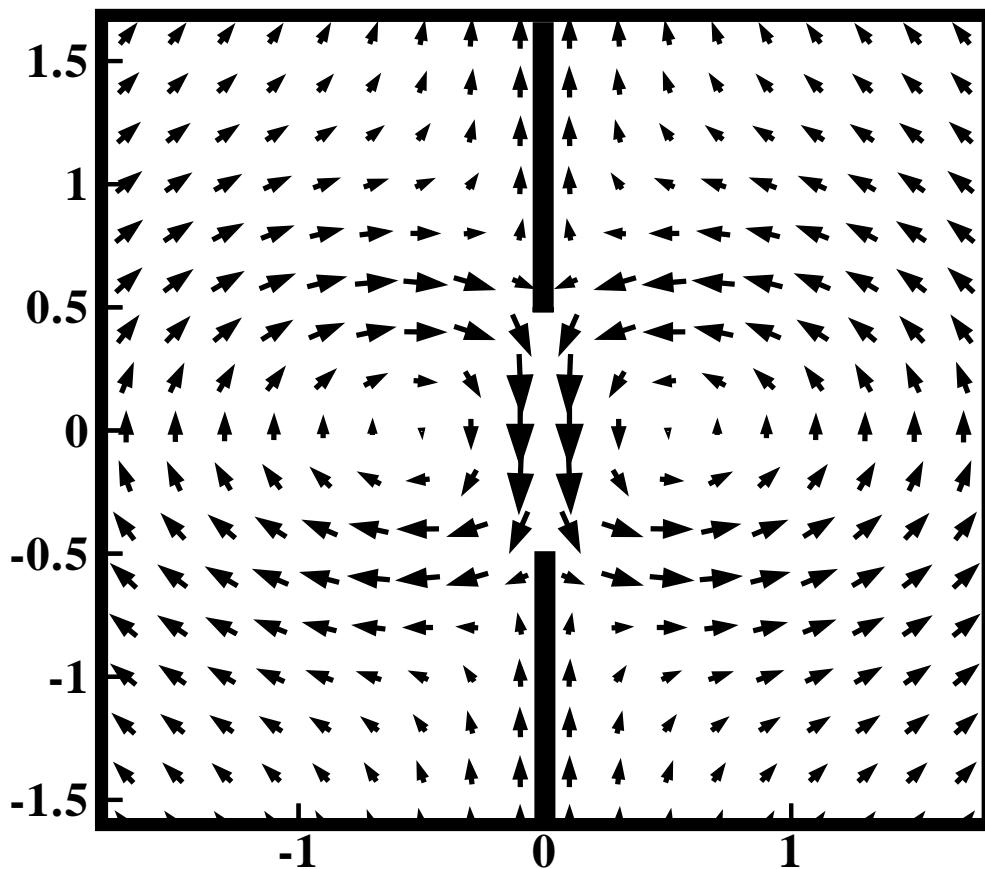


Figure 8. Vector plot of the current for $\phi = \pi$, $q = 0.5$, $T/T_c = 0.1$ and $D = 0.95$. Axes are marked in units of the contact size a .

the tangential current is not disturbed by the contact, it tends to its value on the bank. The Josephson current-phase relation is the same as when the transport current is absent. However, when ϕ tends to π , for the highly transparent contact ($D = 1, 0.9$) the tangential current becomes anti-parallel to the bulk current. But for $D = 0.7$ the "interference" current is strongly suppressed and the tangential current flows parallel to the bulk current. In Fig.7, we plot $j_z(D) = j_T + j_{int}$ at $\phi = \pi$ for different temperatures. These plots show that by increasing the temperature a counter-flow $j_z(D) < 0$ exists in a wider interval of transparency $D_c(T) < D \leq 1$ and $D_c(T \rightarrow T_c) \rightarrow \frac{1}{2}$. This numerical result coincides with analytical results (75,76).

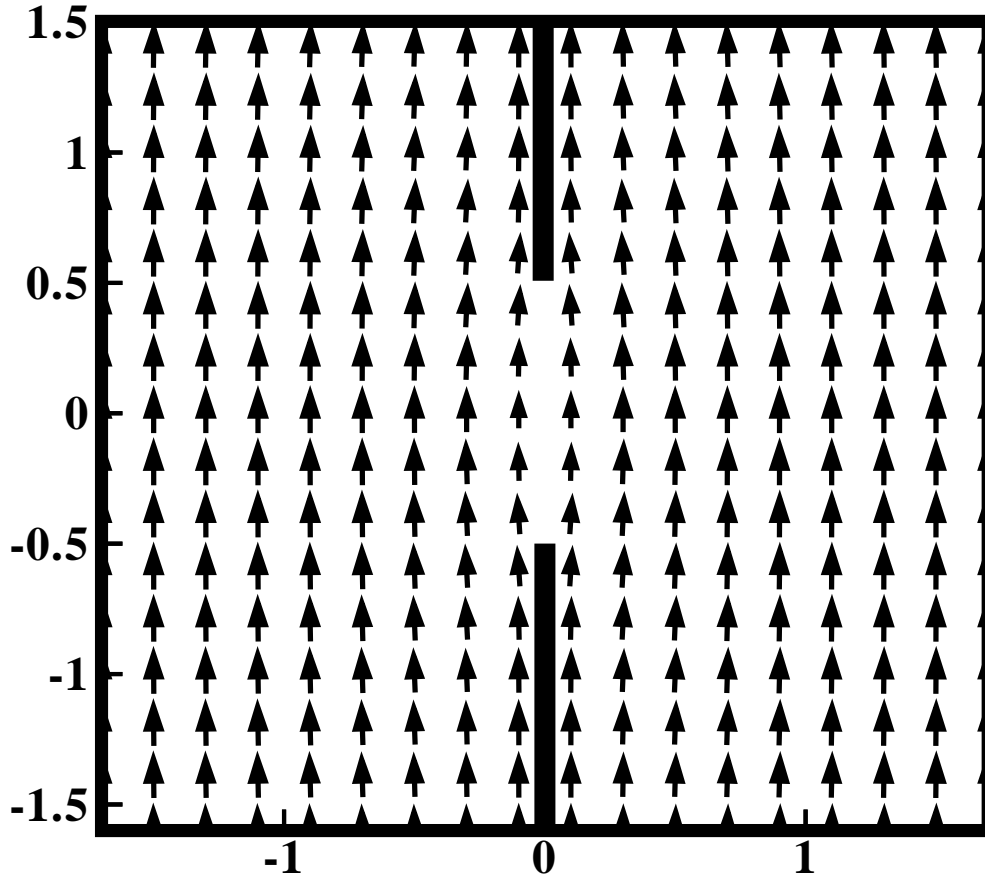


Figure 9. Vector plot of the current for $\phi = \pi$, $q = 0.5$, $T/T_c = 0.1$ and $D = 0.7$.

3.4. Spatial distribution of the current near the contact

In this subsection we consider the spatial distribution of the current near the orifice. The superconducting current (53) can be written as

$$\mathbf{j}(\rho, \mathbf{v}_s) = j_0 \frac{T}{T_c} \sum_{m>0} \langle \hat{\mathbf{v}} g_1(\rho, \mathbf{v}_s) \rangle_{\hat{\mathbf{v}}_{\mathbf{F}}}, \quad (77)$$

where, $j_0 = 4\pi |e| N(0) v_F T_c$. We should note that although the current (77) depends only on the coordinates in the film plane, the integration over velocity directions $\hat{\mathbf{v}}$ is carried out over all of the Fermi sphere as in a bulk sample. This method of calculation is correct only for specular reflection from the film surfaces when there is no back scattering after electron interaction with them. At a point, $\rho = (y, z)$, all ballistic trajectories can be categorized as transit and non-transit trajectories (see, Fig.4). For the transit trajectories "1" (their reflected counterparts marked by "3" in Fig.4) a projection $\hat{\mathbf{v}}_{\parallel}$ of the vector $\hat{\mathbf{v}}$ to the film plane belongs to the angle at which the slit is seen from the

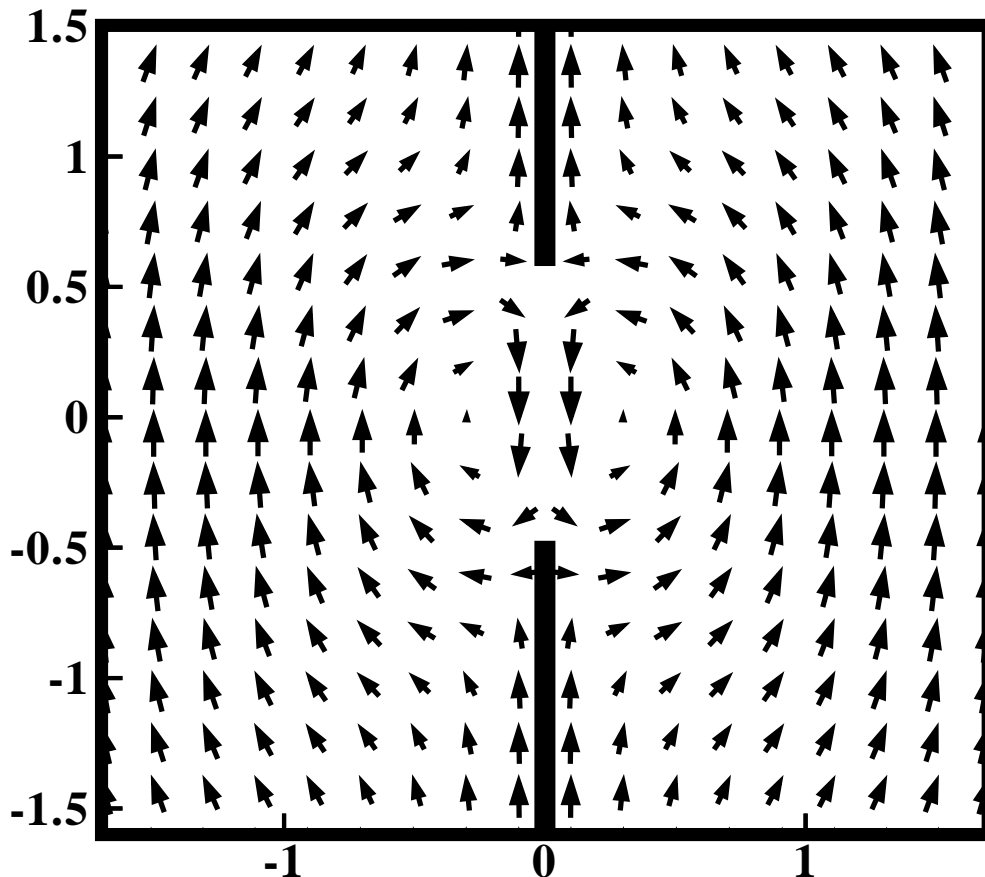


Figure 10. Vector plot of the current for $\phi = \pi$, $q = 0.5$, $D = 0.7$, and $T/T_c = 0.85$.

point ρ , $\hat{\mathbf{v}}_{\parallel} \in \alpha(\rho)$, and for non-transit (marked by "2" in Fig.4) $\hat{\mathbf{v}}_{\parallel} \notin \alpha(\rho)$. For transit trajectories the Green functions satisfy boundary conditions on both banks and at the contact. The non-transit trajectories should satisfy the specular reflection condition [or Zaitsev's boundary conditions (66)-(67) for $D = 0$ at $y = 0, |z| \geq a$]. Then for the current at $T_c - T \ll T_c$ we obtain an analytical formula [56]:

$$\mathbf{j}(\rho, \phi, D, \mathbf{v}_s) = j_c D \langle \sin \phi \hat{\mathbf{v}} \text{sgn}(v_y) + k(1 - \cos \phi) \hat{\mathbf{v}} \hat{v}_z \rangle_{\hat{\mathbf{v}}_{\parallel} \in \alpha} - j_c k \langle \hat{\mathbf{v}} \hat{v}_y \rangle_{\hat{\mathbf{v}}} \quad (78)$$

where, $j_c(T, \mathbf{v}_s) = \frac{\pi |e| N(0) v_F \Delta^2(T, \mathbf{v}_s)}{8 T_c}$. To illustrate how the current flows near the contact, we plot the Fig.8 and Fig.9, for $\phi = \pi$ and temperatures much smaller than critical ($T/T_c = 0.1$), and for different values of transparency. At such value of the phase ϕ there is no Josephson current and at the large $D = 0.95$ the current is disturbed in such a way that there are two anti-symmetric vortices close to the orifice (see Fig. 8). For the such temperature at $D = 0.7$ the vortices are absent in Fig. 9. Near the critical temperature ($T/T_c = 0.85$) the vortex-like currents are restored for $D = 0.7$ (see Fig.10).

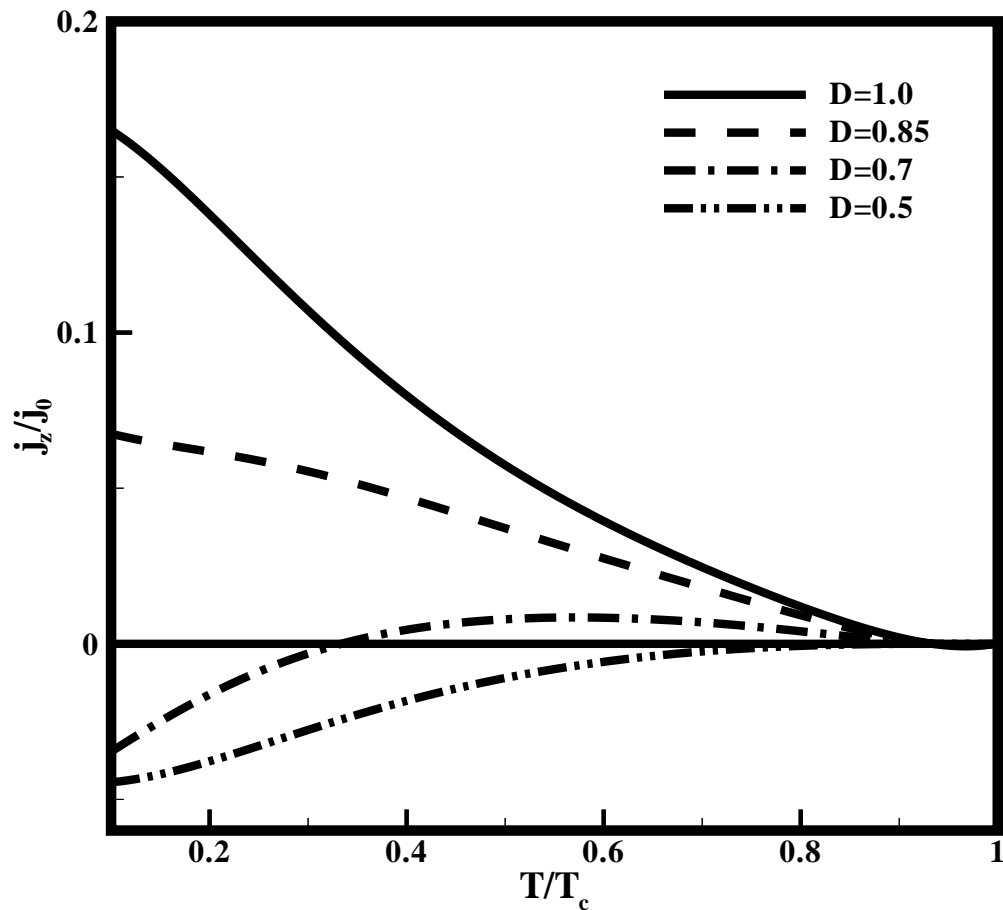


Figure 11. Tangential current j_z versus the temperature T at $\phi = \pi$ and $q = 0.5$.

Far from the orifice (at the distances $l \sim \xi_0 \gg a$) the Josephson current is spread out and the current is equal to its value at infinity. Considering the current distributions and current-phase diagrams, we observed that:

- 1). For fixed values of temperature and superfluid velocity, by decreasing the transparency the vortex-like current disappears at $D = D_c(T)$; $0.5 \leq D_c(T) < 1$
- 2). For intermediate values of transparency D ($D_c(T) < D < 1$) by increasing the temperature the vortex-like currents, which were destroyed by the effect of electron reflection at the contact, may be restored.

It is clear that both Josephson and "interference" currents are the result of the quantum interference between two coherent states. By decreasing the transparency the interference effect will be weaker and these two currents will decrease, while the transport current will remain constant. On the other hand, the presence of vortices depends on the result of competition between transport and "interference" current. Thus, by decreasing the transparency the tunneling and consequently the "interference"

current will decrease and vortices may be destroyed (75,76). Similar to the case $D = 1$ in [32], at high values of transparency, the "interference" current can dominate the transport current and tangential current can be anti-parallel to the transport current, thus the vortices appear. But for low transparency the tangential current will be parallel to the transport current and the vortices disappear.

The second point is an anomalous temperature behavior of the effect. The vortices are the result of the coherent current mixing. One could expect that by increasing the temperature the vortices would disappear whereas, for intermediate values of transparency, by increasing the temperature the vortices will be restored. As considered in Fig.9 and Fig.10 for the transparency $D = 0.7$ the vortices at low temperature are absent but at high temperature they are present. In the plots for tangential current versus transparency, Fig. 7 we can observe this phenomenon (appearance of the counter-flow near the contact at high temperatures).

Usually superconducting currents are monotonic and descendant functions of temperature. Josephson and transport currents have this property, but about the tangential current j_y , the situation is totally different. At high values of transparency the j_y has similar behavior to the two other currents, but at low and intermediate values of transparency at $\phi = \pi$ it has a non-monotonic dependence on the temperature and this is the origin of the anomalous temperature behavior of vortices. As the temperature increases, the tangential current first increases and then decreases. In Fig.11 we plotted the tangential current ("interference" + transport current) versus the temperature for different values of transparency. We observed that for intermediate values of transparency $0.5 < D < 1$, at low temperatures and $\phi = \pi$ the tangential current has anomalous dependence on the temperature. The reason for this dependence is that the "interference" current flows in the opposite direction to the transport current. This current is suppressed by the reflection, but with increasing of the temperature it decreases slowly than the transport current. As a consequence of that with increasing of T the tangential current can change its sign and vortices appear. We found that for low values of transparency $0 < D < 0.5$ the "interference" current cannot dominate the transport current and in addition the tangential current has the same direction as the transport current for any temperature $T < T_c$.

4. Weak link between unitary f -wave superconductors

4.1. Introduction

In this chapter the spin current in the Josephson junction as a weak-link (interface) between misorientated triplet superconductors will be investigated theoretically for the models of the order parameter in UPt_3 . Green functions of the system will be obtained from the quasiclassical Eilenberger equations. The analytical results for the charge and spin currents will be illustrated by numerical calculations for the certain misorientation angles of gap vector of superconductors.

Triplet superconductivity has become one of the most interesting topics of condensed matter physics [5, 7], particularly in view of the recently discovered ferromagnetic superconductivity [13, 14]. The mechanism of pairing, physics of interaction and gap structure in this type of superconductors have been the subject of many experimental and theoretical works [58, 59]. The Cooper pairing in the triplet superconductors has been investigated, for example, using the thermal conductivity in papers [60, 61] and Knight shift experiments in papers [62, 63]. Also, the Josephson effect in the point contact between triplet superconductors has been studied in paper [6]. These weak-link structures have been used to demonstrate the order parameter symmetry in Ref. [64]. Eventually, the f -wave symmetry of order parameter has been proposed for UPt_3 and Sr_2RuO_4 compounds. In addition, the spin polarized transport through the systems consisting of superconductors, normal metals, ferromagnetic layers and other structures as one of the modern topics of mesoscopic physics, has attracted much attention recently [65, 66, 67, 68]. In this chapter, the ballistic Josephson weak-link as the interface between two bulk of f -wave superconductors with different orientations of the crystallographic axes has been investigated. It is shown that the current-phase dependencies are totally different from the current-phase dependencies of the junction between conventional (s -wave) superconductors [30] and high T_c (d -wave) superconductors [48]. It is found that for the certain values of the misorientation, the spin-current in the both directions, tangential and perpendicular to the interface, may exist and it has totally unusual dependence on the external phase difference. The effect of misorientation on the spin current is investigated. It is observed that the misorientation between gap vectors is the origin of the spin current. As the important result of this chapter, it is obtained that, at some of certain values of phase difference, at which the charge current is zero, the spin current has the finite value. Another result of this chapter is the capability of this proposed experiment for polarization of the spin transport using the junction between f -wave superconductors. Eventually, one of the states and geometries of our system can be used as a switch which is able to divide the spin and charge currents into two parts: parallel and perpendicular to the interface.

The arrangement of the rest of this chapter is as follows. In Sec.(4.2) we describe our configuration, which is investigated. For a non-self-consistent model of the order parameter, the quasiclassical Eilenberger equations [31] are solved and suitable Green functions are obtained analytically. In Sec.(4.3) the obtained formulas for the Green

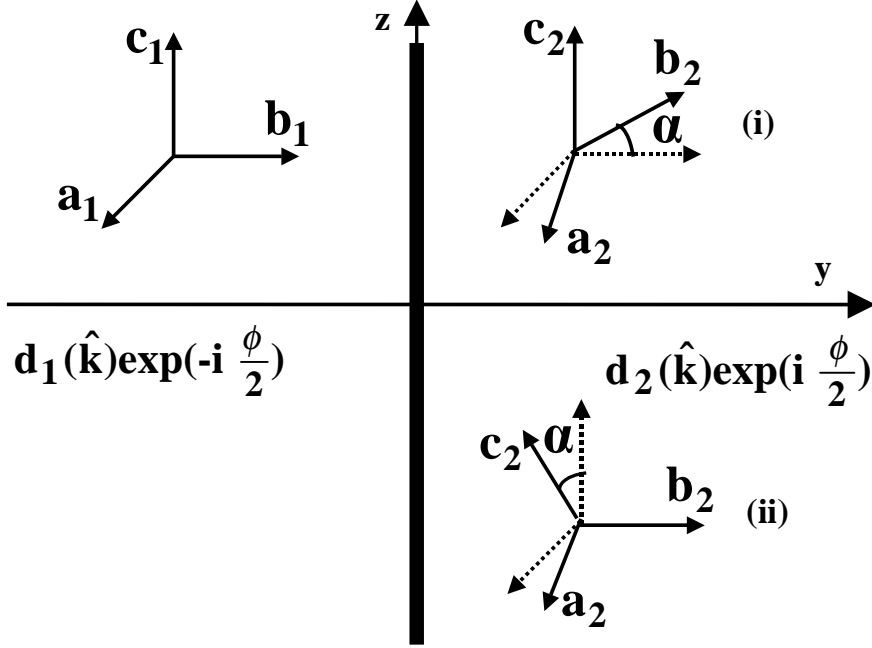


Figure 12. Scheme of a flat interface between two superconducting bulks, which are misorientated as much as α .

functions are used for calculation the charge and spin current densities at the interface. An analysis of numerical results will be done in Sec.(4.4).

4.2. Basic Equations

We consider a model of a flat interface $y = 0$ between two misorientated f -wave superconducting half-spaces (Fig.12) as a ballistic Josephson junction. In the quasiclassical ballistic approach, in order to calculate the charge and spin current, we use “transport-like” equations [31] for the energy integrated Green functions $\check{g}(\hat{\mathbf{v}}_F, \mathbf{r}, \varepsilon_m)$

$$\mathbf{v}_F \nabla \check{g} + \left[\varepsilon_m \check{\sigma}_3 + i \check{\Delta}, \check{g} \right] = 0, \quad (79)$$

and the normalization condition

$$\check{g} \check{g} = \check{1}, \quad (80)$$

where $\varepsilon_m = \pi T(2m + 1)$ are discrete Matsubara energies $m = 0, 1, 2, \dots$, T is the temperature and \mathbf{v}_F is the Fermi velocity and $\check{\sigma}_3 = \hat{\sigma}_3 \otimes \hat{I}$ in which $\hat{\sigma}_j$ ($j = 1, 2, 3$) are Pauli matrices. The Matsubara propagator \check{g} can be written in the standard form:

$$\check{g} = \begin{pmatrix} g_1 + \mathbf{g}_1 \hat{\sigma} & (g_2 + \mathbf{g}_2 \hat{\sigma}) i \hat{\sigma}_2 \\ i \hat{\sigma}_2 (g_3 + \mathbf{g}_3 \hat{\sigma}) & g_4 - \hat{\sigma}_2 \mathbf{g}_4 \hat{\sigma}_2 \end{pmatrix}, \quad (81)$$

where, the matrix structure of the off-diagonal self energy $\check{\Delta}$ in the Nambu space is

$$\check{\Delta} = \begin{pmatrix} 0 & \mathbf{d}\hat{\sigma}i\hat{\sigma}_2 \\ i\hat{\sigma}_2\mathbf{d}^*\hat{\sigma} & 0 \end{pmatrix}. \quad (82)$$

In this chapter, the unitary states, for which $\mathbf{d} \times \mathbf{d}^* = 0$, is investigated. Also, the unitary states vectors $\mathbf{d}_{1,2}$ can be written as

$$\mathbf{d}_n = \Delta_n \exp i\psi_n, \quad (83)$$

where $\Delta_{1,2}$ are the real vectors in the left and right sides of the junction. The gap (order parameter) vector \mathbf{d} has to be determined from the self-consistency equation, near the Fermi surface:

$$\mathbf{d}(\hat{\mathbf{v}}_F, \mathbf{r}) = \pi T N(0) \sum_m \langle V(\hat{\mathbf{v}}_F, \hat{\mathbf{v}}'_F) \mathbf{g}_2(\hat{\mathbf{v}}'_F, \mathbf{r}, \varepsilon_m) \rangle \quad (84)$$

where $V(\hat{\mathbf{v}}_F, \hat{\mathbf{v}}'_F)$, is a potential of pairing interaction, $\langle \dots \rangle$ stands for averaging over the directions of an electron momentum on the Fermi surface $\hat{\mathbf{v}}'_F$ and $N(0)$ is the electron density of states at the Fermi level of energy. Solutions to Eqs. (79) and (84) must satisfy the conditions for Green functions and vector \mathbf{d} in the bulks of the superconductors far from the interface as follow:

$$\check{g}(\pm\infty) = \frac{\varepsilon_m \check{\sigma}_3 + i\check{\Delta}_{2,1}}{\sqrt{\varepsilon_m^2 + |\mathbf{d}_{2,1}|^2}}; \quad (85)$$

$$\mathbf{d}(\pm\infty) = \mathbf{d}_{2,1}(\hat{\mathbf{v}}_F) \exp\left(\mp \frac{i\phi}{2}\right), \quad (86)$$

where ϕ is the external phase difference between the order parameters of the bulks. Eqs. (79) and (84) have to be supplemented by the continuity conditions at the interface between superconductors. For all quasiparticle trajectories, the Green functions satisfy the boundary conditions both in the right and left bulks as well as at the interface.

The set of equations (79) and (84) can be solved only numerically. For unconventional superconductors such solution requires the information of the function $V(\hat{\mathbf{v}}_F, \hat{\mathbf{v}}'_F)$. This information, as that of the nature of unconventional superconductivity in novel compounds, in most cases is unknown. Usually, the spatial variation of the order parameter and its dependence on the momentum direction can be separated in the form of $\Delta(\hat{\mathbf{v}}_F, y) = \Delta(\hat{\mathbf{v}}_F)\Psi(y)$. It has been shown that the absolute value of a self-consistent order parameter and $\Psi(y)$ are suppressed near the interface and at the distances of the order of the coherence length, while its dependence on the direction in the momentum space ($\Delta(\hat{\mathbf{v}}_F)$) remains unaltered [41]. Consequently, this suppression doesn't influence the Josephson effect drastically. This suppression of the order parameter keeps the current-phase dependence unchanged but, it changes the amplitude value of the current. For example, it has been verified in Ref. [48] for the junction between unconventional *d*-wave, in Ref. [41] for the case of “*f*-wave” superconductors and in Refs. [69, 70] for pinholes in ${}^3\text{He}$ that, there is a good qualitative agreement between self-consistent and non-self-consistent results. Also, it has been observed that the results of the non-self-consistent investigation of ferromagnet-*d*-wave proximity structure in Ref. [71] are

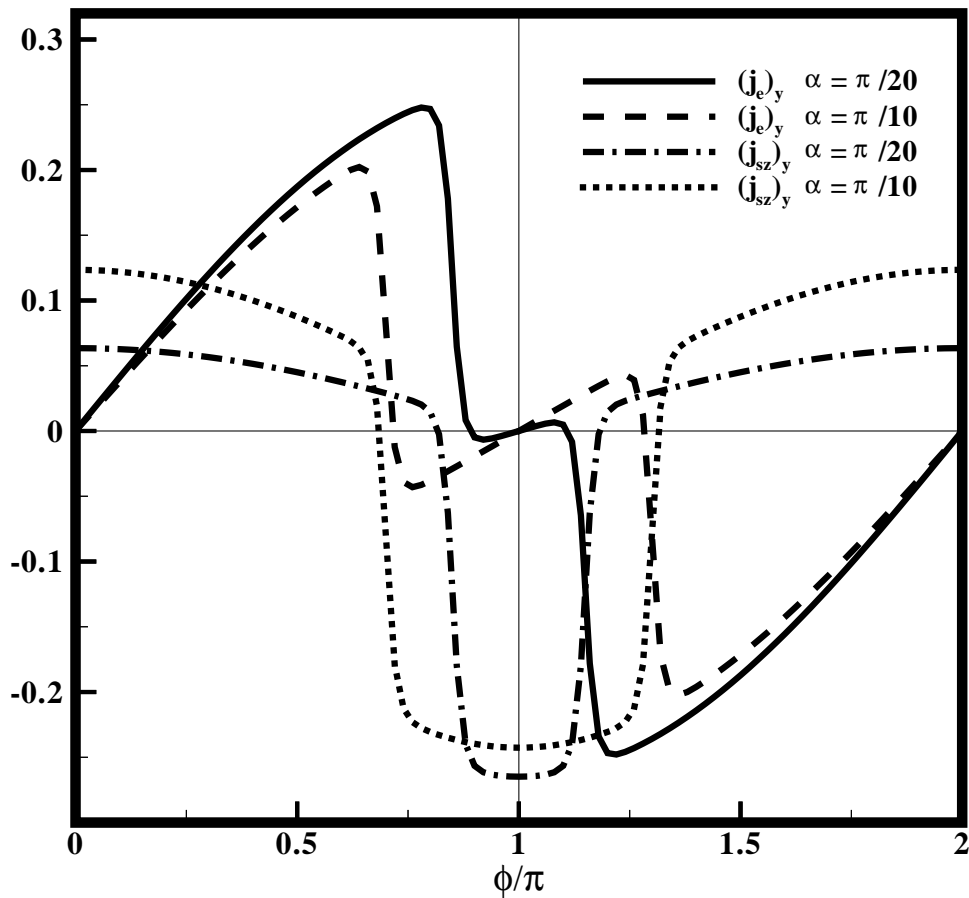


Figure 13. Charge and spin current (s_z) versus the phase difference ϕ for the planar state (103), geometry (i) and the different misorientations. Currents are given in units of $j_{0,e} = \frac{\pi}{2}eN(0)v_F\Delta_0(0)$ and $j_{0,s} = \frac{\pi}{4}\hbar N(0)v_F\Delta_0(0)$ respectively.

coincident with the experimental results of the paper [72] and the results of the non-self-consistent model in paper [45] are similar to the superfluid weak-link experiment [73]. In the paper [71], they have investigated the proximity effect between a ferromagnet and a high- T_c superconductor. They have solved the Eilenberger equation and using the obtained Green function investigated the Andreev bound states. The density of states in this system has been studied and the spatial oscillations have been observed in this nonselfconsistent paper. The results of this paper had been observed before in an experimental report in paper [72]. In addition, there are many published papers [69, 70, 71] and [74, 75, 76, 77] in which, such approximation has been used for different systems containing unconventional superconductors and important analytical results have been obtained. In Refs. [69, 70, 71] Eilenberger equation has been solved and Bogoliobov- Degennes equation has been considered in papers [74, 75, 76, 77] non-

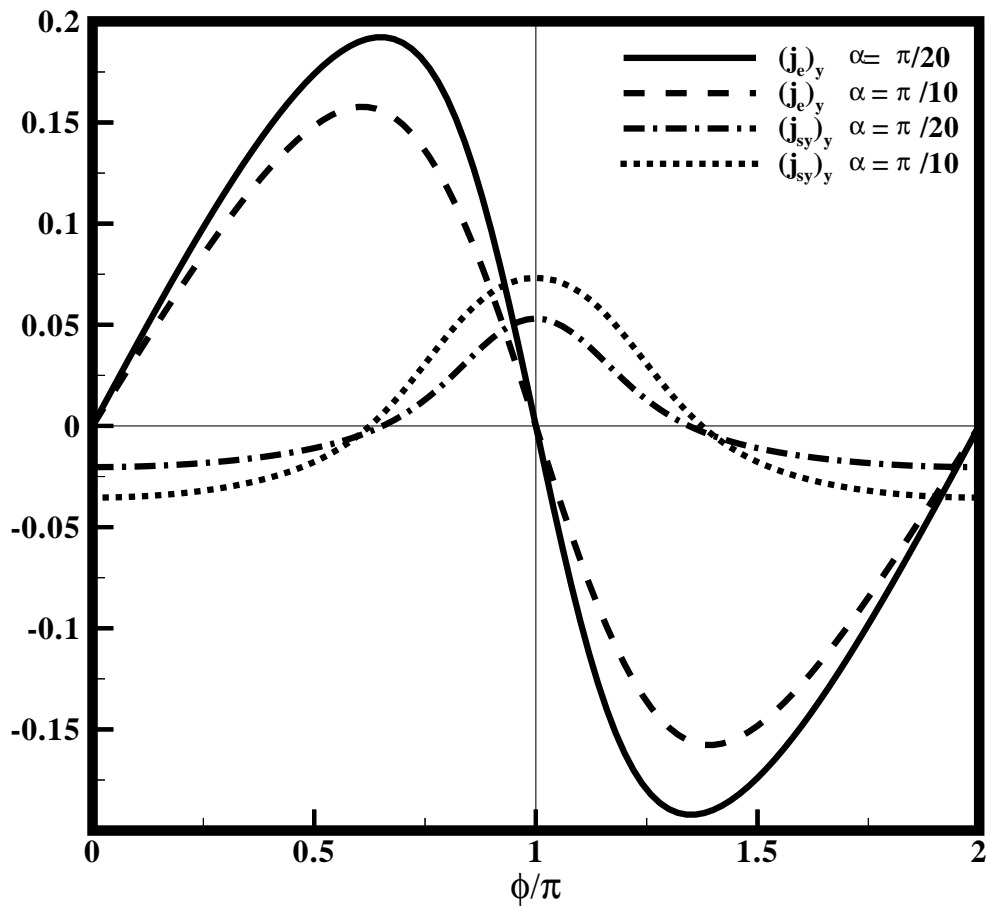


Figure 14. Charge and spin current (s_y) versus the phase difference ϕ for the axial state (102), geometry (ii) and the different misorientations (y -component).

self-consistently. Consequently, despite the fact that this estimation cannot be applied directly for a quantitative analyze of the real experiment, only a qualitative comparison of calculated and experimental current-phase relations is possible. In our calculations, a simple model of the constant order parameter up to the interface is considered and the pair breaking and the scattering on the interface are ignored. We believe that under these strong assumptions our results describe the real situation qualitatively. In the framework of such model, the analytical expressions for the charge and spin current can be obtained for an arbitrary form of the order parameter. Also, we have done our calculations for the small misorientations $\alpha = \frac{\pi}{20}$, $\alpha = \frac{\pi}{15}$ and $\alpha = \frac{\pi}{10}$. As the results of paper [48], for the small misorientations, selfconsistent and nonselfconsistent calculations have the same results approximately. Consequently, authors of paper [48] concluded that the nonselfconsistent formalism can be used for the junction between unconventional superconducting bulks with small misorientations.

4.3. Analytical Green functions

The solution of Eqs. (79) and (84) allows us to calculate the charge and spin current densities. The expression for the charge current is:

$$\mathbf{j}_e(\mathbf{r}) = 2i\pi eTN(0) \sum_m \langle \mathbf{v}_F g_1(\hat{\mathbf{v}}_F, \mathbf{r}, \varepsilon_m) \rangle \quad (87)$$

and for the spin current we have:

$$\mathbf{j}_{s_i}(\mathbf{r}) = 2i\pi \left(\frac{\hbar}{2}\right) TN(0) \sum_m \langle \mathbf{v}_F(\hat{\mathbf{e}}_i \mathbf{g}_1(\hat{\mathbf{v}}_F, \mathbf{r}, \varepsilon_m)) \rangle \quad (88)$$

where, $\hat{\mathbf{e}}_i = (\hat{\mathbf{x}}, \hat{\mathbf{y}}, \hat{\mathbf{z}})$. We assume that the order parameter does not depend on coordinates and in each half-space it equals to its value (112) far from the interface in the left or right bulks. For such a model, the current-phase dependence of a Josephson junction can be calculated analytically. It enables us to analyze the main features of current-phase dependence for the different models of the order parameter of “*f*-wave” superconductivity. The Eilenberger equations (79) for Green functions \check{g} , which are supplemented by the condition of continuity of solutions across the interface, at $y = 0$, and the boundary conditions at the bulks, should be solved for a non-self-consistent model of the order parameter analytically. In a ballistic case the system of equations for functions g_i and \mathbf{g}_i can be decomposed on independent blocks of equations. The set of equations which enables us to find the Green function g_1 is:

$$v_F \hat{\mathbf{k}} \nabla g_1 = i(\mathbf{d} \cdot \mathbf{g}_3 - \mathbf{d}^* \cdot \mathbf{g}_2); \quad (89)$$

$$v_F \hat{\mathbf{k}} \nabla \mathbf{g}_- = -2(\mathbf{d} \times \mathbf{g}_3 + \mathbf{d}^* \times \mathbf{g}_2); \quad (90)$$

$$v_F \hat{\mathbf{k}} \nabla \mathbf{g}_2 = -2\varepsilon_m \mathbf{g}_2 + 2ig_1 \mathbf{d} + \mathbf{d} \times \mathbf{g}_-; \quad (91)$$

$$v_F \hat{\mathbf{k}} \nabla \mathbf{g}_3 = 2\varepsilon_m \mathbf{g}_3 - 2ig_1 \mathbf{d}^* + \mathbf{d}^* \times \mathbf{g}_-; \quad (92)$$

where $\mathbf{g}_- = \mathbf{g}_1 - \mathbf{g}_4$. The Eqs. (89)-(92) can be solved by integrating over ballistic trajectories of electrons in the right and left half-spaces. The general solution satisfying the boundary conditions (109) at infinity is

$$g_1^{(n)} = \frac{\varepsilon_m}{\Omega_n} + a_n \exp(-2s\Omega_n t); \quad (93)$$

$$\mathbf{g}_-^{(n)} = \mathbf{C}_n \exp(-2s\Omega_n t); \quad (94)$$

$$\mathbf{g}_2^{(n)} = \frac{i\mathbf{d}_n}{\Omega_n} - \frac{2ia_n \mathbf{d}_n + \mathbf{d}_n \times \mathbf{C}_n}{2s\eta\Omega_n - 2\varepsilon_m} \exp(-2s\Omega_n t); \quad (95)$$

$$\mathbf{g}_3^{(n)} = \frac{i\mathbf{d}_n^*}{\Omega_n} + \frac{2ia_n \mathbf{d}_n^* - \mathbf{d}_n^* \times \mathbf{C}_n}{2s\eta\Omega_n + 2\varepsilon_m} \exp(-2s\Omega_n t); \quad (96)$$

where t is time of flight along the trajectory, $sgn(t) = sgn(y) = s$ and $\eta = sgn(v_y)$. By matching the solutions (93-96) at the interface ($y = 0, t = 0$), we find constants a_n and \mathbf{C}_n . Indices $n = 1, 2$ label the left and right half-spaces respectively. The function $g_1(0) = g_1^{(1)}(-0) = g_1^{(2)}(+0)$, which is a diagonal term of Green matrix and determines the current density at the interface, $y = 0$, is as follows: Two diagonal terms of Green matrix which determine the current densities at the interface, $y = 0$, are following. For

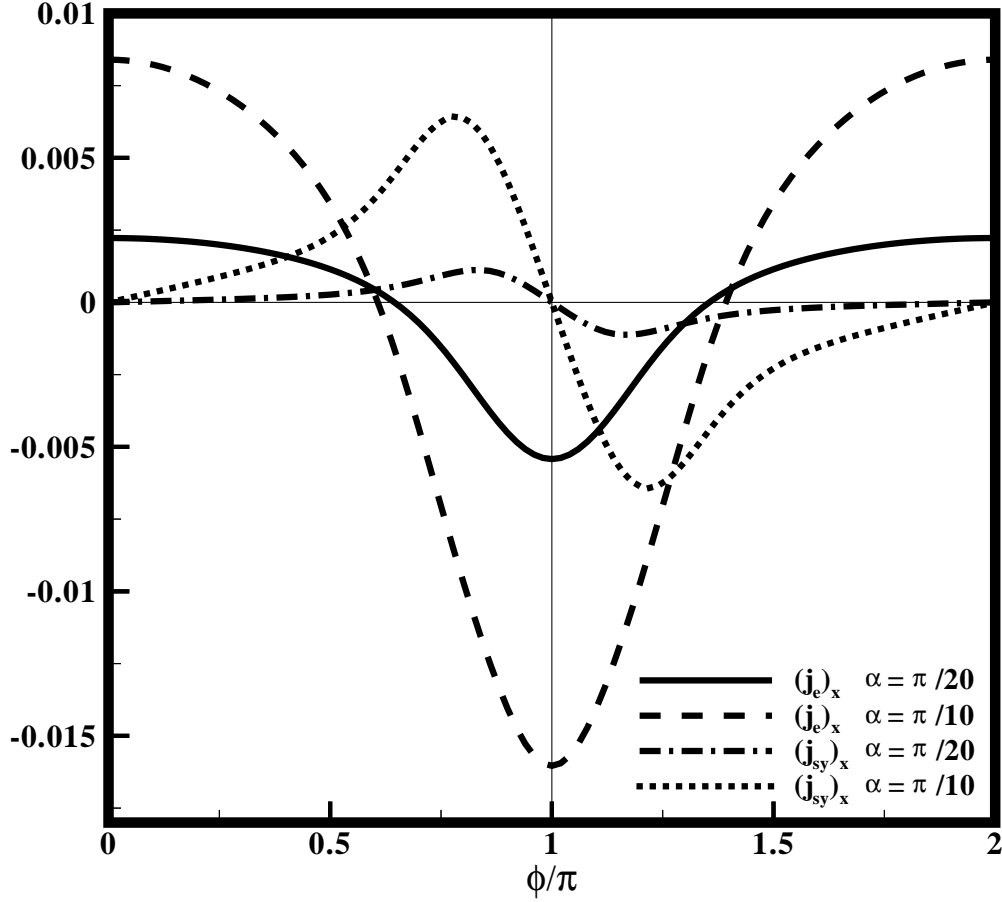


Figure 15. Charge and spin current (s_y) versus the phase difference ϕ for the axial state (102), geometry (ii) and the different misorientations (x -component)

the relative term to the charge current we obtain:

$$g_1(0) = \frac{\varepsilon_m(\Omega_1 + \Omega_2) \cos \beta + i\eta \sin \beta(\Omega_1\Omega_2 + \varepsilon_m^2)}{i\eta \sin \beta \varepsilon_m(\Omega_1 + \Omega_2) + \cos \beta(\Omega_1\Omega_2 + \varepsilon_m^2) + \Delta_1\Delta_2} \quad (97)$$

and for the case of spin current we have:

$$\mathbf{g}_1(0) = \quad (98)$$

$$\mathbf{M}[(B-1)^2 \exp(i\beta)(\eta\Omega_1 + \varepsilon_m)(\eta\Omega_2 + \varepsilon_m) - (B+1)^2 \exp(-i\beta)(\eta\Omega_2 - \varepsilon_m)(\eta\Omega_1 - \varepsilon_m)]$$

where $\eta = \text{sgn}(v_y)$, $\Omega_n = \sqrt{\varepsilon_m^2 + |\mathbf{d}_n|^2}$, $\beta = \psi_1 - \psi_2 + \phi$,

$$B = \frac{\eta\varepsilon_m(\Omega_1 + \Omega_2) \cos \beta + i \sin \beta(\Omega_1\Omega_2 + \varepsilon_m^2)}{i\eta \sin \beta \varepsilon_m(\Omega_1 + \Omega_2) + \cos \beta(\Omega_1\Omega_2 + \varepsilon_m^2) + \Delta_1\Delta_2}, \quad (99)$$

$$A = \frac{\Delta_1\Delta_2(B-1) \exp(i\beta)}{(\eta\Omega_1 - \varepsilon_m)(\eta\Omega_2 - \varepsilon_m)} + \frac{\Delta_1\Delta_2(B+1) \exp(-i\beta)}{(\eta\Omega_1 + \varepsilon_m)(\eta\Omega_2 + \varepsilon_m)} \quad (100)$$

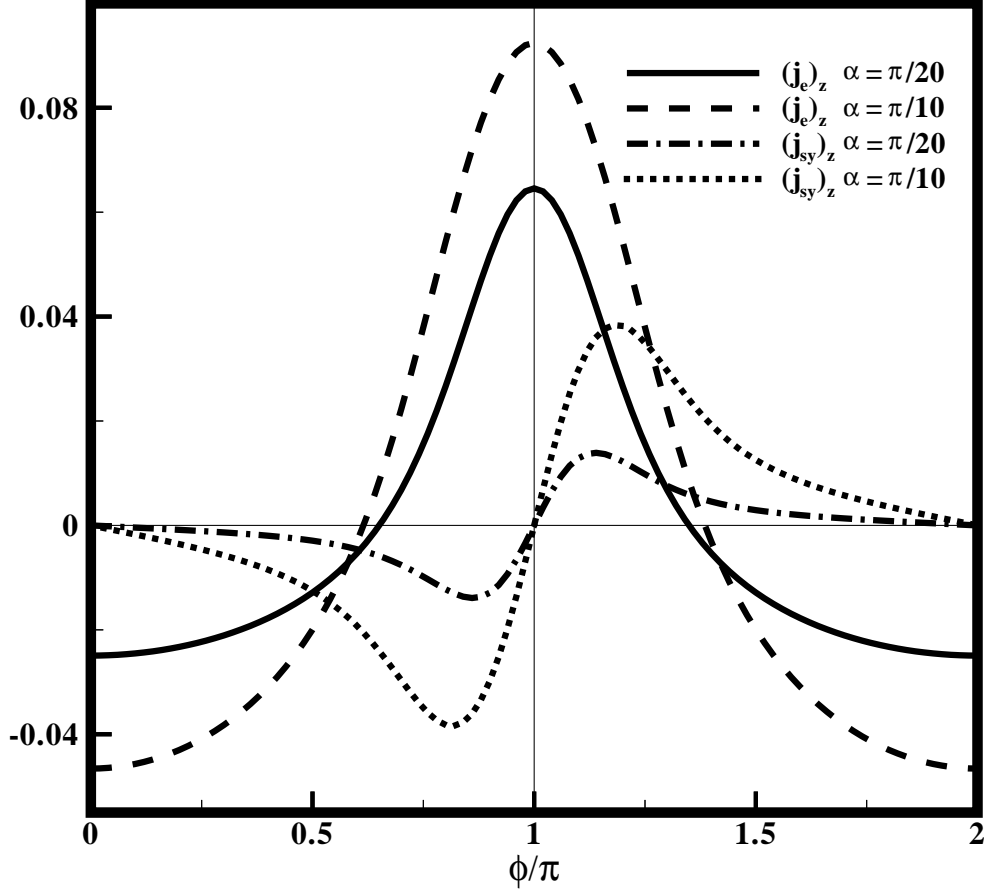


Figure 16. Charge and spin current (s_y) versus the phase difference ϕ for the axial state (102), geometry (ii) and the different misorientations (z -component)

and

$$\mathbf{M} = \frac{\eta \Delta_1 \times \Delta_2}{(A + 2B) |\mathbf{d}_1|^2 |\mathbf{d}_2|^2} \quad (101)$$

Also, $n = 1, 2$ label the left and right half-spaces respectively. We consider a rotation \check{R} only in the right superconductor (see, Fig.12), (i.e., $\mathbf{d}_2(\hat{\mathbf{k}}) = \check{R} \mathbf{d}_1(\check{R}^{-1} \hat{\mathbf{k}})$, $\hat{\mathbf{k}}$ is the unit vector in the momentum space). The crystallographic \mathbf{c} -axis in the left half-space is selected parallel to the partition between the superconductors (along \mathbf{z} -axis in Fig.2). To illustrate the results obtained by computing the formula (97,98), we plot the current-phase diagrams for the different models of the “ f -wave” pairing symmetry (102,103) and for two different geometries. These two geometries are corresponding to the different orientations of the crystals in the right and left sides of the interface (see, Fig.12):

- (i) The basal ab -plane in the right side has been rotated around the c -axis by α ; $\hat{\mathbf{c}}_1 \parallel \hat{\mathbf{c}}_2$.
- (ii) The c -axis in the right side has been rotated around the axis perpendicular to the

interface (y -axis in Fig.12) by α ; $\hat{\mathbf{b}}_1 \parallel \hat{\mathbf{b}}_2$.

Further calculations require a certain model of the gap vector (vector of order parameter) \mathbf{d} .

4.4. Numerical results

In this chapter, two most possible forms of the f -wave order parameter vector in UPt_3 are considered. The first model which is successful to explain the properties of the B -phase of UPt_3 is the axial state. This state describes the strong spin-orbital coupling with vector \mathbf{d} directed along the \mathbf{c} axis of the lattice and it is:

$$\mathbf{d}(T, \mathbf{v}_F) = \Delta_0(T) \hat{\mathbf{z}} k_z (k_x + ik_y)^2. \quad (102)$$

The coordinate axes $\hat{\mathbf{x}}, \hat{\mathbf{y}}, \hat{\mathbf{z}}$ here and below are chosen along the crystallographic axes $\hat{\mathbf{a}}, \hat{\mathbf{b}}, \hat{\mathbf{c}}$ in the left side of Fig.12. The function $\Delta_0 = \Delta_0(T)$ in Eq. (102) and below describes the dependence of the order parameter \mathbf{d} on the temperature T (our numerical calculations have been done at the temperatures close to the $T = 0$). The second model of the order parameter which describes the weak spin-orbital coupling in UPt_3 states, is the unitary planar state. The planar model of gap vector is:

$$\mathbf{d}(T, \mathbf{v}_F) = \Delta_0(T) k_z (\hat{\mathbf{x}} (k_x^2 - k_y^2) + \hat{\mathbf{y}} 2k_x k_y). \quad (103)$$

Using these two models of order parameters (102,103) and solutions to the Eilenberger equations (97) and (98), we have calculated the spin current and charge current densities at the interface numerically. These numerical results are listed below:

1) The spin current can be present, only when misorientation between gap vectors exists. Because in our Green function (98), the spin current is proportional to the “cross product” between the left and right gap vectors. For instance, the spin current for the case of the axial state (102) and geometry (i) is zero, because both of the gap vectors are in the same direction ($\hat{\mathbf{z}}$). (Geometry (i) is a rotation as much as α , around the z axis).

2) In Fig.13 it is shown that for the planar state and geometry (i), it is possible to observe the current of s_z in the direction perpendicular to the interface, but in Figs.14,15 and 16, it is demonstrated that, for the axial state and geometry (ii), only the current of s_y can be observed. Consequently, this kind of junction can be applied as a polarizer or filter for the spin currents.

However, for the planar state and geometry (ii), all terms of the spin current (s_x, s_y and s_z) can be observed (see Eq.98).

3) In Figs.14-20 (planar states), it is shown that the value of the phase differences in which the currents are in the maxima, minima and zero values, are not very sensitive to the misorientation angle α , while the amplitude of maxima and minima, are strongly dependent on the value of misorientation α .

4) In the Figs.13,14 and Fig.17, 18, while the charge currents are the odd functions of ϕ with respect to the line of $\phi = \pi$, the spin currents are even functions of the phase difference; $\mathbf{j}_e(\phi = \pi + \delta\phi) = -\mathbf{j}_e(\phi = \pi - \delta\phi)$ and for the spin current

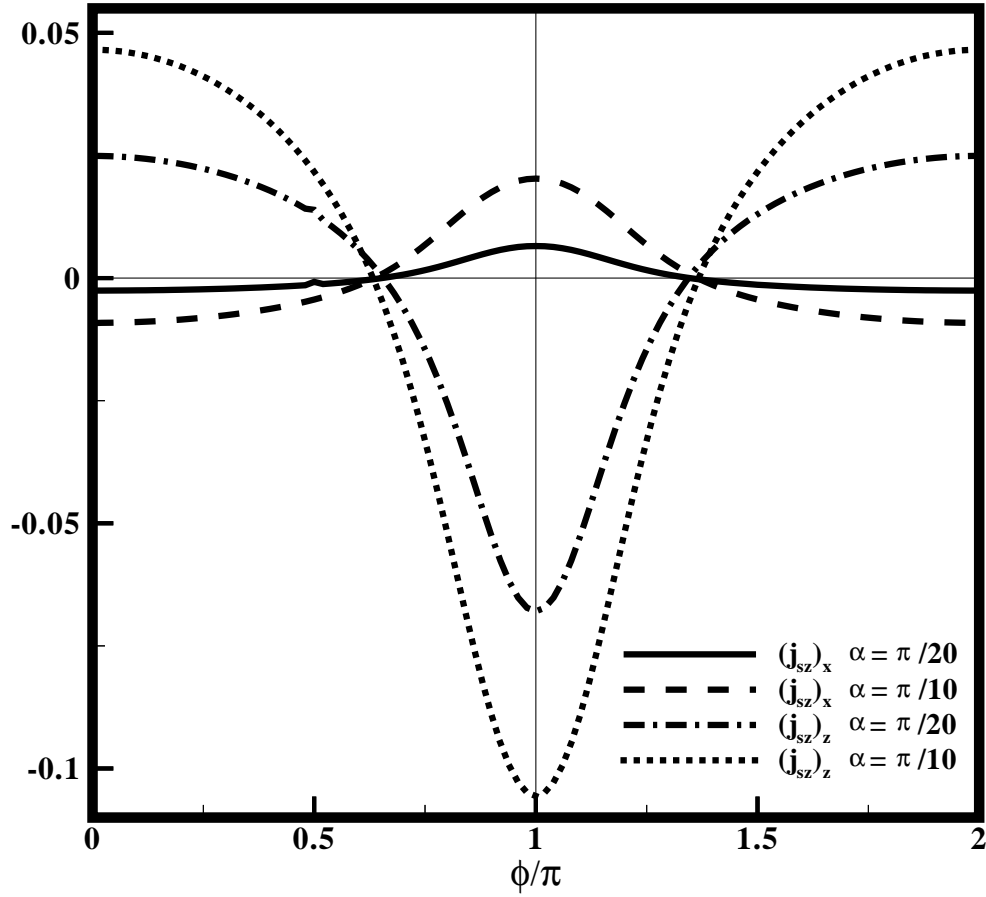


Figure 17. Tangential spin current (s_z) versus the phase difference ϕ for the planar state (103), geometry (ii) and the different misorientations. The perpendicular component (y -direction) of the spin current is absent.

$\mathbf{j}_{s_i}(\phi = \pi + \delta\phi) = \mathbf{j}_{s_i}(\phi = \pi - \delta\phi)$. On the contrary, in the Figs.15 and 16, the charge and spin currents are even and odd functions of ϕ with respect to the line of $\phi = \pi$, respectively; $\mathbf{j}_e(\phi = \pi + \delta\phi) = \mathbf{j}_e(\phi = \pi - \delta\phi)$ and $\mathbf{j}_{s_i}(\phi = \pi + \delta\phi) = -\mathbf{j}_{s_i}(\phi = \pi - \delta\phi)$.

5) In Fig.13, the perpendicular component of the spin and charge current in terms of the external phase difference ϕ for the case of the planar state (103), geometry (i) and for two different misorientations are plotted. The solid line is the charge current-phase dependence [6]. Also, at the $\phi = 0$, $\phi = \pi$ and $\phi = 2\pi$, the charge current (Josephson current) is zero while the spin current has the finite value.

6) The perpendicular component of the charge (Josephson current) and spin current for the case of the axial state (102) and geometry (ii) are plotted in Fig.14, and the tangential components of them, are plotted in Figs.15,16. The charge current-phase diagrams have been obtained before in paper [6] and they are totally different from the

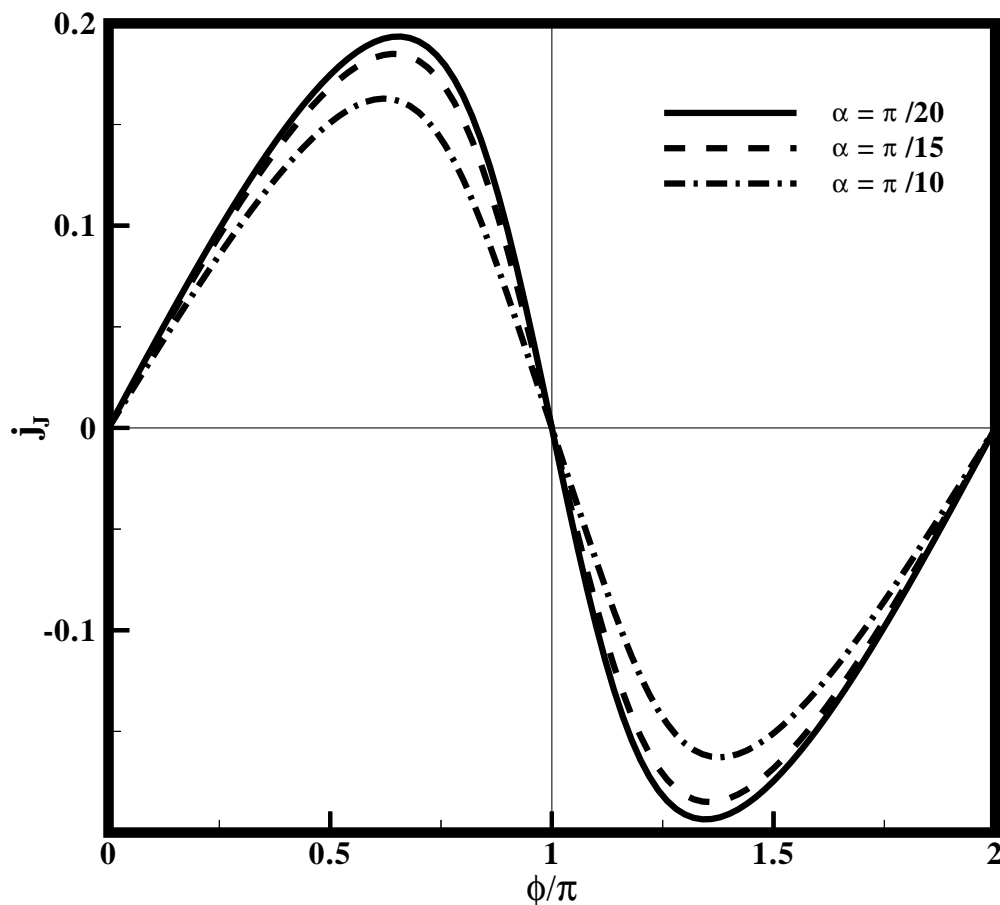


Figure 18. The perpendicular component of the charge current (Josephson) versus the phase difference ϕ for the planar state (103), geometry (ii) and the different misorientations. The tangential components (x and z -directions) are absent.

case of conventional superconductors in the paper [30]. At the phase values of $\phi = 0$, $\phi = \pi$ and $\phi = 2\pi$, in which the charge current is exactly zero, the spin current has the finite values and may select its maximum value. In Figs.13,14 and specially Fig.20, for a small value of misorientation we have a very long but narrow peak in the spin current phase diagram, close to the $\phi = \pi$.

7) Both the planar state with geometry (i) and the axial state with geometry (ii) can be applied as the filter for polarization of the spin transport (see Figs13-16), the former transports only the s_z but the latter case flows the s_y (see .98). In addition, the planar states with geometry (ii) can be used as a switch for the spin and charge current into two directions: parallel and perpendicular to the interface. In this case, the spin and charge currents select only one of the directions parallel or perpendicular to the interface. Namely, it is impossible to observe the tangential and perpendicular components of the

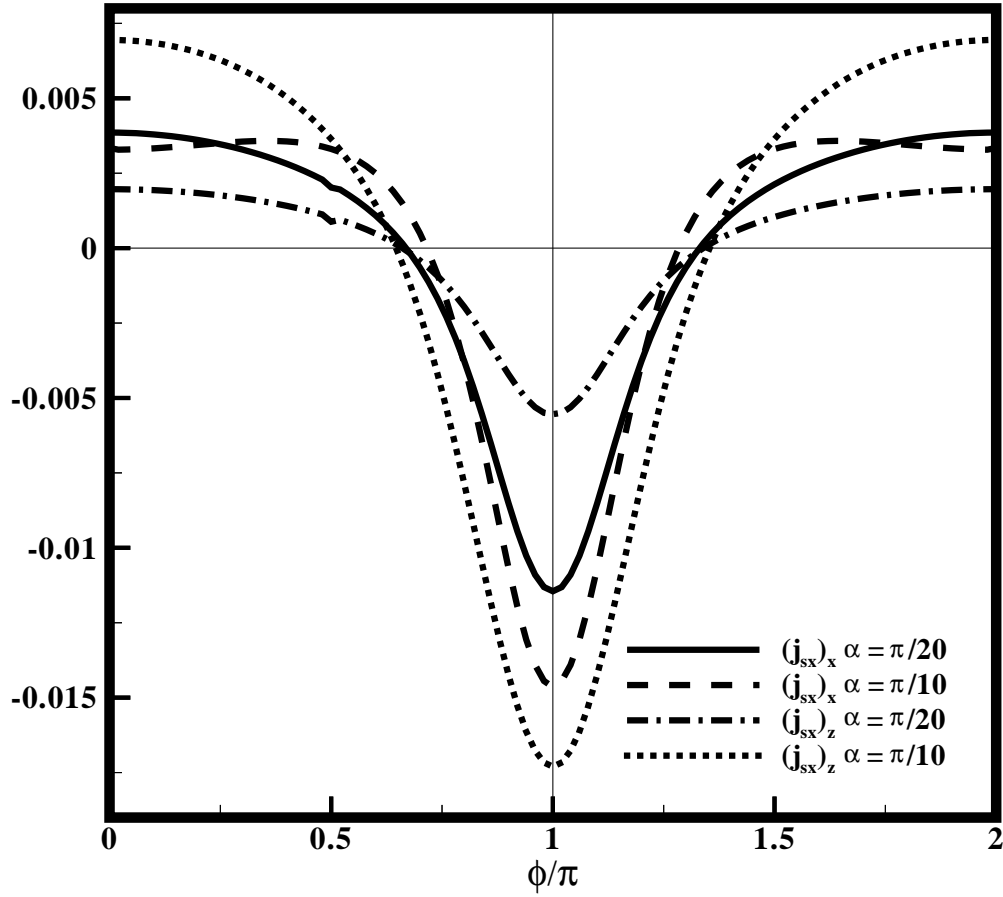


Figure 19. Tangential spin currents (s_x) versus the phase difference ϕ for the planar state (103), geometry (ii) and the different misorientations. The perpendicular component (y -direction) of the spin current is absent.

currents at the same time for planar state with geometry (ii)(Figs.17-20).

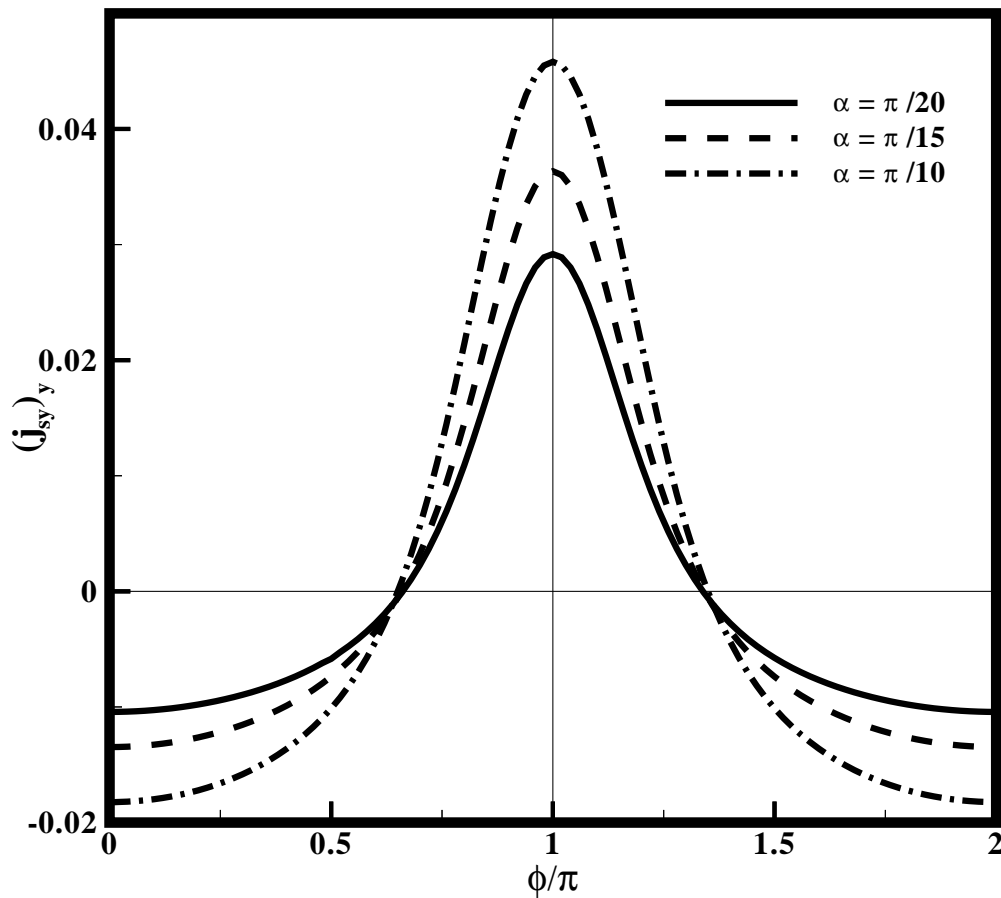


Figure 20. Perpendicular component of the spin current (s_y) versus the phase difference ϕ for the planar state (103), geometry (ii) and the different misorientations. The tangential components (x and z directions) are absent.

5. Weak link between $PrOs_4Sb_{12}$ superconducting banks

5.1. Introduction

The “ $(p + h)$ -wave” form of pairing symmetry has been considered for the superconductivity in $PrOs_4Sb_{12}$ compound, recently. In this chapter, a stationary Josephson junction as a weak-link between $PrOs_4Sb_{12}$ triplet superconductors is theoretically investigated. The Eilenberger equation is solved for two distinct models of the order parameter (A and B -phases). The spin and charge current-phase diagrams are plotted and the effect of misorientation between crystals on the Josephson, spontaneous and spin current is studied. It is obtained that such experimental investigations of the current-phase diagrams can be used to test the pairing symmetry in the above-mentioned superconductors. In this chapter, it is shown that this apparatus can be applied as a

polarizer for the spin current. Furthermore, it is observed that at some certain values of the phase differences in which the charge current is zero, the spin current exists while carriers of both of charge and spin are the same (electrons).

The pairing symmetry of the recently discovered superconductor compound $PrOs_4Sb_{12}$ is an interesting topic of research in the field of superconductivity [8, 25, 78]. Superconductivity in this compound has been discovered in papers [79, 80, 81] and two different phases (A and B) have been considered for this kind of superconductor in papers [25, 26]. Although people at first have considered the spin-singlet “ $(s+g)$ –wave” pairing symmetry to this superconductor [25] but later it has been specified that the spin-triplet is the real pairing symmetry of $PrOs_4Sb_{12}$ complex [8, 82]. Authors of paper [82], using the knight shift in NMR measurement estimated the spin-triplet pairing symmetry for the superconductivity in $PrOs_4Sb_{12}$. Consequently, the “ $(p+h)$ –wave” proposed for the pairing symmetry of the superconductivity in $PrOs_4Sb_{12}$ compound, recently [8]. In this chapter, the self-consistent equation for the gap vectors (BCS gap equation) have been solved for the finite temperature numerically and for the temperatures close to the zero and the critical temperature analytically. For this compound and using the “ $(p+h)$ –wave” symmetry for the order parameter vector (gap function), the value of the order parameter at the zero temperature has been obtained for both A and B -phases, in terms of the critical temperature of this type of superconductivity (T_c). In addition, the gap dependence on the temperature close to the zero and critical temperatures have been obtained. Authors of paper [8] have investigated the critical magnetic field and the temperature dependence of critical field, specific heat and heat conduction.

Also, the Josephson effect in the point contact between triplet superconductors has been studied in paper [6]. In this chapter, the effect of misorientation on the charge transport has been studied and a spontaneous current tangential to the interface between the f –wave superconductors has been observed. Additionally, the spin-current in the weak-link between the f –wave superconductors has been investigated in the paper [83]. The authors of paper [83], have proposed this kind of weak-link device as the filter for polarization of the spin-current. These weak-link structures have been used to demonstrate the order parameter symmetry in paper [64].

In this chapter, the ballistic Josephson weak-link via an interface between two bulk of “ $(p+h)$ –wave” superconductors with different orientations of the crystallographic axes is investigated. It is shown that the spin and charge current-phase diagrams are totally different from the current-phase diagrams of the junction between conventional (s -wave) superconductors [30], high T_c (d -wave) superconductors [48] and from the spin-current phase diagrams in the weak-link between the f -wave superconductors [83]. In this weak-link structure between the “ $(p+h)$ –wave” superconductors, the spontaneous current parallel to the interface as the characteristic of unconventional superconductivity can be present. The effect of misorientation on the spontaneous, Josephson and spin currents for the different models of the pairing symmetry (A – and B – phases in Fig.5.1) are investigated. It is possible to find the value of the phase difference in which the Josephson current is zero but the spontaneous current tangential to the interface, which

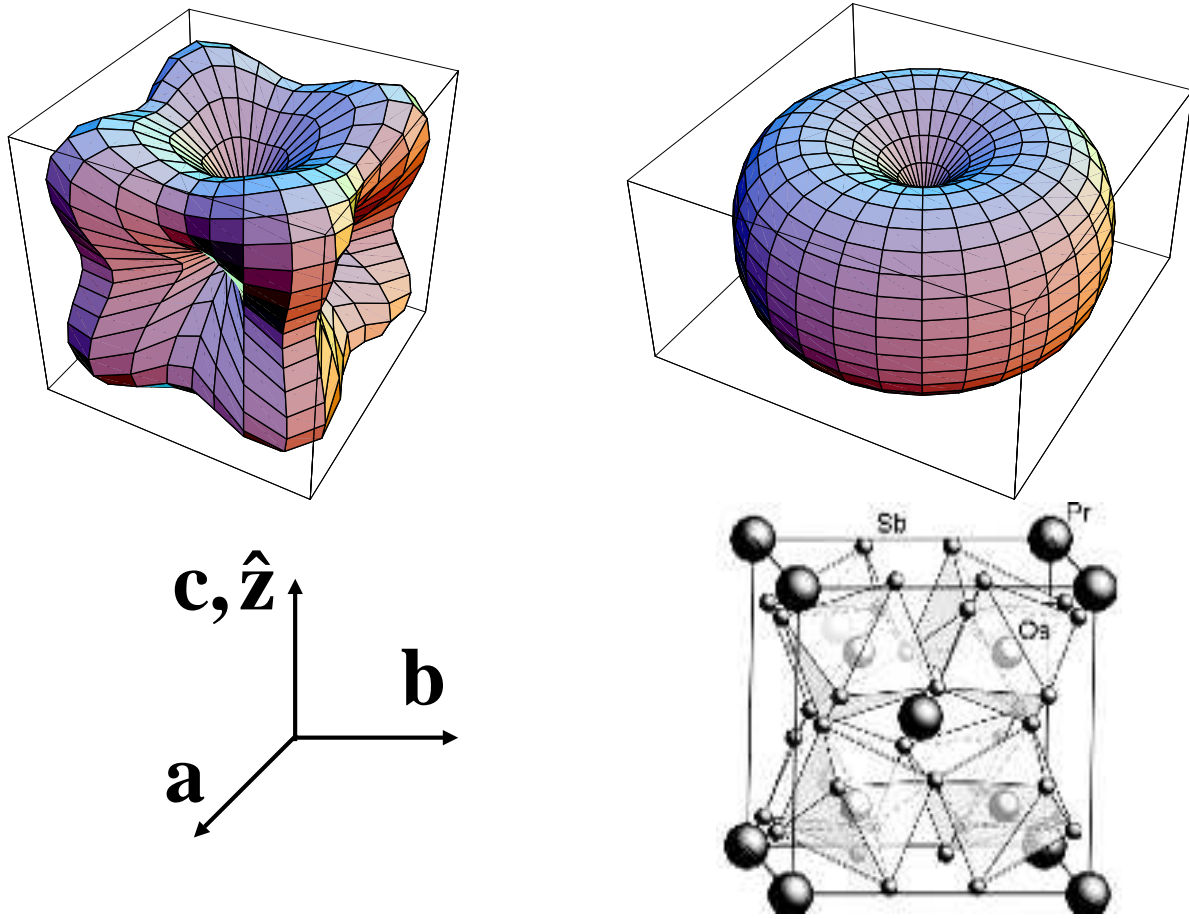


Figure 21. *A*-phase (left-above), *B*-phase (right-above) order parameters, direction of *a*, *b*, *c* and \hat{z} unit vectors (left-below) and chemical structure of $PrOs_4Sb_{12}$ molecule [25]. *A*- and *B*- phases are high field (high temperature) and low field (low temperature) phases, respectively [27].

is produced by the interface, exists. In some of configurations and at the zero phase difference, the Josephson current is not zero and it has a finite value, this finite value corresponds to a spontaneous phase difference which is related to the misorientation between the gap vectors.

Finally, It is observed that at the some certain values of the phase differences ϕ in which the charge current is zero the spin current exists and vice versa. In addition, in this configuration in which the gap vectors are selected along the \hat{z} direction and the unit vector perpendicular to the interface is \hat{y} direction, only the spin current of the s_y can be present and the other terms of the spin current are absent totally. Consequently, this structure can be used as a filter for polarization of the spin transport. Furthermore, our analytical and numerical calculations have shown that the misorientation is the origin of the spin current and in the absence of the misorientation spin current is absent while

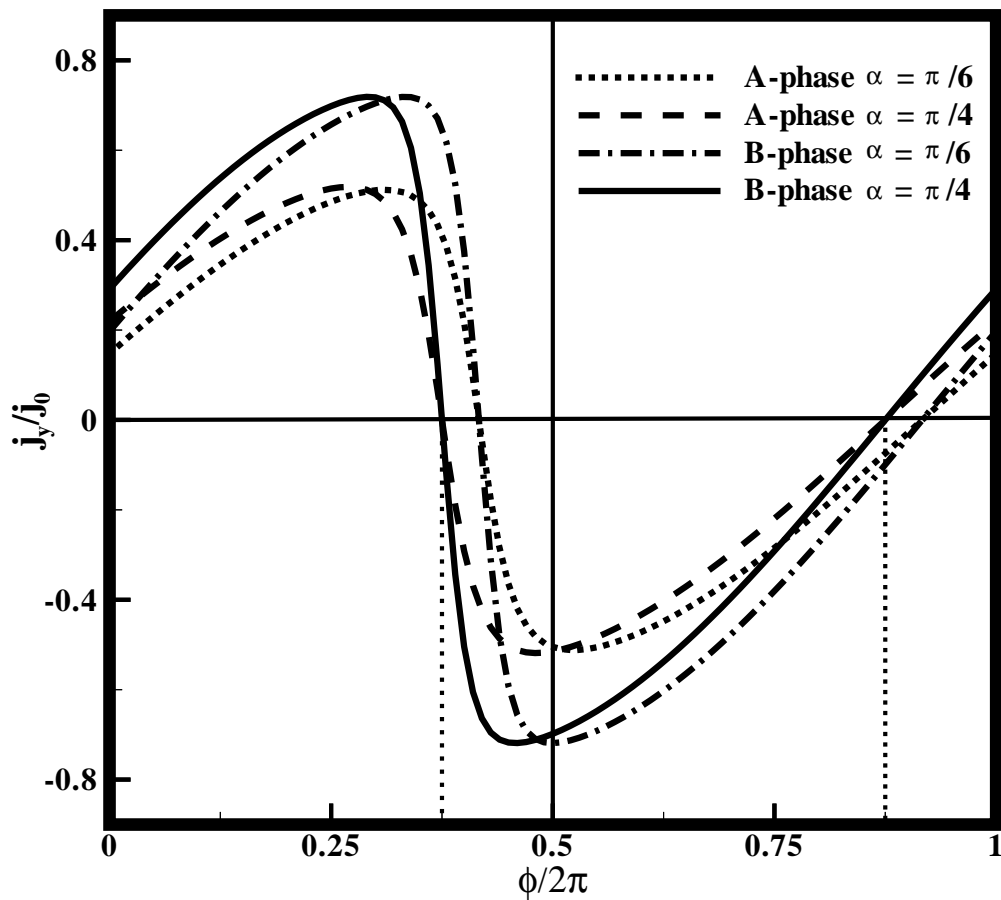


Figure 22. Perpendicular component of current (Josephson current) versus the phase difference ϕ for *A* and *B*-phases, geometry (i), $T/T_c = 0.08$ and the different misorientations. Currents are given in units of $j_0 = \frac{\pi}{2}eN(0)v_F\Delta_0(0)$.

the charge current flows.

In Sec.(5.2) the obtained formulas for the Green functions will be discussed and an analysis of numerical results will be done.

5.2. Discussions

In this chapter again we consider a model of a flat interface $y = 0$ between two misorientated “ $(p + h)$ -wave” superconducting half-spaces (Fig.12) as a ballistic Josephson junction. As same as the previous chapter, in our calculations, a simple model of the constant order parameter up to the interface is considered and the pair breaking and the scattering on the interface are ignored. The solution of Eqs. (1) and (84) allows us to calculate the charge and spin current densities. Again, we assume that the order parameter does not depend on coordinates and in each half-space it equals

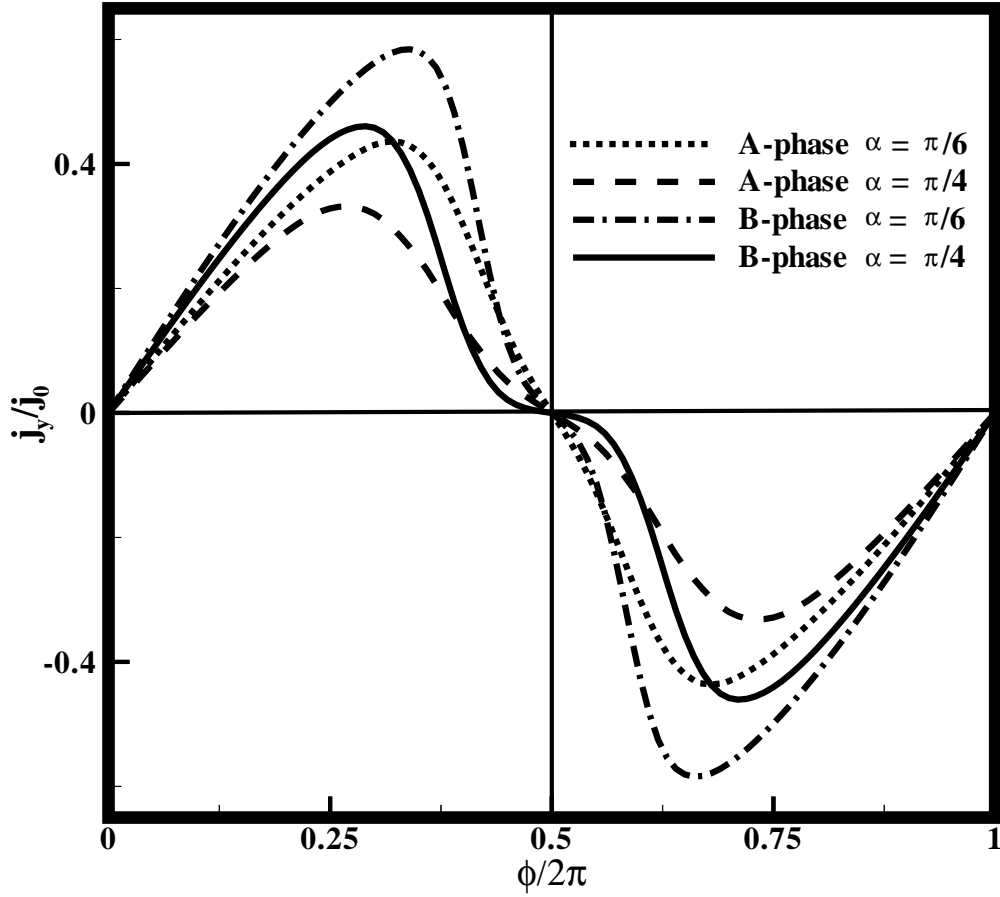


Figure 23. Perpendicular component of current (Josephson current) versus the phase difference ϕ for *A* and *B*-phases, geometry (ii), $T/T_c = 0.08$ and the different misorientations.

to its value (112) far from the interface in the left or right bulks. For such a model, the current-phase dependence of a Josephson junction can be calculated analytically. It enables us to analyze the main features of current-phase dependence for the different models of the order parameter of “ $(p + h)$ -wave” superconductivity. To illustrate the results obtained by computing the formula (97), we plot the current-phase diagrams for the different models of the “ $(p + h)$ -wave” pairing symmetry (104,105) and for two different geometries. These geometries are corresponding to the different orientations of the crystals in the right and left sides of the interface (Fig.12):

- (i) The basal *ab*-plane in the right side has been rotated around the *c*-axis by α ; $\hat{\mathbf{c}}_1 \parallel \hat{\mathbf{c}}_2$.
- (ii) The *c*-axis in the right side has been rotated around the *b*-axis by α (*y*-axis in Fig.12); $\hat{\mathbf{b}}_1 \parallel \hat{\mathbf{b}}_2$.

Further calculations require a certain model of the gap vector (vector of order parameter)

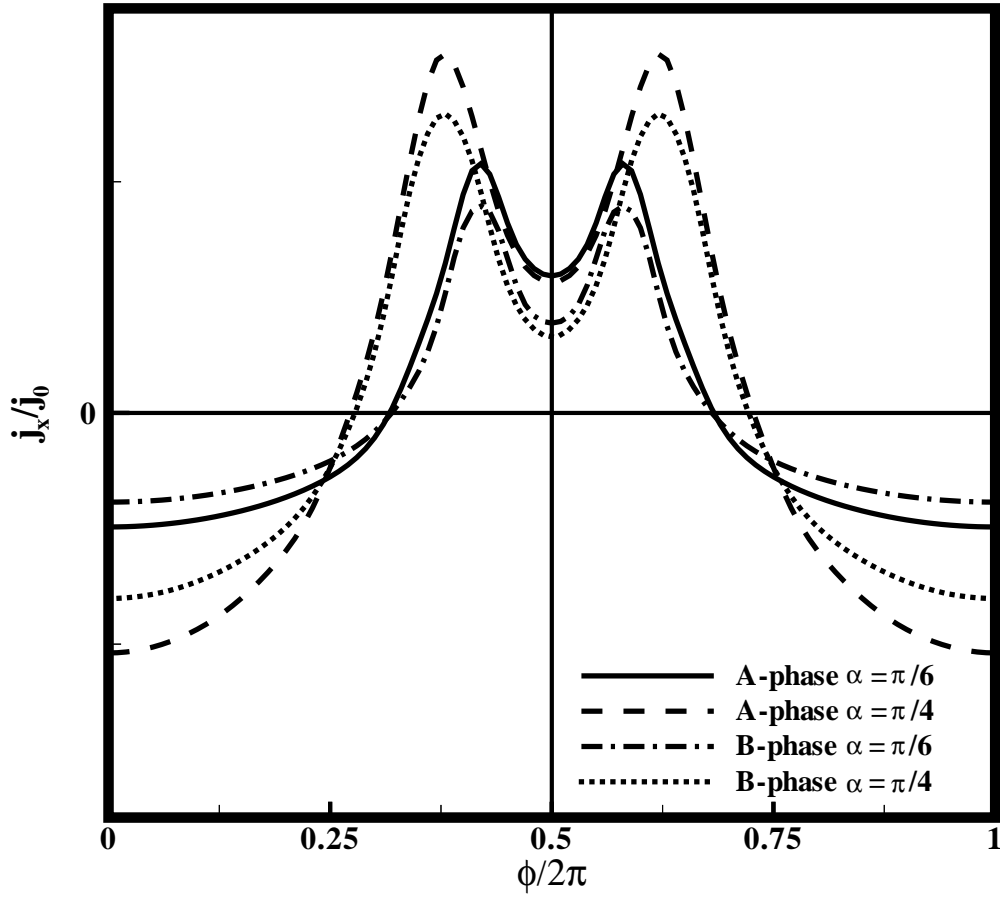


Figure 24. Tangential (to the interface) component of current versus the phase difference ϕ for *A* and *B*-phases, geometry (ii), $T/T_c = 0.08$ and the different misorientations (x -component).

d.

In this chapter, two forms of the “ $(p+h)$ -wave” unitary gap vector in $PrOs_4Sb_{12}$ are considered. The first model to explain the properties of the *A*-phase of $PrOs_4Sb_{12}$ is:

$$\mathbf{d}(T, \hat{\mathbf{k}}) = \Delta_0(T)(k_x + ik_y)\frac{3}{2}(1 - \hat{k}_x^4 - \hat{k}_y^4 - \hat{k}_z^4)\hat{\mathbf{z}} \quad (104)$$

The coordinate axes $\hat{\mathbf{x}}, \hat{\mathbf{y}}, \hat{\mathbf{z}}$ here and below are chosen along the crystallographic axes $\hat{\mathbf{a}}, \hat{\mathbf{b}}, \hat{\mathbf{c}}$ in the left side of Fig.12. The function $\Delta_0 = \Delta_0(T)$ in Eq. (104) and below describes the dependence of the gap vector \mathbf{d} on the temperature T . The second model to describe the gap vector of the *B*-phase of $PrOs_4Sb_{12}$ is:

$$\mathbf{d}(T, \hat{\mathbf{k}}) = \Delta_0(T)(k_x + ik_y)(1 - \hat{k}_z^4)\hat{\mathbf{z}} \quad (105)$$

Our numerical calculations are done at the low temperatures, $T/T_c = 0.08$, and

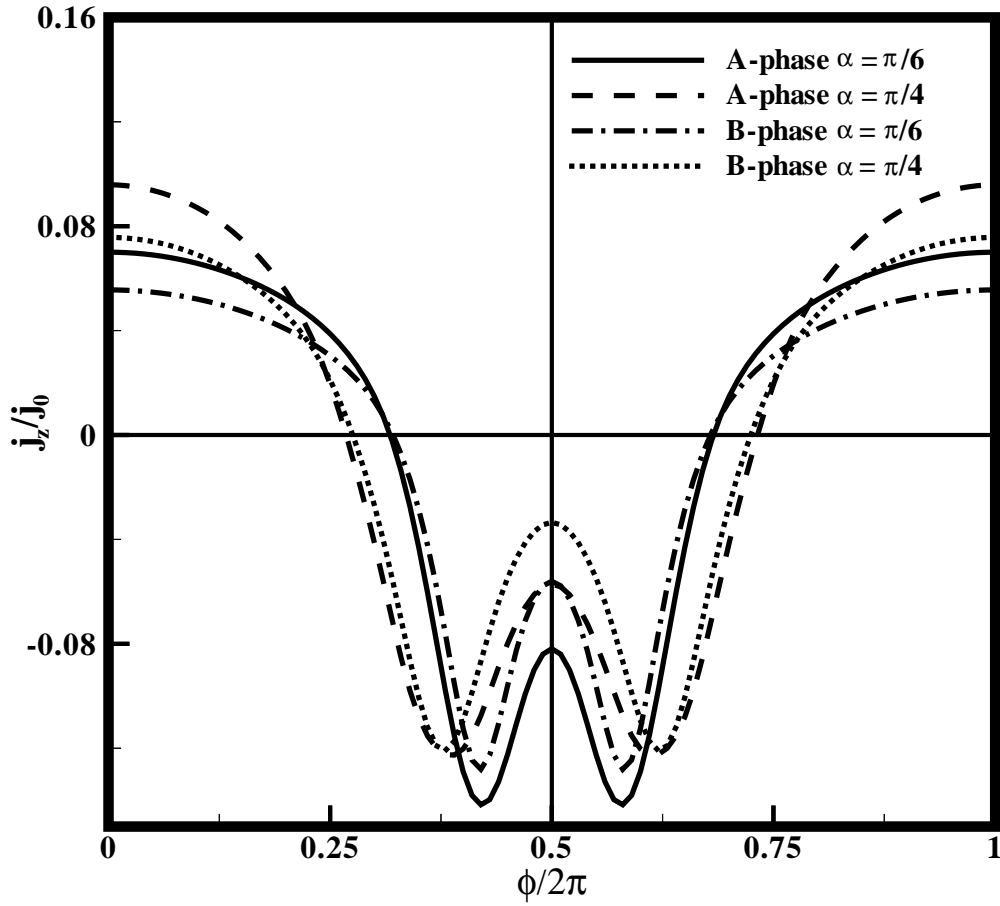


Figure 25. Tangential (to the interface) component of current versus the phase difference ϕ for the both A and B -phases, geometry (ii), $T/T_c = 0.08$ and the different misorientations(z -component).

we have used the formulas $\ln(\Delta(T)/\Delta(0)) = -\frac{7\pi\zeta(3)}{8}\left(\frac{T}{\Delta(0)}\right)^3$ for the A -phase and $\ln(\Delta(T)/\Delta(0)) = -\frac{135\pi\zeta(3)}{512}\left(\frac{T}{\Delta(0)}\right)^3$ for the B -phase, from the paper [8], for temperature dependence of the gap functions $\Delta_0(T)$ at the low temperatures ($T \ll T_c$). Also, in the mentioned paper [8] the value of $\Delta_0(T)$ in terms of the critical temperatures has been calculated for both A and B - phases. They are $\Delta(0)/T_c = 2.34$ and $\Delta(0)/T_c = 1.93$ for A and B - phases, respectively. Using these two models of order parameters (104,105) and solution to the Eilenberger equations (97,98), we have calculated the current density at the interface numerically. These numerical results are listed below [84]:

1) In Fig.22, the perpendicular component of current (perpendicular to the interface) which is called Josephson current is plotted for both A and B -phases, geometry (i), misorientations $\alpha = \pi/4$ and $\alpha = \pi/6$. It is observed that the critical values of current for B -phase is greater than A -phase. Also, in spite of junction between the

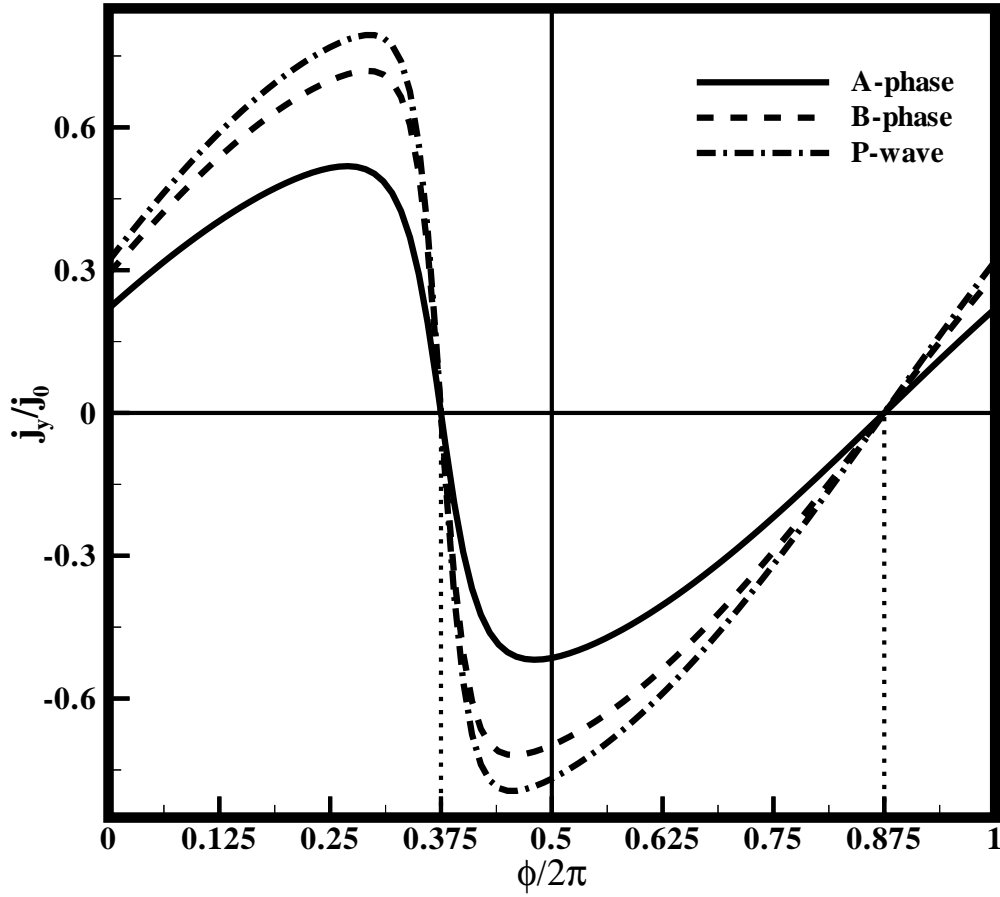


Figure 26. Perpendicular component of current (Josephson current) versus the phase difference ϕ for geometry (i), $\frac{T}{T_c} = 0.08$, $\alpha = \frac{\pi}{4}$, A -phase, B -phase and p -wave pairing symmetry.

conventional superconductors and planar Josephson junction, at the $\phi = 0$, the current is not zero. The current is zero at the phase difference value $\phi = \phi_0$, which depends on the misorientation between the gap vectors. In Fig.22, the value of the spontaneous phase difference ϕ_0 is close to the misorientation α .

2) In Fig.23, Josephson current is plotted for both A and B -phases, geometry (ii) and different misorientations. Again, the maximum value of the current for the B -phase is greater than A -phase. Increasing the misorientation between the gap vectors, the maximum value of current decreases. It is demonstrated that at the phase difference values $\phi = 0$, $\phi = \pi$ and $\phi = 2\pi$, the Josephson current is zero while, both of spontaneous and spin currents are not zero and have the finite value. Increasing the misorientation between the gap vectors decreases the derivative of the current with respect to the phase difference ($\frac{dj_y}{d\phi}$) close to the $\phi = \pi$.

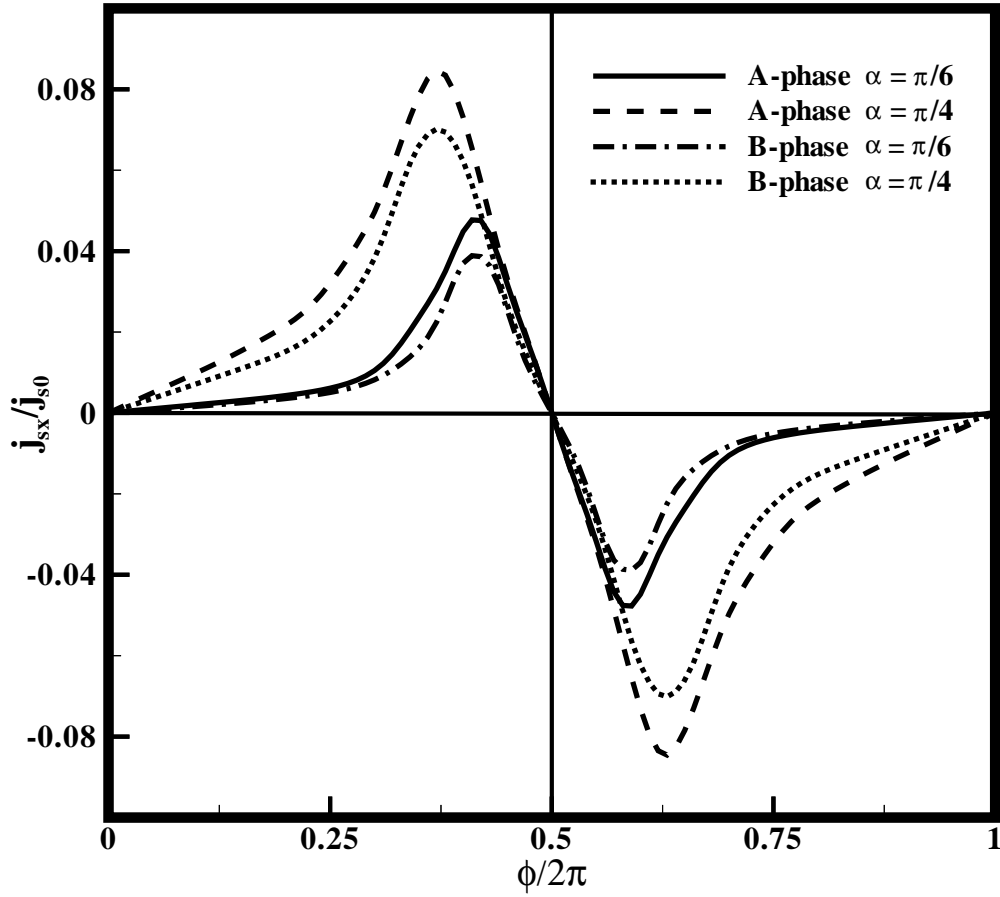


Figure 27. Tangential component of spin (s_y) current (x -component) versus the phase difference ϕ for geometry (ii), $\frac{T}{T_c} = 0.08$ and different misorientations between the A and B -phase of “ $(p+h)$ -wave” pairing symmetry.

3) In Figs.24,25, the tangential components of charge current (x and z -components) in terms of the phase difference ϕ are plotted. It is seen that at the $\phi = 0$, $\phi = \pi$ and $\phi = 2\pi$ in which the Josephson current is zero the parallel spontaneous currents have the finite values. Although the perpendicular component of charge current (see Fig.23) is an odd function of the phase difference with respect to the line of $\phi = \pi$ but the parallel charge currents are even functions at the phase differences close to $\phi = \pi$ (see Fig.24 and Fig.25).

4) In Fig.26, the Josephson current in terms of the phase difference is plotted for the case of p -wave, and A and B -phases of “ $(p+h)$ -wave”. The p -wave pairing symmetry as the first candidate for the superconducting state in Sr_2RuO_4 is as follows [19]:

$$\mathbf{d}(T, \hat{\mathbf{k}}) = \Delta_0(T)(k_x + ik_y)\hat{\mathbf{z}} \quad (106)$$

It is observed that the maximum value of Josephson current (j_y) of junction between

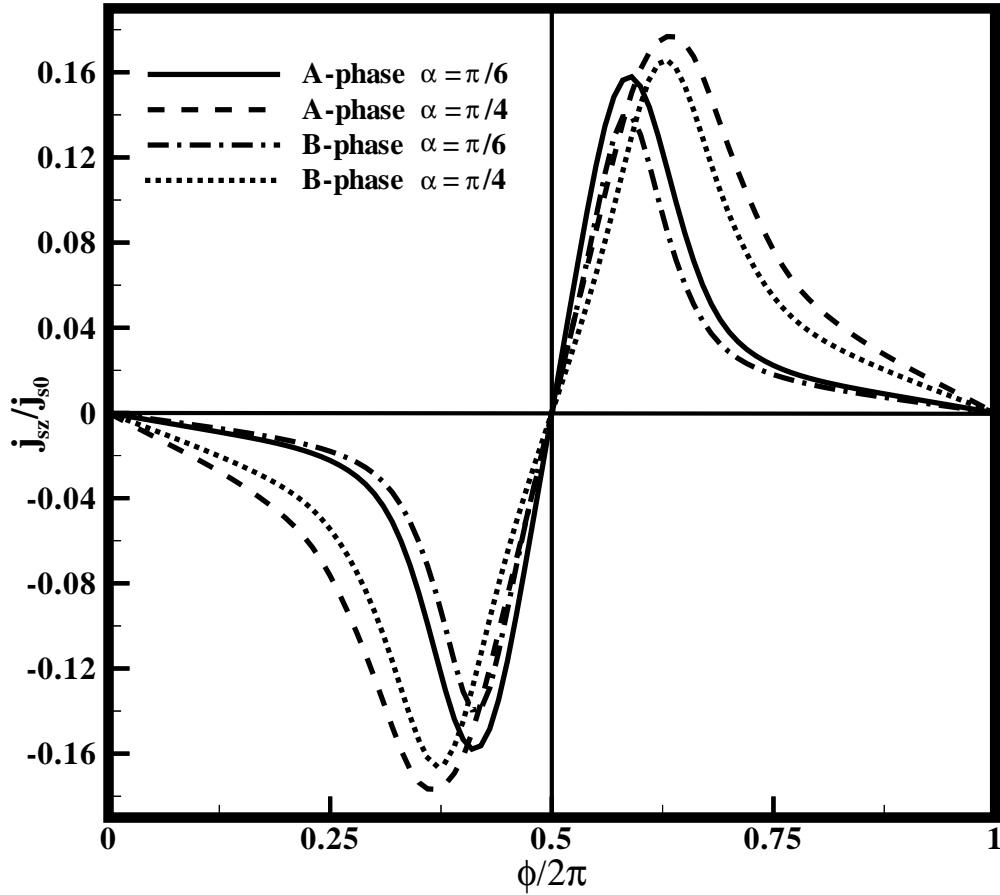


Figure 28. Tangential component of spin (s_y) current (z -component) versus the phase difference ϕ for geometry (ii), $\frac{T}{T_c} = 0.08$ and different misorientations between the A and B -phase of “ $(p+h)$ -wave” pairing symmetry.

the p -wave superconductors, is greater than the B -phase of “ $(p+h)$ -wave” and the Josephson current of second is greater than its A -phase counterpart. Also, the place of the zero of the current is at the spontaneous phase difference which is close to the misorientation $\phi_0 = \alpha$ (look at the Fig.32).

5) In Figs.27,28, the tangential spin (s_y) currents in terms of the phase difference is plotted for different misorientations and geometry (ii). By increasing the misorientation the maximum value of spin current increases. In spite of the charge current for this state, the spin current at the phase differences $\phi = 0$, $\phi = \pi$ and $\phi = 2\pi$ is exactly zero (compare Figs.24 and 25 with Figs.27 and 28).

6) In Figs.29,30, the perpendicular component of charge and spin current (j_y and j_{sy}) are plotted for different misorientations and A and B -phases respectively. An interesting case in our observations is the finite value of the perpendicular spin current at the $\phi = 0$,

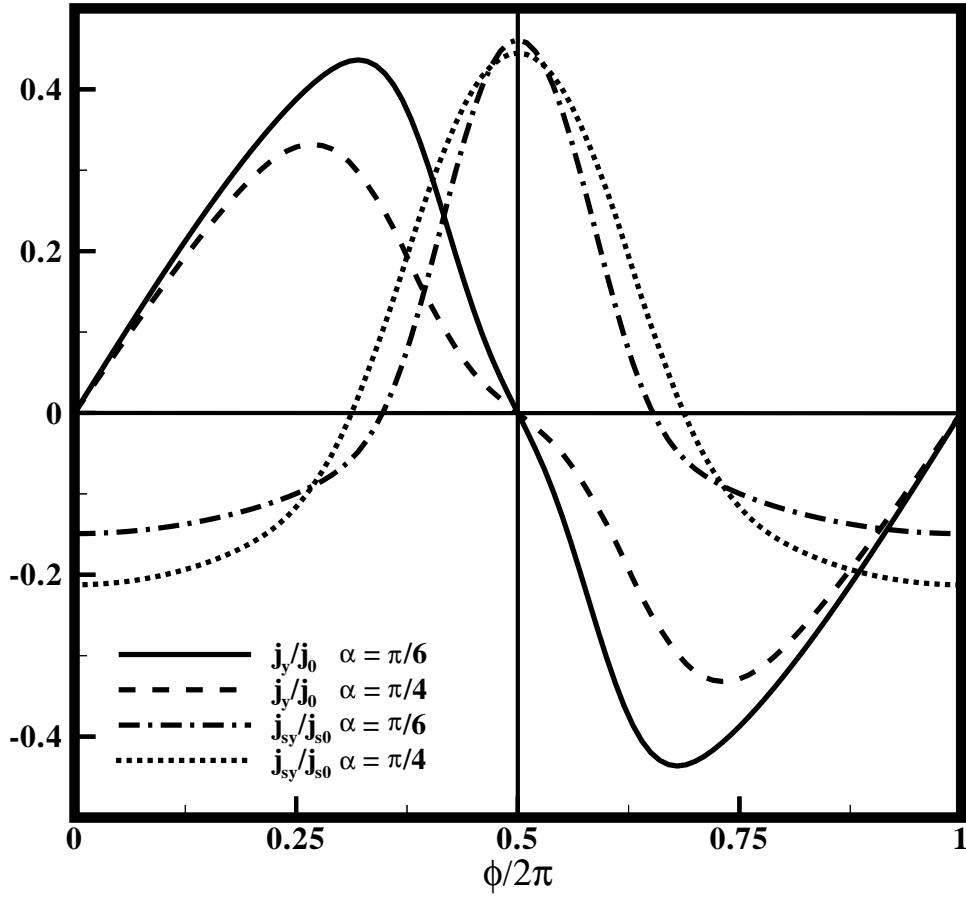


Figure 29. Perpendicular component of charge and spin current (j_y and j_{sy}) versus the phase difference ϕ for A -phase, geometry (ii), $\frac{T}{T_c} = 0.08$, $\alpha = \frac{\pi}{6}$ and $\alpha = \frac{\pi}{4}$.

$\phi = \pi$ and $\phi = 2\pi$ at which the perpendicular charge current (j_y) is zero (see Figs.29 and 30).

7) In Fig.31, the perpendicular component of the spin current is plotted for p -wave, A and B -phases of “ $(p + h)$ -wave” pairing symmetries and for a specified value of misorientation $\alpha = \frac{\pi}{4}$. In both Figs.26 and 31 the maximum value of current of junction between the p -wave is greater than B -phase and B -phase has the maximum value greater than junction between the A -phase. This different character of the current-phase diagrams enables us to distinguish between the three states. Also, It is observed that at the phase differences $\phi = 0$, $\phi = \pi$ and $\phi = 2\pi$, the spin current has the finite value and may have its maximum value. This is a counterpart of Fig.23, in that figure the charge currents are zero at the mentioned value of the phase difference but the spin current has the finite value.

Furthermore, our analytical and numerical calculations have shown that the origin of

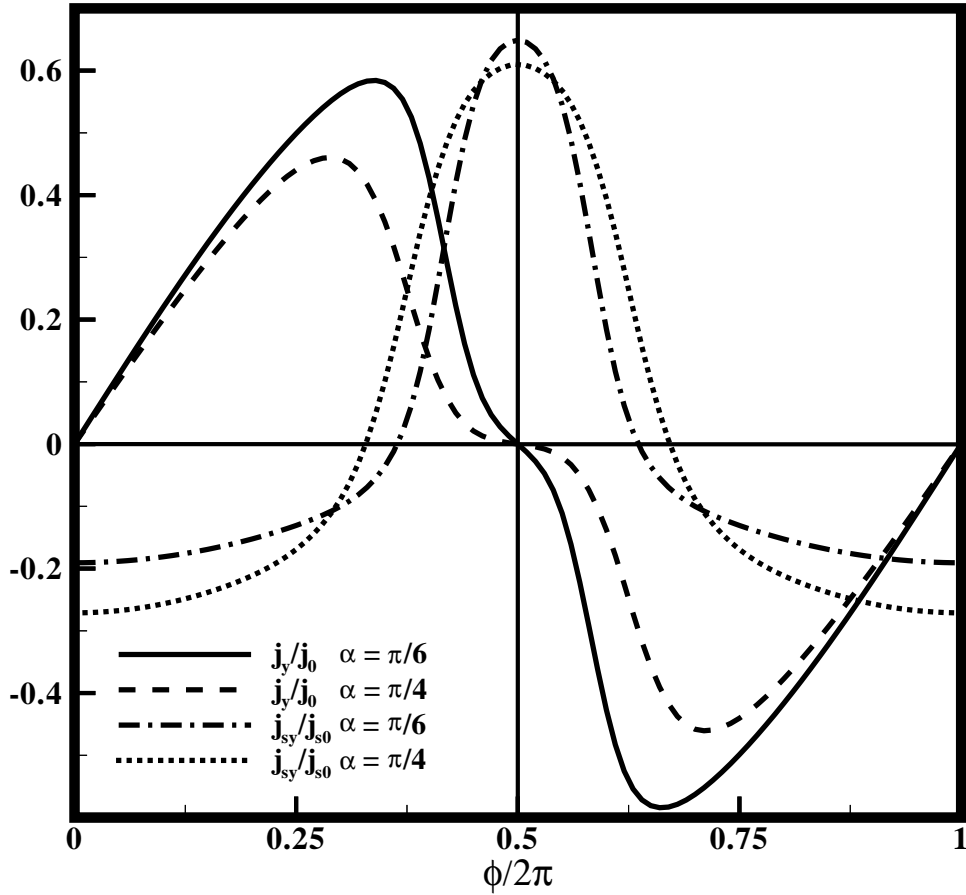


Figure 30. Perpendicular component of charge and spin current (j_y and j_{sy}) versus the phase difference ϕ for B -phase, geometry (ii), $\frac{T}{T_c} = 0.08$, $\alpha = \frac{\pi}{6}$ and $\alpha = \frac{\pi}{4}$.

the spin current is misorientation between the gap vectors (cross product in Eq.98). Thus the spin current in the weak link between geometry (i) misorientated crystals is zero. Because the geometry (i) is a rotation by α around the \hat{z} -axis and both of the left and right gap vectors are in the same direction and cross product between them is zero. Also, it is shown that in this structure (y -direction is perpendicular to the interface, gap vectors c -axis are selected in the z -direction and rotation is done around the y -direction) only the current of the s_y flows and other terms of the spin current are totally absent. So, this kind of weak-link experiment can be used as the filter for polarization of spin transport. Since the spin is a vector, the spin current is a tensor and we have the current of spin s_y in the three \hat{x} , \hat{y} and \hat{z} directions.

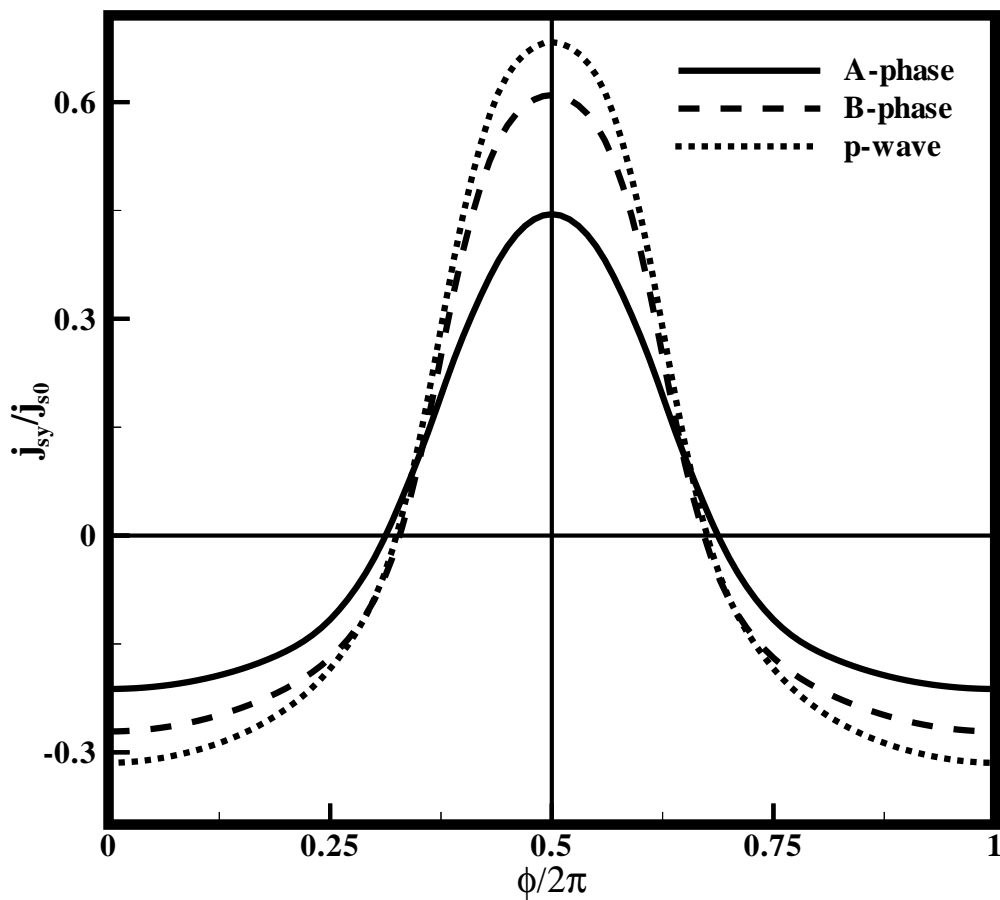


Figure 31. Perpendicular component of spin current (j_{sy}) versus the phase difference ϕ for geometry (ii), $\frac{T}{T_c} = 0.08$, $\alpha = \frac{\pi}{4}$, A -phase, B -phase and p -wave pairing symmetry.

6. Weak link between nonunitary triplet superconductors

6.1. Introduction

A stationary Josephson effect in a weak-link between misorientated nonunitary triplet superconductors is investigated theoretically. The non-self-consistent quasiclassical Eilenberger equation for this system has been solved analytically. As an application of this analytical calculation, the current-phase diagrams are plotted for the junction between two nonunitary bipolar f -wave superconducting banks. A spontaneous current parallel to the interface between superconductors has been observed. Also, the effect of misorientation between crystals on the Josephson and spontaneous currents is studied. Such experimental investigations of the current-phase diagrams can be used to test the pairing symmetry in the above-mentioned superconductors.

In the recent years, the triplet superconductivity has become one of the modern subjects for researchers in the field of superconductivity [5, 7, 85]. Particularly, the nonunitary spin triplet state in which, Cooper pairs may carry a finite averaged intrinsic spin momentum, has attracted much attention in the last decade [15, 86]. A triplet state in the momentum inverse space (\mathbf{k}) can be described by the order parameter $\hat{\Delta}(\mathbf{k}) = i(\mathbf{d}(\mathbf{k}) \cdot \hat{\sigma})\hat{\sigma}_y$ in a 2×2 matrix form in which $\hat{\sigma}_j$ s are 2×2 Pauli matrices. The three dimensional complex vector $\mathbf{d}(\mathbf{k})$ demonstrates the triplet pairing state exactly. In the nonunitary state, the product $\hat{\Delta}(\mathbf{k})\hat{\Delta}(\mathbf{k})^\dagger = \mathbf{d}(\mathbf{k}) \cdot \mathbf{d}^*(\mathbf{k}) + i(\mathbf{d}(\mathbf{k}) \times \mathbf{d}^*(\mathbf{k})) \cdot \hat{\sigma}$ is not a multiple of unit matrix. Thus in a non-unitary state time reversal symmetry necessarily is broken spontaneously and spontaneous moment $\mathbf{m}(\mathbf{k}) = i\mathbf{d}(\mathbf{k}) \times \mathbf{d}^*(\mathbf{k})$ appears at each point (\mathbf{k}). In this case the macroscopic averaged moment $\langle \mathbf{m}(\mathbf{k}) \rangle$ integrated on the Fermi surface non-vanishes. The variable $\mathbf{m}(\mathbf{k})$ is related to the net spin average of state \mathbf{k} by $\text{tr}[\hat{\Delta}(\mathbf{k})^\dagger \hat{\sigma}_j \hat{\Delta}(\mathbf{k})]$, it is clear that the total spin average over the Fermi surface can be nonzero. As an application, the nonunitary bipolar state of f -wave pairing symmetry has been considered for the B -phase of superconductivity in the UPt_3 compound which has been created in the low temperatures T and low values of H [15, 16]. In this chapter, we want to investigate the weak link between two nonunitary superconducting bulks. This type of weak link structure can be used to demonstrate and to test the pairing symmetry in the superconducting phase [64]. Consequently, we generalize the formalism of paper [6] for the case of weak link between nonunitary triplet superconducting bulks. In the paper [6], the Josephson effect in the point contact between unitary f -wave triplet superconductors has been studied. Also, the effect of misorientation on the charge transport has been investigated and a spontaneous current tangential to the interface between the f -wave superconductors, has been observed. In this chapter, the ballistic Josephson weak-link via an interface between two bulks of nonunitary bipolar f -wave superconductivity with different orientations of the crystallographic axes is investigated. It is shown that the current-phase diagrams are totally different from the current-phase diagrams of the junction between conventional (s -wave) superconductors [30], high T_c (d -wave) superconductors [48] and unitary triplet (axial and planar) f -wave superconductors [6]. This different characters can be used to distinct between nonunitary bipolar f -wave superconductivity from the other types of superconductivity, roughly speaking. In this weak-link structure between the nonunitary f -wave superconductors, the spontaneous current parallel to the interface as a fingerprint of unconventional superconductivity and spontaneous time reversal symmetry breaking, has been observed. The effect of misorientation on the spontaneous and Josephson currents is investigated. It is possible to find the value of the phase difference in which the Josephson current is zero but the spontaneous current tangential to the interface, which is produced by the interface, is present. In some configurations and at the zero phase difference, the Josephson current is not zero generally and it has a finite value. This finite value corresponds to a spontaneous phase difference which is related to the misorientation between the gap vectors.

The arrangement of the rest of this chapter is as follows. In Sec.(6.2) we describe our

configuration, which has been investigated. For a non-self-consistent model of the order parameter, the quasiclassical Eilenberger equations [31] are solved and suitable Green functions have been obtained analytically. In Sec.(6.3) the obtained formulas for the Green functions have been used for calculation the current densities at the interface and an analysis of numerical results will be done.

6.2. Quasiclassical equations

We consider a model of a flat interface $y = 0$ between two misoriented nonunitary f -wave superconducting half-spaces (Fig.12) as a ballistic Josephson junction. In order to calculate the current, we use quasiclassical Eilenberger equations [31] for Green functions (2) The Matsubara propagator \check{g} here, like the unitary triplet superconductor case, can be written in the form:

$$\check{g} = \begin{pmatrix} g_1 + \mathbf{g}_1 \cdot \hat{\sigma} & \mathbf{g}_2 \cdot \hat{\sigma} i \hat{\sigma}_2 \\ i \hat{\sigma}_2 \mathbf{g}_3 \cdot \hat{\sigma} & g_4 - \hat{\sigma}_2 \mathbf{g}_4 \cdot \hat{\sigma} \hat{\sigma}_2 \end{pmatrix}, \quad (107)$$

where, the matrix structure of the off-diagonal self energy $\check{\Delta}$ in the Nambu space is

$$\check{\Delta} = \begin{pmatrix} 0 & \mathbf{d} \cdot \hat{\sigma} i \hat{\sigma}_2 \\ i \hat{\sigma}_2 \mathbf{d}^* \cdot \hat{\sigma} & 0 \end{pmatrix}. \quad (108)$$

In this chapter, the nonunitary states, for which $\mathbf{d} \times \mathbf{d}^* \neq 0$, is investigated. Fundamentally, the gap vector (order parameter) \mathbf{d} has to be determined numerically from the self-consistency equation [85], while in this chapter, we use a non-self-consistent model for the gap vector which is much more suitable for the analytical calculations. Solutions to Eq. (1) must satisfy the conditions for Green functions and gap vector \mathbf{d} in the bulks of the superconductors far from the interface as follow:

$$\check{g} = \frac{1}{\Omega_n} \begin{pmatrix} \varepsilon(1 - \mathbf{A}_n \cdot \hat{\sigma}) & [i\mathbf{d}_n - \mathbf{d}_n \times \mathbf{A}_n] \cdot \hat{\sigma} i \hat{\sigma}_2 \\ i \hat{\sigma}_2 [i\mathbf{d}_n^* + \mathbf{d}_n^* \times \mathbf{A}_n] \cdot \hat{\sigma} & -\varepsilon \hat{\sigma}_2 (1 + \mathbf{A}_n \cdot \hat{\sigma}) \hat{\sigma}_2 \end{pmatrix} \quad (109)$$

where,

$$\mathbf{A}_n = \frac{i\mathbf{d}_n \times \mathbf{d}_n^*}{\varepsilon^2 + \mathbf{d}_n \cdot \mathbf{d}_n^* + \sqrt{(\varepsilon^2 + \mathbf{d}_n \cdot \mathbf{d}_n^*)^2 + (\mathbf{d}_n \times \mathbf{d}_n^*)^2}} \quad (110)$$

and,

$$\Omega_n = \sqrt{\frac{2[(\varepsilon^2 + \mathbf{d}_n \cdot \mathbf{d}_n^*)^2 + (\mathbf{d}_n \times \mathbf{d}_n^*)^2]}{\varepsilon^2 + \mathbf{d}_n \cdot \mathbf{d}_n^* + \sqrt{(\varepsilon^2 + \mathbf{d}_n \cdot \mathbf{d}_n^*)^2 + (\mathbf{d}_n \times \mathbf{d}_n^*)^2}}} \quad (111)$$

$$\mathbf{d}(\pm\infty) = \mathbf{d}_{2,1}(T, \hat{\mathbf{v}}_F) \exp\left(\mp \frac{i\phi}{2}\right) \quad (112)$$

where ϕ is the external phase difference between the order parameters of the bulks and $n = 1, 2$ label the left and right half spaces respectively. It is clear that, poles of Green function in the energy space, are in

$$\Omega_{2,1} = 0 \quad (113)$$

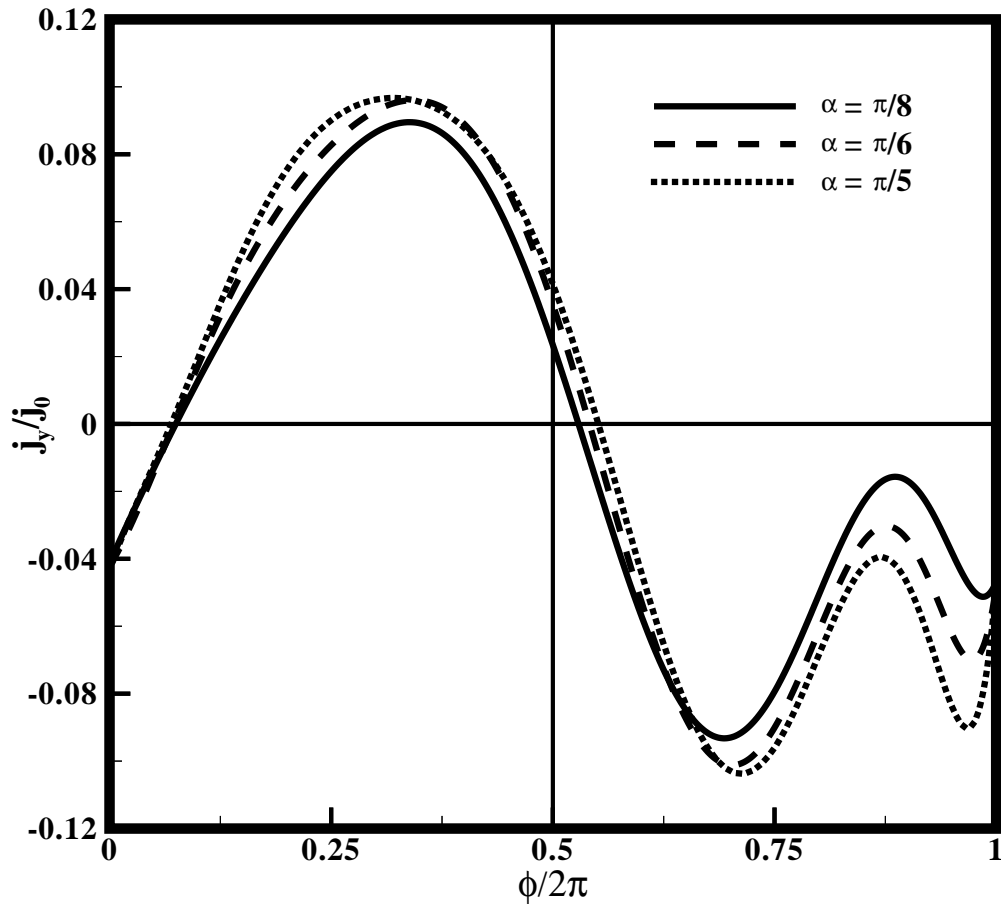


Figure 32. Component of current normal to the interface (Josephson current) versus the phase difference ϕ for the junction between nonunitary bipolar f -wave bulks, $T/T_c = 0.15$, geometry (i) and different misorientations. Currents are given in units of $j_0 = \frac{\pi}{2} e N(0) v_F \Delta_0(0)$.

consequently,

$$((iE)^2 + \mathbf{d}_{2,1} \cdot \mathbf{d}_{2,1}^*)^2 + (\mathbf{d}_{2,1} \times \mathbf{d}_{2,1}^*)^2 = 0 \quad (114)$$

and

$$E = \pm \sqrt{\mathbf{d}_{2,1} \cdot \mathbf{d}_{2,1}^* \mp i \mathbf{d}_{2,1} \times \mathbf{d}_{2,1}^*} \quad (115)$$

in which E is the energy place of poles. Eq. (1) have to be supplemented by the continuity conditions at the interface between superconductors. For all quasiparticle trajectories, the Green functions satisfy the boundary conditions both in the right and left bulks as well as at the interface.

The system of equations (1) and the self-consistency equation [85] can be solved only numerically. For unconventional superconductors such solution requires the information

of the interaction between the electrons in the Cooper pairs and nature of unconventional superconductivity in novel compounds which, in most cases are unknown. Also, It has been shown that the absolute value of a self-consistent order parameter is suppressed near the interface and at the distances of the order of the coherence length, while its dependence on the direction in the momentum space almost remains unaltered [41]. This suppression of the order parameter which keeps the current-phase dependence unchanged but changes the amplitude value of the current, doesn't influence the Josephson effect drastically. For example, it has been verified in paper [48] for the junction between unconventional d -wave, in paper [41] for the case of unitary “ f -wave” superconductors and in paper [70] for pinholes in ${}^3\text{He}$ that, there is a good qualitative agreement between self-consistent and non-self-consistent results. Also, it has been observed that results of the non-self-consistent model in [45] are similar to the experiment [73]. Consequently, despite the fact that this estimation cannot be applied directly for a quantitative analyze of the real experiment, only a qualitative comparison of calculated and experimental current-phase relations is possible. In our calculations, a simple model of the constant order parameter up to the interface is considered and the pair breaking and the scattering on the interface are ignored. We believe that under these strong assumptions our results describe the real situation qualitatively. In the framework of such model, the analytical expressions for the current can be obtained for a certain form of the order parameter.

6.3. Analytical and numerical results

The solution of Eq. (1) allows us to calculate the current densities. The expression for current is:

$$\mathbf{j}(\mathbf{r}) = 2i\pi eTN(0) \sum_m \langle \mathbf{v}_F g_1(\hat{\mathbf{v}}_F, \mathbf{r}, \varepsilon_m) \rangle \quad (116)$$

where, $\langle \dots \rangle$ stands for averaging over the directions of an electron momentum on the Fermi surface $\hat{\mathbf{v}}_F$ and $N(0)$ is the electron density of states at the Fermi level of energy. We assume that the order parameter is constant in space and in each half-space it equals to its value (112) far from the interface in the left or right bulks. For such a model, the current-phase dependence of a Josephson junction can be calculated analytically. It enables us to analyze the main features of current-phase dependence for a certain model of the order parameter of nonunitary f -wave superconductivity (bipolar). The Eilenberger equations (1) for Green functions \check{g} , which are supplemented by the condition of continuity of solutions across the interface, $y = 0$, and the boundary conditions at the bulks, are solved for a non-self-consistent model of the order parameter analytically. In a ballistic case the system of equations for functions g_i and \mathbf{g}_i can be decomposed on independent blocks of equations. The set of equations which enables us to find the Green function g_1 is:

$$v_F \hat{\mathbf{k}} \nabla g_1 = i(\mathbf{d} \cdot \mathbf{g}_3 - \mathbf{d}^* \cdot \mathbf{g}_2); \quad (117)$$

$$v_F \hat{\mathbf{k}} \nabla g_- = -2(\mathbf{d} \times g_3 + \mathbf{d}^* \times g_2); \quad (118)$$

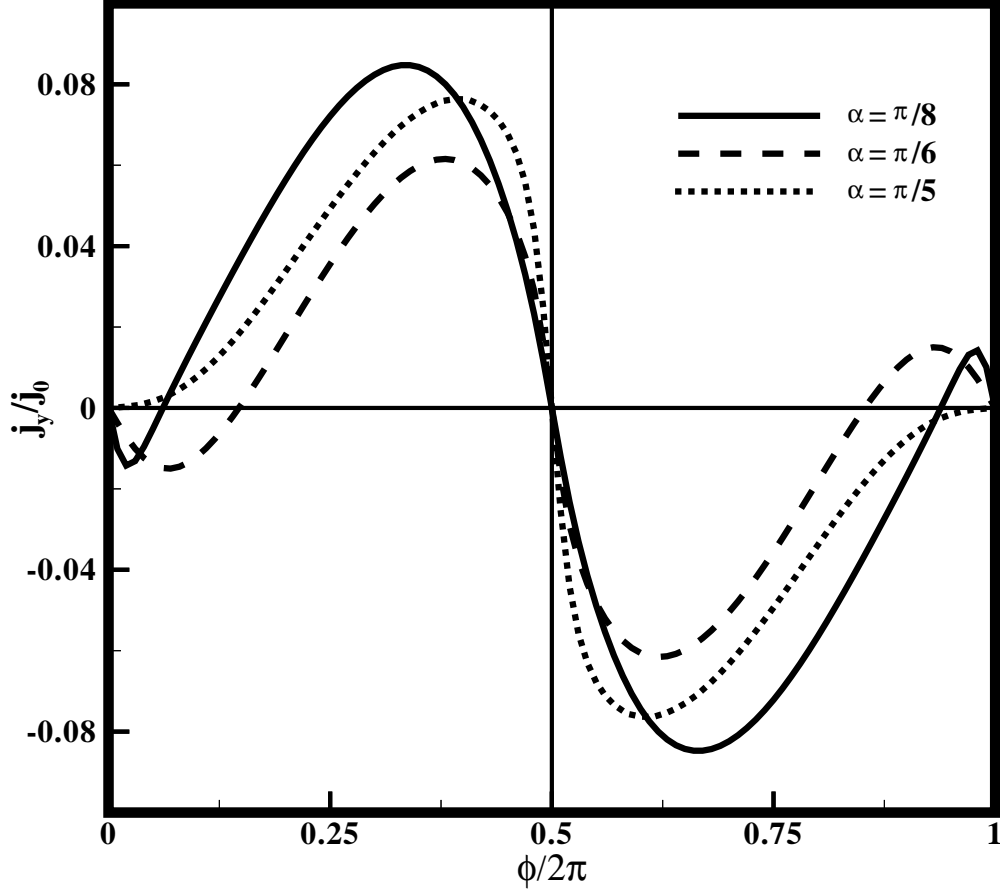


Figure 33. Component of current normal to the interface (Josephson current) versus the phase difference ϕ for the junction between nonunitary bipolar f -wave bulks, $T/T_c = 0.15$, geometry (ii) and different misorientations.

$$v_F \hat{\mathbf{k}} \nabla \mathbf{g}_2 = -2\varepsilon_m \mathbf{g}_2 + 2ig_1 \mathbf{d} + \mathbf{d} \times \mathbf{g}_-; \quad (119)$$

$$v_F \hat{\mathbf{k}} \nabla \mathbf{g}_3 = 2\varepsilon_m \mathbf{g}_3 - 2ig_1 \mathbf{d}^* + \mathbf{d}^* \times \mathbf{g}_-; \quad (120)$$

where $\mathbf{g}_- = \mathbf{g}_1 - \mathbf{g}_4$. The Eqs. (117)-(119) can be solved by integrating over ballistic trajectories of electrons in the right and left half-spaces. The general solution satisfying the boundary conditions (109) at infinity is

$$g_1^{(n)} = \frac{\varepsilon_m}{\Omega_n} + a_n e^{-2s\Omega_n t}; \quad (121)$$

$$\mathbf{g}_-^{(n)} = -2 \frac{\varepsilon_m}{\Omega_n} \mathbf{A}_n + \mathbf{C}_n e^{-2s\Omega_n t}; \quad (122)$$

$$\mathbf{g}_2^{(n)} = \frac{i\mathbf{d}_n - \mathbf{d}_n \times \mathbf{A}_n}{\Omega_n} - \frac{2ia_n \mathbf{d}_n + \mathbf{d}_n \times \mathbf{C}_n}{2s\eta\Omega_n - 2\varepsilon_m} e^{-2s\Omega_n t}; \quad (123)$$

$$\mathbf{g}_3^{(n)} = \frac{i\mathbf{d}_n^* + \mathbf{d}_n^* \times \mathbf{A}_n}{\Omega_n} + \frac{2ia_n\mathbf{d}_n^* - \mathbf{d}_n^* \times \mathbf{C}_n}{2s\eta\Omega_n + 2\varepsilon_m} e^{-2s\Omega_n t}, \quad (124)$$

where t is time of flight along the trajectory, $\text{sgn}(t) = \text{sgn}(y) = s$ and $\eta = \text{sgn}(v_y)$. By matching the solutions (121-124) at the interface ($y = 0, t = 0$), we find constants a_n and \mathbf{C}_n . Indices $n = 1, 2$ label the left and right half-spaces respectively. The function $g_1(0) = g_1^{(1)}(-0) = g_1^{(2)}(+0)$, which is a diagonal term of Green matrix and determines the current density at the interface, $y = 0$, is as follows:

$$g_1(0) = \frac{\eta(\mathbf{d}_2 \cdot \mathbf{d}_2(\eta\Omega_1 + \varepsilon)^2 - \mathbf{d}_1 \cdot \mathbf{d}_1(\eta\Omega_2 - \varepsilon)^2 + B)}{[\mathbf{d}_2(\eta\Omega_1 + \varepsilon) + \mathbf{d}_1(\eta\Omega_2 - \varepsilon)]^2} \quad (125)$$

where $B = i\mathbf{d}_1 \times \mathbf{d}_2 \cdot (\mathbf{A}_1 + \mathbf{A}_2)(\eta\Omega_2 - \varepsilon)(\eta\Omega_1 + \varepsilon)$. We consider a rotation \check{R} only in the right superconductor (see, Fig.12), i.e., $\mathbf{d}_2(\hat{\mathbf{k}}) = \check{R}\mathbf{d}_1(\check{R}^{-1}\hat{\mathbf{k}})$; $\hat{\mathbf{k}}$ is the unit vector in the momentum space. The crystallographic c -axis in the left half-space is selected parallel to the partition between the superconductors (along z -axis in Fig.12). To illustrate the results obtained by computing the formula (125), we plot the current-phase diagrams for two different geometries. These geometries are corresponding to the different orientations of the crystals in the right and left sides of the interface (Fig.12):
(i) The basal ab -plane in the right side has been rotated around the c -axis by α ; $\hat{\mathbf{c}}_1 \parallel \hat{\mathbf{c}}_2$.
(ii) The c -axis in the right side has been rotated around the b -axis by α ; $\hat{\mathbf{b}}_1 \parallel \hat{\mathbf{b}}_2$.

Further calculations require a certain model of the gap vector (order parameter) \mathbf{d} .

In this chapter, the nonunitary f -wave gap vector in the B -phase (low temperature T and low field H) of superconductivity in UPt_3 compound has been considered. This nonunitary bipolar state which explains the weak spin-orbit coupling in UPt_3 is [15]:

$$\mathbf{d}(T, \mathbf{v}_F) = \Delta_0(T)k_z(\hat{\mathbf{x}}(k_x^2 - k_y^2) + \hat{\mathbf{y}}2ik_x k_y), \quad (126)$$

The coordinate axes $\hat{\mathbf{x}}, \hat{\mathbf{y}}, \hat{\mathbf{z}}$ are selected along the crystallographic axes $\hat{\mathbf{a}}, \hat{\mathbf{b}}, \hat{\mathbf{c}}$ in the left side of Fig.12. The function $\Delta_0 = \Delta_0(T)$ describes the dependence of the gap vector on the temperature T (our numerical calculations are done at the low value of temperature $T/T_c = 0.1$). Using this model of the order parameter (126) and solution to the Eilenberger equations (125), we have calculated the current density at the interface numerically. These numerical results are listed below [87]:

1) The nonunitary property of Green's matrix diagonal term consists of two part. The explicit part which is in the B mathematical expression in Eq. (125) and the implicit part in the $\Omega_{1,2}$ and $\mathbf{d}_{1,2}$ terms. These $\Omega_{1,2}$ and $\mathbf{d}_{1,2}$ terms are different from their unitary counterparts. In the mathematical expression for $\Omega_{1,2}$ the nonunitary mathematical terms $\mathbf{A}_{1,2}$ are presented. The explicit part will be present only in the presence of misorientation between gap vectors,

$B = i\mathbf{d}_1 \times \mathbf{d}_2 \cdot (\mathbf{A}_1 + \mathbf{A}_2)(\eta\Omega_2 - \varepsilon)(\eta\Omega_1 + \varepsilon)$, but the implicit part will be present always. So, in the absence of misorientation ($\mathbf{d}_1 \parallel \mathbf{d}_2$), although the implicit part of nonunitary exists but the explicit part is absent. This means that, in the absence of misorientation current-phase diagrams for planar unitary and nonunitary bipolar systems are the same but the maximum values is different slightly.

2) A component of current parallel to the interface j_z for geometry (i) is zero as same as

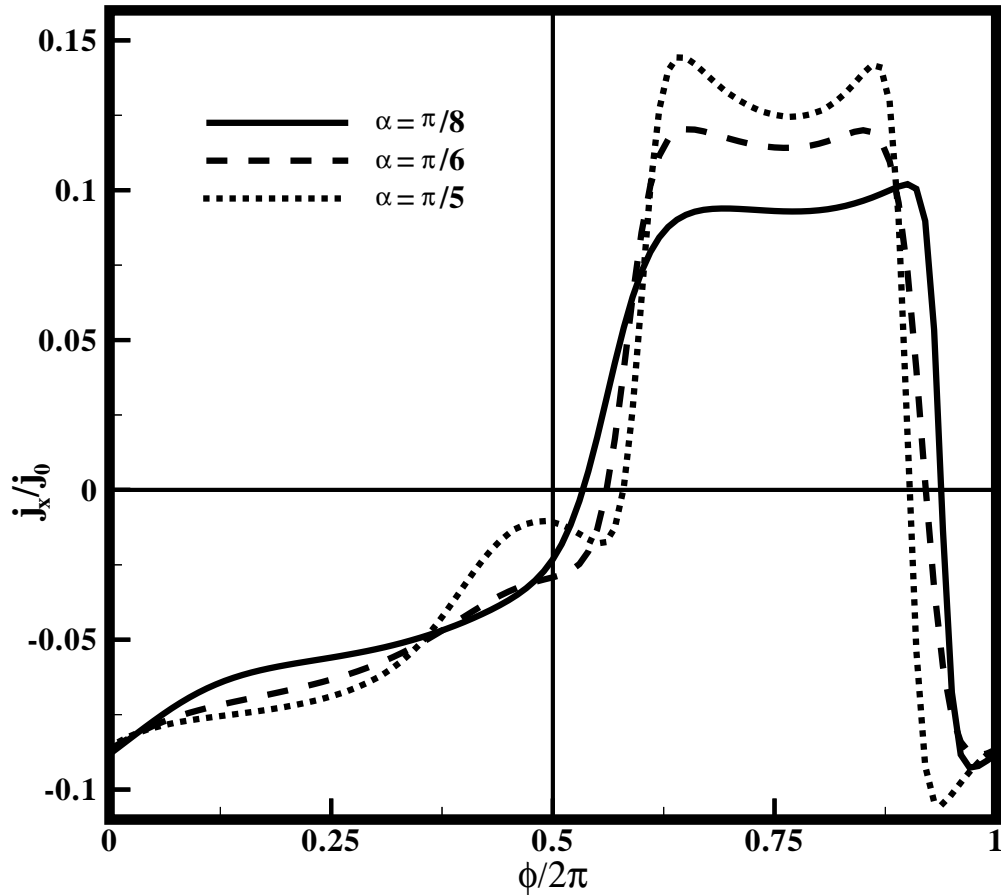


Figure 34. The x -component of charge current tangential to the interface versus the phase difference ϕ for the junction between nonunitary bipolar f -wave superconducting bulks, $T/T_c = 0.15$, geometry (i) and the different misorientations.

the unitary case [6] while the other parallel component j_x has a finite value (see Fig.34). This later case is a difference between unitary and nonunitary cases. Because in the junction between unitary f -wave superconducting bulks all parallel components of the current (j_x and j_z) for geometry (i) are absent [6].

3) In Figs.32,33, the Josephson current j_y is plotted for certain nonunitary model of f -wave and different geometries. Figs.32,33 are plotted for the geometry (i) and geometry (ii) respectively. They are completely unusual and totally different from their unitary counterparts which have been obtained in [6].

4) In Fig.32 for geometry (i), it is observed that by increasing the misorientation, some small oscillations, as the result of non-unitary property of the order parameter, appear in the current-phase diagrams. Also, the Josephson current at the zero external phase difference $\phi = 0$ is not zero but it has a finite value. The Josephson current will be zero

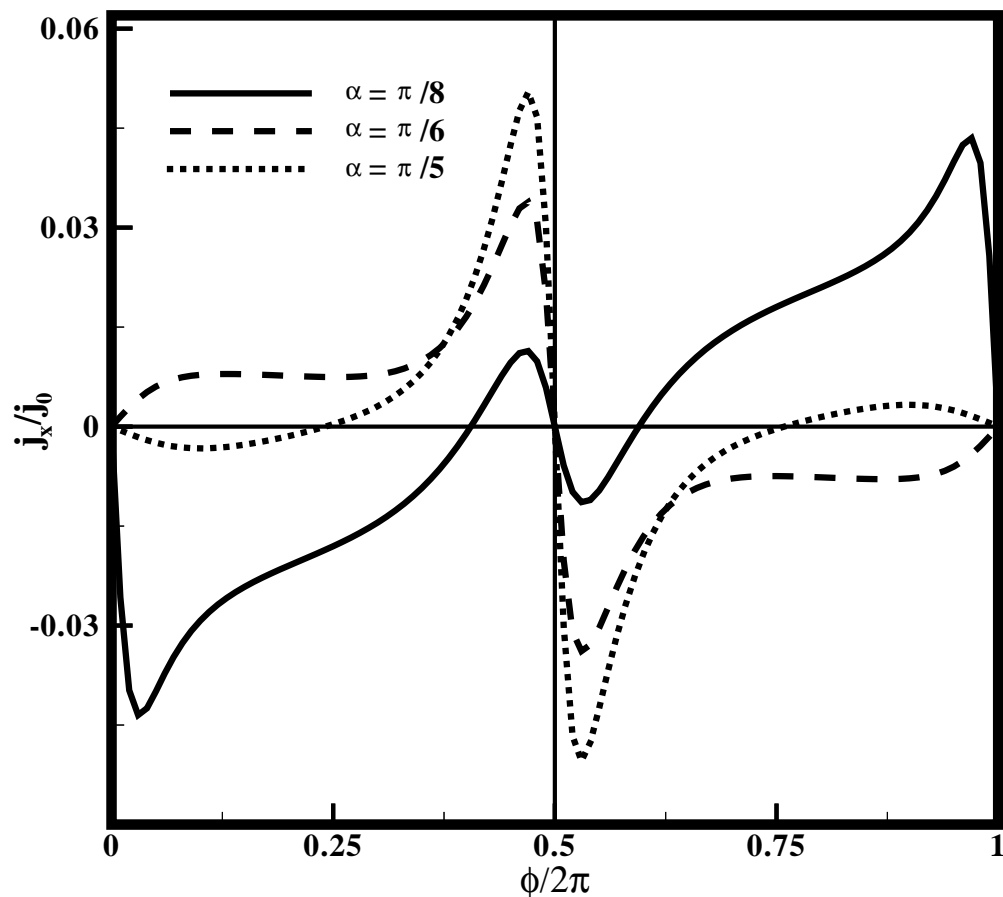


Figure 35. Current tangential to the interface versus the phase difference ϕ for the junction between nonunitary bipolar f -wave superconducting bulks, $T/T_c = 0.15$, geometry (ii) and the different misorientations (x component) .

at the some finite values of the phase difference.

5) In Fig.33 for geometry (ii), it is observed that by increasing the misorientation the new zeros in current-phase diagrams appear and the maximum value of current will be changed non-monotonically. In spite of the Fig32 for geometry (i), the Josephson current at the phase differences $\phi = 0$, $\phi = \pi$ and $\phi = 2\pi$ is zero exactly.

6) The current-phase diagram for geometry (i) and x -component (Fig.34) is totally unusual. By increasing the misorientation, the maximum value of current increases. The components of current parallel to the interface for geometry (ii) are plotted in Fig.35 and Fig36. All of terms at the phase differences $\phi = 0$, $\phi = \pi$ and $\phi = 2\pi$ are zero. The maximum value of the current-phase diagrams is not a monotonic function of the misorientation.

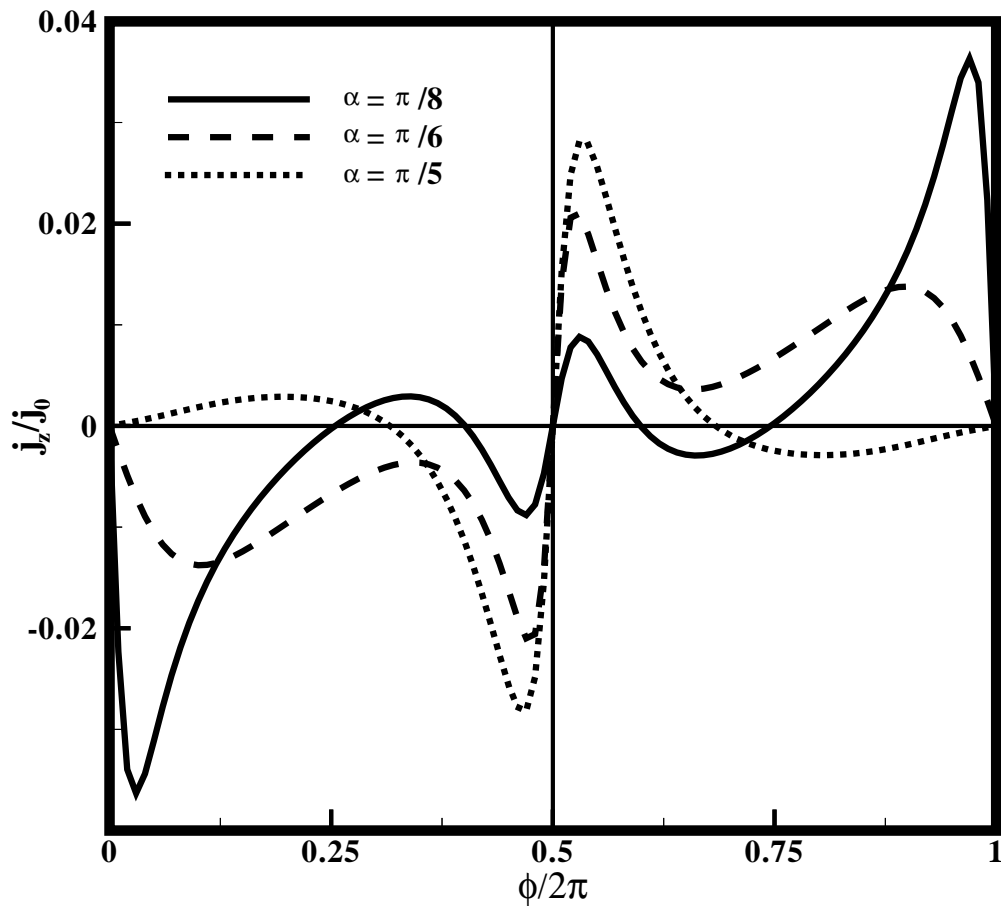


Figure 36. Current tangential to the interface versus the phase difference ϕ for the junction between nonunitary bipolar f -wave superconducting bulks, $T/T_c = 0.15$, geometry (ii) and the different misorientations (z -component).

7. Conclusions

At first, in the Chapter 3 of this thesis, we have studied the stationary Josephson effect in the ballistic point contact with transport current on the banks in the model $S-c-S$ taking into account the reflection of electrons from the contact. The contact is subject to the phase difference ϕ and the transport current tangential to the boundary of the contact. As it was shown in [32], in the ideal transparent point-contact at $\phi = \pi$ and near the orifice the tangential current flows in the opposite direction to the transport current, and there are two anti-symmetric vortex-like structures. It is observed that, by decreasing the transparency $D_c < D < 1$ the vortex-like current is destroyed. The critical value of $D = D_c(T)$ depends on the temperature T and $D_c(T \rightarrow 0) \rightarrow 1$, $D_c(T \rightarrow T_c) \rightarrow \frac{1}{2}$, so that we can never find a vortex for transparency values lower than

$\frac{1}{2}$. This anomalous temperature behavior of the vortices is the result of non-monotonic dependence of the interference current on the temperature.

Then, we have studied the spin current in the ballistic Josephson junction in the model of an ideal transparent interface between two misorientated f -wave superconductors which are subject to a phase difference ϕ , in Chapter (4). Our analysis has shown that the misorientation and different models of triplet gap vectors influence the spin current [83]. This has been shown for the charge current in the paper [6]. Misorientation between the left and right gap vectors changes strongly the critical values of both of the spin current and charge current. It has been obtained that the spin current is the result of the misorientation between the gap vectors. Furthermore, as an interesting and new result, it is observed that the different models of the gap vectors and geometries can be applied for the polarization of the spin transport. Another result of these calculations is the state in which the currents select one of the two possible directions (perpendicular and parallel to the interface) to flow. This property can be used as a switch to control the direction of the charge and spin current. Finally, it is observed that at some certain values of the phase difference ϕ , the charge-current vanishes while the spin-current flows, although the carriers of both spin and charge are the same (electrons). The spatial variation of the phase of the order parameter plays a role as the origin of the charge current and, similarly, due to a spatial difference of the gap vectors in two half-spaces causes spin currents. This is because there is a position-dependent phase difference between “spin up” and “spin down” Cooper pairs and, although the total charge current vanishes, there can be a net transfer of the spin. Therefore, in our system, there is a discontinuous jump between the gap vectors and, consequently the spin currents should generally be present. For instance, if spin-up states and spin-down states have a velocity in the opposite directions, the charge currents cancel each other whereas the spin current is being transported. Mathematically speaking, $\mathbf{j}_{\text{charge}} = \mathbf{j}_{\uparrow} + \mathbf{j}_{\downarrow}$, $\mathbf{j}_{\text{spin}} = \mathbf{j}_{\uparrow} - \mathbf{j}_{\downarrow}$, so it is possible to find the state in which one of these current terms is zero and the other term has a finite value [68]. In addition, the spin imbalance which is the result of the different density of states for “spin-up” and “spin-down” can be other reason of spin current [67]. In conclusion, the spin current in the absence of the charge current can be observed.

Also, the weak link between two misorientated $PrOs_4Sb_{12}$ superconducting bulks has been investigated in Chapter (5) of this thesis. We have considered the transportation of the spin and charge in the ballistic Josephson junction between two $PrOs_4Sb_{12}$ crystals with “ $(p+h)$ -wave” pairing symmetry which are subject to a phase difference ϕ . In this case as same as the case of f -wave junctions in Chapter (4), the different misorientations and different models of the gap vectors influence the spin and charge currents and it is shown that the misorientation of the superconductors leads to a spontaneous phase difference that corresponds to the zero Josephson current. This phase difference depends on the misorientation angle. A spontaneous charge current tangential to the interface which is not equal to zero in the absence of the Josephson current is observed in this junction. It has been obtained that the spin current is the result of the misorientation between the gap vectors which is the characteristic of unitary triplet superconductors.

Again in this case as same as the case of f -wave superconductors, it is observed that the certain model of the gap vectors and geometries can be applied to polarize of the spin transport. Finally, it is observed that at some certain values of the phase difference ϕ , the charge-current vanishes while the spin-current flows. The reason for this case is the above-mentioned discussion for f -wave. The spin and charge currents can be used to recognize the A -phase and B -phase of “ $(p+h)$ -wave” and the pure p -wave pairing symmetry and can be used to determine the pairing symmetry. Particularly, this proposed experiment can be used to demonstrate the “ $(p+h)$ -wave” pairing symmetry for which many doubts and challenges exist.

Finally, in Chapter (7), we have theoretically studied the charge currents in the ballistic Josephson junction in the model of an ideal transparent interface between two misoriented UPt_3 crystals with nonunitary bipolar f -wave superconducting bulks which are subject to a phase difference ϕ . Our analysis has shown that misorientation between the gap vectors create a current parallel to the interface and the different misorientations between gap vectors influence the spontaneous parallel and normal Josephson currents. These have been shown for the currents in the point contact between two bulks of unitary axial and planar f -wave superconductor in [6] separately. Also, It is shown that the misorientation of the superconductors leads to a spontaneous phase difference that corresponds to the zero Josephson current and to the minimum of the weak link energy in the presence of the finite spontaneous current. This phase difference depends on the misorientation angle. Again in this case, the tangential spontaneous charge current is not equal to zero in the absence of the Josephson current. The difference between junction behavior of unitary planar and nonunitary bipolar superconductivity can be used to distinct between them. This experiment can be used to test the pairing symmetry and recognize the different phases of UPt_3 which has two unitary and a nonunitary triplet pairing symmetry.

References

- [1] H.K. Onnes, Commun. Phys. Lab. **12**, 120 (1911).
- [2] J. Bardeen, L.N. Cooper, and J.R. Schrieffer, Phys. Rev. **108**, 1175 (1957).
- [3] L. N. Cooper, Phys. Rev. **104**, 1189 (1956).
- [4] V.L. Ginzburg and L.D. Landau, Zh. Eksp. Teor. Fiz. **20**, 1064 (1950).
- [5] Y. Maeno, H. Hashimoto, K. Yoshida, S. Nashizaki, T. Fujita, J.G. Bednorz, and F. Lichtenberg, Nature **372**, 532 (1994).
- [6] R. Mahmoodi, S.N. Shevchenko and Yu.A. Kolesnichenko, Fiz. Nizk. Temp. **28**, 262(2002) [Sov. J. Low Temp. Phys. **28**, 184 (2002)].
- [7] A.P. Mackenzie and Y. Maeno, Rev. Mod. Phys. **75**, 657 (2003).
- [8] D. Parker, K. Maki, S. Haas, cond-mat/0407254 (Accepted in Europhys. Lett).
- [9] V.P. Mineev, K.V. Samokhin, *Introduction to Unconventional Superconductivity* (CRC Pr I Llc, 1999).
- [10] Yu.S. Barash and I.V. Bobkova, Phys. Rev. B **65**, 144502 (2002).
- [11] Yu.S. Barash, I.V. Bobkova, and T. Kopp, Phys. Rev. B **66**, 140503 (2002).
- [12] A. Brataas and Y. Tserkovnyak, Phys. Rev. Lett. **93**, 087201 (2004).
- [13] V.P. Mineev and T. Champel, Phys. Rev. B **69**, 144521 (2004).
- [14] M.B. Walker and K.V. Samokhin, Phys. Rev. Lett. **88**, 207001 (2002).
- [15] K. Machida, T. Nishira, and T. Ohmi, J. Phys. Soc. Jpn. **67**, 1122 (1998).
- [16] T. Ohmi and K. Machida, Phys. Rev. Lett. **71**, 625 (1993).
- [17] C. Pfleiderer and A. D. Huxley, Phys. Rev. Lett. **89**, 147005 (2002).
- [18] I. Sheikin, A. Huxley, D. Braithwaite, J. P. Brison, S. Watanabe, K. Miyake, and J. Flouquet, Phys. Rev. B **69**, 180513 (2004).
- [19] T.M. Rice and M. Sgrist, J. Phys.: Condens. Matter **7**, L643 (1995).
- [20] D.F. Agterberg, T.M. Rice and M. Sgrist, Phys. Rev. Lett. **78**, 3374 (1997).
- [21] V. Müller, Ch. Roth, D. Maurer, E.W. Scheidt, K. Lüders, E. Bucher, and H.E. Bömmel, Phys. Rev. Lett. **58**, 1224 (1987).
- [22] Y.J. Qian, M.F. Hu, A. Schedenstrom, H.P. Baum, J.B. Ketterson, D. Hinks, M. Levy, and B.K. Sarma, Solid State Commun. **63**, 599 (1987).
- [23] Y. Maeno, Physica C, **282-287**, 206 (1997).
- [24] M.J. Graf, S.-K. Yip, and J.A. Sauls, Phys. Rev. B **62**, 14393 (2000).
- [25] K. Maki, H. Won, P. Thalmeier, Q. Yuan, K. Izawa, and Y. Matsuda, Europhys. Lett. **64**, (4), 496 (2003).
- [26] K. Izawa, Y. Nakajima, J. Goryo, Y. Matsuda, S. Osaki, H. Sugawara, H. Sato, P. Thalmeier, and K. Maki, Phys. Rev. Lett. **90**, 117001 (2003).
- [27] Goryo J, Phys. Rev. B **67**, 184511 (2003).
- [28] J.G. Bednorz and K.A. Muller, Z. Phys. B **64**, 189 (1986).
- [29] B.D. Josephson, Phys. Lett. **1**, 251 (1962).
- [30] I.O. Kulik and A.N. Omelyanchouk, Fiz. Nizk. Temp. **4**, 296 (1978) [Sov. J. Low Temp. Phys. **4**, 142 (1978)].
- [31] G. Eilenberger, Z. Phys., **214**, 195 (1968).
- [32] Yu.A. Kolesnichenko, A.N. Omelyanchouk, S. N. Shevchenko, Phys. Rev. B. **67**, 172504 (2003).
- [33] Y. Aharonov and D. Bohm, Phys. Rev. **115**, 485 (1959).
- [34] A.V. Zaitsev, JETP **59**, 1015 (1984).
- [35] A. A. Abrikosov, L. P. Gorkov, and I. E. Dzyaloshinskii, *Methods of Quantum Field Theory in Statistical Physics* (Prentice Hall, 1963).
- [36] A. L. Fetter, J. D. Walecka, *Quantum theory of many-particle systems* (McGraw-Hill, New York, 1971).
- [37] J. W. Serene, and D. Rainer, Phys. Rep. **101**, 221 (1983).
- [38] M. Zareyan, PhD Thesis Inst. for Adv. Studies in Basic Sciences Zanjan (2000).

- [39] V. Ambegaokar and A. Baratof, Phys. Rev. Lett. **10**, 486 (1963).
- [40] Yu. V. Sharvin Sov. Phys. JETP **21**, 655 (1965).
- [41] Yu. S. Barash, A. M. Bobkov, and M. Fogelstrom, Phys. Rev. B **64**, 214503 (2001).
- [42] M.H.S. Amin, A.N. Omelyanchouk, A.M. Zagoskin Phys. Rev. B **62**, R6131 (2000).
- [43] T. Lofwander, V.S. Shumeiko, and G. Wendin, Phys. Rev. B **62**, R14653 (2000).
- [44] J. Kurkijarvi. Phys. Rev. B **38**, 11184 (1988).
- [45] S.-K. Yip, Phys. Rev. Lett. **83**, 3864 (1999).
- [46] M. Fogelstrom, S. Yip and J. Kurkijarvi. Physica C **294**, 289 (1998).
- [47] M.H.S. Amin, A.N. Omelyanchouk, and A.M. Zagoskin, Phys. Rev. B **63**, 212502 (2001)
- [48] M.H.S. Amin, M.Coury, S.N. Rashkeev, A.N. Omelyanchouk, and A.M. Zagoskin, Physica B **318**, 162 (2002).
- [49] Yu.S. Barash, A.V. Galaktionov, and A.D. Zaikin, Phys. Rev. B **52** 665 (1995).
- [50] J.P.Heida, B.J. van Wees, T.M. Klapwijk, and G. Borghs, Phys. Rev. B **57**, R5618 (1998).
- [51] V. Barzykin and A.M. Zagoskin, Superlatt. and Microstr., **25**, 797 (1999).
- [52] Urs. Lederman, A.L. Fauchere, and G. Blatter, Phys. Rev. B **59**, R9027 (1999).
- [53] M.H.S. Amin, A.N. Omelyanchouk, and A.M.Zagoskin, Low Temp.Phys. **27**, 616 (2001).
- [54] W. Belzig, F. K. Wilhelm, C. Bruder, G. Schon and A. Zaikin, Superlatt. and Microstruc. **25**, 1251 (1999).
- [55] G. Rashedi, Superlatt. and Microstruc. **35**, 155 (2004).
- [56] G. Rashedi and Yu.A. Kolesnichenko, Phys. Rev. B **69**, 024516 (2004).
- [57] J. Bardeen, Rev. Mod. Phys. **34**, 667 (1962).
- [58] K. Ishida, H. Mukuda, Y. Kitaoka, Z.Q. Mao, Y. Mori, and Y. Maeno, Phys. Rev. Lett. **84**, 5387 (2000).
- [59] K. Deguchi, Z.Q. Mao, H. Yaguchi, and Y. Maeno, Phys. Rev. Lett. **92**, 047002 (2004).
- [60] K. Izawa, H. Takahashi, H.Yamaguchi, Y. Matsuda, M. Suzuki, T. Sasaki, T. Fukase, Y. Yoshida, R. Settai, and Y. Onuki, Phys. Rev. Lett. **86**, 2653 (2001).
- [61] M.J. Graf and A.V. Balatsky, Phys. Rev. B **62**, 9697 (2000).
- [62] H. Tou, Y. Kitaoka, K. Ishida, K. Asayama, N. Kimura, Y Onuki, E. Yamamoto, and K. Maezawa, Phys. Rev. Lett. **77**, 1374 (1996).
- [63] K. Ishida, H. Mikuda, Y. Kitaoka, K. Asayama, Z.Q. Mao,Y. Mori, and Y. Maeno, Nature **396**, 658 (1998).
- [64] N. Stefanakis, Phys. Rev. B **65**, 064533 (2002).
- [65] T. Yamashita, S. Takahashi, H. Imamura, and S. Maekawa, Phys. Rev. B **65**, 172509 (2002).
- [66] N.M. Chtchelkatchev JETP Lett. **78**, 230 (2003) [Pis'ma Zh. Eksp. Teor. Fiz. **78**, 265 (2003)].
- [67] G. Sun, Z. Zheng, D. Y. Xing, J. Dong and Z. D. Wang, J. Phys.:Condens. Matter **13**, 627 (2001).
- [68] S. Maekawa, J. Magn. Magn. Mater. **272**, 1459 (2004).
- [69] J.K. Viljas, E.V. Thuneberg, Phys. Rev. B **65**, 64530 (2002).
- [70] J. Viljas, cond-mat/0004246.
- [71] Z. Faraii and M. Zareyan, Phys. Rev. B **69**, 014508 (2004).
- [72] M. Freamat, K.-W. Ng, Phys. Rev. B **68**, 060507 (2003).
- [73] S. Backhaus, S. Pereverzev, R.W. Simmonds, A. Loshak, J.C. Davis, and R.E. Packard, Nature **392**, 687 (1998).
- [74] S. Kashiwaya, Y. Tanaka, N. Yoshida and M. R. Beasley, Phys. Rev. B **60**, 3572 (1999).
- [75] Y. Tanaka, T. Hirai, K. Kusakabe and S. Kashiwaya, Phys. Rev. B **60**, 6308 (1999).
- [76] N. Yoshida, Y. Tanaka, J. Inoue and S. Kashiwaya, J. Phys. Soc. Jpn **68**, 1071 (1999).
- [77] Y. Asano, Phys. Rev. B **64**, 224515 (2001).
- [78] K. Maki, S. Haas, D. Parker, H. Won, K. Izawa, Y. Matsuda, cond-mat/0406492.
- [79] E.D. Bauer, N.A. Frederick, P.-C. Ho, V.S. Zapf, and M.B. Maple, Phys. Rev. B **65**, R100506 (2002).
- [80] R. Vollmer, A. Faißt, C. Pfeleiderer, H. v. Löhneysen, E. D. Bauer, P.-C. Ho, V. Zapf, and M. B. Maple, Phys. Rev. Lett. **90**, 57001 (2003).

- [81] H. Kotegawa, M. Yogi, Y. Imamura, Y. Kawasaki, G.-Q. Zheng, K. Kitaoka, S. Ohsaki, H. Sugawara, Y. Aoki, and H. Sato, *Phys. Rev. Lett.* **90**, 027001 (2003).
- [82] H. Tou, K. Ishida, Y. Kitaoka, cond-mat/0308562.
- [83] G. Rashedi and Yu. A. Kolesnichenko, cond-mat/0501211.
- [84] G. Rashedi and Yu. A. Kolesnichenko, *Supercond. Sci. Technol.* **18**, 482 (2005).
- [85] M. Sigrist and K. Ueda, *Rev. Mod. Phys.* **63**, 239 (1991).
- [86] H. Tou, Y. Kitaoka, K. Ishida, K. Asayama, N. Kimura, Y. Onuki, E. Yamamoto, Y. Haga, and K. Maezawa, *Phys. Rev. Lett.* **80**, 3129 (1998).
- [87] G. Rashedi and Yu. A. Kolesnichenko, *Fiz. Nizk. Temp.* **31**, 634 (2005) [*Low Temp. Phys.* **31**, ??? (2005)].

